



NTNU – Trondheim
Norwegian University of
Science and Technology

TPG 4920: Petroleum Engineering Master's Thesis

Numerical Study on Autonomous Inflow Control Devices: Their
Performance and Effects on the Production from Horizontal Oil Wells
with an Underlying Aquifer

Melckzedeck Michael Mgimba

Petroleum Engineering

Supervisor: Prof. Milan Stanko, NTNU

Co-supervisor: Dr. Karim Baruti, UDSM

Department of Petroleum Engineering and Applied Geophysics

Submission date: August 2018

Norwegian University of Science and Technology

Department of Petroleum Engineering and Applied Geophysics

PREFACE

The idea of this Thesis comes as the extension of my specialization course which had the title “*Numerical Evaluation of the Effect of Ideal Autonomous Inflow Control Devices (AICDs) in the Recovery Factor of a Horizontal Well*”. This course covered the study of the oil recovery by horizontal well completed with AICDs perforating the oil reservoir with a gas cap. In this Thesis the work was extended to the title “*Numerical Study on Autonomous Inflow Control Devices: Their Performance and Effects on the Production from Horizontal Oil Wells with an Underlying Aquifer*” where it involves the study of DFCs (ICDs, AICDs, and AICVs) in the horizontal well perforating the oil reservoir with an underlying aquifer. The performance of DFCs in different oil reservoirs were covered, including in the heavy oil reservoir, thin oil layer reservoir, low viscous oil reservoir, and homogeneous reservoir.

I would like to thank God for the nice health I had during the time of doing my Thesis, My special gratitude goes to my Supervisor Prof. Milan Stanko for the suggestion of my topic and his guidelines for all works which I had been consulting him. Also, I would like to thank my co-supervisor Dr. Karim Baruti for the advice and guidelines which he provided to me during the time of doing my Thesis.

I would like to thank Angolan Norwegian Tanzanian Higher Education Initiative (ANTHEI) program coordinators Dr. Ambrose Itika from University of Dar es Salaam (UDSM) and Prof. Jon Kleppe from Norwegian University of Science and Technology (NTNU) for solving various studying challenges and making good studying environment.

Lastly but not least I would like to thank my family, friends and all people around who had been with me when I was doing Thesis tasks at home and college for encouraging me to do the work and also for their advice when I faced difficulties.

ABSTRACT

Oil is among one of the main sources of energy in the world and is mostly used by automobiles. However, oil production currently has challenges such as excessive water production, which reduces the cumulative oil recovery, this occurs due to water coning in the reservoir which resulted to earlier water breakthrough in the wellbore. Various Downhole Flow control Devices (DFCs) including ICDs, AICDs, and AICVS are typically installed in the horizontal section of oil wells to mitigate the problem. The devices constructed with new technology called Autonomous ICDs (AICDs and AICVs) according to data in the literature reportedly to perform better when compared against the passive ICDs. This thesis focuses on studying the performance of these technologies.

The study of autonomous ICDs was done by comparing the long term flow performance of such devices against passive ICDs. The study was carried out with a reservoir model representing a single horizontal well with four completion alternatives: open hole, ICD, AICDs, and AICVs, which were perforating in four different numerical reservoir models including heavy oil reservoir, thin oil reservoir, low viscous oil reservoir, and homogeneous reservoir. These cases were run in the Eclipse simulator and their results were compared with the open hole in each reservoir model.

The results show the installation of Autonomous ICDs (AICDs and AICVs) allowed to produce more oil when compared against using passive ICDs. As it was found in three cases, for the case of an heterogeneous reservoir with heavy oil, production with AICD increased the overall oil recovery by 0.73% as compared against an open hole completion, whereas production with ICD increased the overall oil recovery by 0.33% as compared against an open hole completion. For the case of an heterogeneous reservoir with thin layer of oil, production with AICD increased the overall oil recovery by 0.9% as compared against an open hole completion, whereas production with ICD increased the overall oil recovery by 0.14% as compared against an open hole completion. And for the case of an homogeneous reservoir with heavy oil, production with AICD increased the overall oil recovery by 0.03% as compared against an open hole completion, whereas production with ICD increased the overall oil recovery by 0.02% as compared against an open hole completion. But, for the case of an heterogeneous reservoir with low viscous oil (light oil), production with AICD increased the overall oil recovery by 0.2% as compared against an open hole completion which was lower compared against production with ICD which increased the overall oil recovery by 0.21% as compared against an open hole completion. Also, production with DFC reduces the water production and

increases the production time as it was proved by all cases, whereby production with DFC reduced the WC when compared to the open hole completion and we're having longer production time when compared against the open hole completion.

TABLE OF CONTENTS

PREFACE	i
ABSTRACT	ii
TABLE OF CONTENTS	iv
List of figures.....	viii
List of Tables	xi
NOMENCLATURE	xii
Abbreviations	xii
Symbols	xii
Subscripts	xv
1 INTRODUCTION	1
1.1 Problem description.....	5
1.2 Main objective.....	5
1.3 Specific objectives.....	5
1.4 Scope of the Thesis	5
2 LITERATURE REVIEW	7
2.1 The pressure in the Oil reservoir and Production well.....	7
2.1.1 Inflow performance relationship (IPR) for the oil reservoir.....	7
2.1.2 Pressure drop in the fluids flowing into the wellbore	10
2.1.3 Flow of fluids.....	11
2.1.4 Pressure drop for multiphase flow in a horizontal well	12
2.2 Horizontal oil wells/ Open hole	14
2.2.1 The advantage of the horizontal well.....	14
2.2.2 Factors affecting oil production in the open hole	15
2.3 Inflow control devices (ICDs).....	18
2.3.1 Types of ICDs	19
2.3.2 Steps to design inflow control devices.....	22

2.4	Autonomous Inflow Control Devices (AICDs)	26
2.4.1	Application of AICDs	27
2.4.2	Features of AICDs	27
2.4.3	Different technologies of AICDs	27
2.5	Autonomous Inflow control Valve (AICV)	32
2.5.1	Forces on the AICV	33
2.5.2	The AICV features	34
2.5.3	The advantage of AICVs	34
2.6	Factors affecting the horizontal well completion	35
2.7	The underlying aquifer/ Natural water drive	36
2.7.1	Water influx	36
2.7.2	Classifications of aquifer	36
2.7.3	Aquifer models.....	38
3	ADVANCE WELL COMPLETIONS	42
3.1	Introduction	42
3.2	The reservoir modelling	42
3.2.1	The Reservoir properties.....	42
3.2.2	The reservoir fluids (PVT data on Eclipse simulator)	43
3.2.3	Reservoir models used in this Thesis.....	48
3.2.4	The Aquifer	49
3.3	Modelling of DFCs.....	49
3.3.1	The number of DFCs in the horizontal well	50
3.3.2	Modelling of the ICDs	51
3.3.3	Modelling of AICDs and AICVs	55
3.4	Pressures and saturation distribution in the reservoir.....	59
3.5	Results	60
3.5.1	The results for model 1	60

3.5.2	The results for model 2	61
3.5.3	The results for model 3	62
3.5.4	The results for model 4	64
3.6	Discussions.....	65
4	OPTIMIZATION.....	67
4.1	The optimization of the cross sectional area of ICDs	67
4.2	The optimization of the strength of AICD/Vs (a) and Viscosity function exponent (y) 68	
4.3	Thesis process	71
4.4	Economic evaluation	73
4.5	Results	74
4.5.1	Results for model 1	74
4.5.2	Results for model 2	76
4.5.3	Results for model 3	78
4.5.4	Results for model 4	80
4.6	Sensitivity analysis of the oil price	82
4.7	Discussions.....	83
5	CONCLUSIONS AND RECOMMENDATIONS	85
5.1	CONCLUSIONS.....	85
5.2	RECOMMENDATIONS	86
6	REFERENCES	88
7	APPENDICES	92
	Appendix 1: The oil properties used in the reservoir model.....	92
	Appendix 2: The flowing rate through the DFCs	94
	Appendix 3: Procedure to design AICD function's parameters	95
	Appendix 4: Procedure to design AICV model parameters.....	97
	Appendix 5: Procedure to design AICD function's parameters for low viscous oil reservoir	99

Appendix 6: Procedure to design AICV model parameters for low viscous oil reservoir model.....	101
Appendix 7: MATLAB code for optimization of the cross sectional area of ICDs by using the Golden ratio search method	103
Appendix 8: MATLAB code for optimization of the strength of A ICDs (a) and Viscosity exponent (y) by using the Nelder - Mead method.	104
Appendix 9: Designed cross sectional areas of the ICDs	107
Appendix 10: Results for all four models	108
Appendix 11: Other attachment of the results for all four models	109

List of figures

Figure 1-1: Horizontal well showing heel-toe effect	2
Figure 1-2: ICD installation in the horizontal well to balance inflow in the wellbore	3
Figure 2-1: IPR for single phase oil flow	8
Figure 2-2: IPR for multiphase fluid flow	9
Figure 2-3: Pressure drop along the horizontal well	11
Figure 2-4: Laminar and Turbulent flow regimes.....	12
Figure 2-5: Perforating a reservoir with the horizontal well.....	14
Figure 2-6: Reservoir heterogeneity	15
Figure 2-7: The variation of cumulative oil production with the well length.....	17
Figure 2-8: Schematic diagram of orifice ICD	18
Figure 2-9: Helical-channel type ICD.....	19
Figure 2-10: Nozzle type ICD.....	20
Figure 2-11: Section view of Tube type and Hybrid channel ICDs	21
Figure 2-12: Pressure drop for different types of ICD.....	22
Figure 2-13: The variation of pressure drop with flow rate per ICD.....	24
Figure 2-14: Inflow rate throughout the wellbore	24
Figure 2-15: Horizontal well completion with Autonomous inflow control devices (AICDs)26	
Figure 2-16: ER –AICD system mounted in the production pipe	28
Figure 2-17: Fluidic diode type AICD. (a) Is the streamline for oil flow and (b) is the streamline for water and (c) Simplified model of AICD.....	29
Figure 2-18: RCP valve (AICDs)	30
Figure 2-19: Cross section view of AICV	32
Figure 2-20: Pressures in the AICV.....	33
Figure 2-21: Forces acting on the AICV.....	34
Figure 2-22: Types of aquifer based on the location from the reservoir	38
Figure 2-23: Determination of constant C and a graphically.....	39
Figure 3-1: Horizontal well perforating in the oil reservoir	42
Figure 3-2: Permeability in the heterogeneous reservoir along the x-direction.....	43
Figure 3-3: Solution GOR for heavy oil reservoir models	44
Figure 3-4: Solution GOR for low viscous oil reservoir models	45
Figure 3-5: Variation of viscosity of oil with the pressure in the heavy oil reservoir models.46	

Figure 3-6: Variation of viscosity of oil with the pressure in the low viscous oil reservoir models	46
Figure 3-7: Variation of viscosity of gas (μg) with the pressure in the reservoir	48
Figure 3-8: Variation of formation volume factor of gas (Bg) with the pressure in the reservoir	48
Figure 3-9: Sketch of the reservoir model which shows the pressure losses from the reservoir to the wellbore.....	50
Figure 3-10: Performance curve for AICDs	57
Figure 3-11: Performance curve for AICDs	57
Figure 3-12: Fluids performance curve of AICV for heavy oil	58
Figure 3-13: Fluids performance curve of AICV for low viscous oil.....	59
Figure 3-14: The oil recovery factor in the reservoir model 1	60
Figure 3-15: The WC in the reservoir model 1	61
Figure 3-16: The oil recovery in the reservoir model 2	61
Figure 3-17: The WC in the reservoir model 2.....	62
Figure 3-18: The oil recovery in the reservoir model 3	63
Figure 3-19: The WC in the reservoir model 3.....	63
Figure 3-20: The oil recovery in the reservoir model 4	64
Figure 3-21: The WC in the reservoir model 4.....	65
Figure 4-1: Trend line of cumulative Oil production versus cross sectional area	68
Figure 4-2: Cumulative oil production against AICDs strength for the horizontal well completed with AICDs	69
Figure 4-3: Cumulative oil production against AICDs strength for the horizontal well completed with AICDs	70
Figure 4-4: Solver for adjusting the w	70
Figure 4-5: Procedure to model DFCs	72
Figure 4-6: Oil recovery factor by horizontal well perforating a heterogeneous reservoir with 150 ft oil thickness (oil viscosity is 90 cp).	74
Figure 4-7: Net revenue of the increased oil for model 1	75
Figure 4-8: WC in the wellbore perforating the heterogeneous reservoir with a 150 ft oil thickness (Viscosity of 90 cp).....	76
Figure 4-9: Oil recovery factor by horizontal well perforating a heterogeneous reservoir with 100 ft oil thickness (oil viscosity is 90 cP).	77
Figure 4-10: Net revenue of the increased oil for model 2	77

Figure 4-11: WC in the horizontal well perforating the heterogeneous reservoir with a 100 ft oil thickness (viscosity of 90 cp).	78
Figure 4-12: Oil recovery factor by horizontal well perforating a heterogeneous reservoir with 150 ft oil thickness (oil viscosity is 2.7 cP).	79
Figure 4-13: Net revenue of the increased oil for model 3	79
Figure 4-14: WC in the horizontal well perforating the heterogeneous reservoir with a 150 ft oil thickness (viscosity of 2.7 cP).	80
Figure 4-15: Oil recovery factor by horizontal well perforating a homogeneous reservoir with 150 ft oil thickness (Oil viscosity is 90 cP)	81
Figure 4-16: Net revenue of the increased oil for model 4	81
Figure 4-17: WC in the horizontal well perforating in the homogeneous reservoir with a 150 ft oil thickness (Viscosity of 90 cP).	82
Figure 4-18: Sensitivity analysis of the oil price	83
Figure 7-1: The variaton of formation volume factor with the reservoir pressure for heavy oil	92
Figure 7-2: The variaton of formation volume factor with the reservoir pressure for light oil	93
Figure 7-3: Performance curve of AICD in heavy oil	95
Figure 7-4: Digitized AICV fluid performance curve	97
Figure 7-5: Performance curve of AICD in the low viscous oil reservoir	99
Figure 7-6: Digitized AICV fluid performance curve for low viscous oil reservoir	101

List of Tables

Table 3-1: Fluids properties found in the reservoir models	43
Table 3-2: Reservoir models used.....	49
Table 3-3: Conversion factor (Cu) when finding the pressure drop across the ICDs (Schlumberger, 2015).....	52
Table 3-4: The designed diameter and cross sectional area of the ICDs in the reservoir model 1.....	53
Table 3-5: The designed diameter and area of the ICDs in the homogeneous reservoir	54
Table 3-6: Parameters used in AICDs completion	58
Table 3-7: Parameters used in AICVs completion	59
.Table 4-1: Optimal cross sectional area of ICDs for different cases	68
Table 4-2: The optimization of the strength of AICDs (a) and Viscosity function exponent (y)	71
Table 4-3: Parameters for economic evaluation	73
Table 7-1: The designed diameter and cross sectional area of the ICDs in the reservoir model 2.....	107
Table 7-2: The designed diameter and cross sectional area of the ICDs in the reservoir model 3.....	107
Table 7-3: The results for model 1.....	108
Table 7-4: The results for model 2.....	108
Table 7-5: The results for model 3.....	108
Table 7-6: The results for model 4.....	108

NOMENCLATURE

Abbreviations

AICD/V	Autonomous Inflow Control Device/Valve
BHP	Bottom hole pressure
BO	Black Oil
DFC	Downhole flow control
EOS	Equation of State
ER -AICDs	Electrical resistivity AICDs
FVF	Formation Volume Factor
GOR	Gas Oil Ratio
GORM	Gas Oil Ratio Model
GVF	Gas Volume Fraction
ICD/V	Inflow Control Device/Valve
IPR	Inflow Performance Relationship
RCP	Rate Controlled Production
RCP- AICDs	Rate controlled Production AICDs
WC	Water Cut

Symbols

Symbol	Meaning	SI Unit	Field unit
ΔP_h	The pressure drop at the heel	<i>Bara</i>	<i>Psia</i>
ΔP_n	The total pressure drop	<i>Bara</i>	<i>Psia</i>
ΔP_t	The pressure drop at the toe	<i>Bara</i>	<i>Psia</i>
$\alpha_{o,w,g}$	The volume fraction of the free oil, water and gas phases at local conditions		

A_c	The cross sectional area of the valve constriction	m^2	ft^2
B_o	The formation volume factor		
C_u	A unit conversion constant		
C_v	The flow coefficient for the valve		
C_w	The rate of water influx	m^3/day	bbl/day
L_{DFC}	The length of DFC across which single DFC is installed	m	ft
L_{tubing}	The length of tubing segment	m	ft
P_{wf}	Well potential pressure	$Bara$	$Psia$
P_D	The dimensionless pressure		
P'_D	The dimensionless pressure derivative		
P_R	Reservoir pressure	$Bara$	$Psia$
P_i	The initial reservoir pressure	$Bara$	$Psia$
W_e	The cumulative water influx	m^3	ft^3
q_0	The oil flowing rate	Sm^3 / d	ft^3 / d
q_{DFC}	The modified flow rate through the DCFs	Sm^3 / d	ft^3 / d
q_{cell}	Volume flow rate through the segment	Sm^3 / d	ft^3 / d
q_g	The gas flowing rate	Sm^3 / d	ft^3 / d
q_o	Production rate	Sm^3 / d	ft^3 / d
q_t	The total flowing rate	Sm^3 / d	ft^3 / d
r_a	The radius of the aquifer	m	ft

r_e	The radius of the reservoir	m	ft
R_s	Solution GOR	sm^3/sm^3	scf/stb
t_D	The dimensionless time		
λ_l	The liquid fraction (volume)		
μ_{cal}	The viscosity of fluid to calibrate AICD	pas	cp
μ_g	The viscosity of the gas	pas	cp
μ_m	The viscosity of the mixture	pas	cp
μ_{mix}	The viscosity of mixture	pas	cp
$\mu_{o,w,g}$	The viscosity of the oil, water and gas phases at local conditions	pas	cp
μ_o	The viscosity of oil	pas	cp
ρ_{cal}	The density of fluid to calibrate AICD	kg/m^3	lbm/ft^3
ρ_{mix}	The density of mixture	kg/m^3	lbm/ft^3
$\rho_{o,w,g}$	The density of the free oil, water and gas phases at local conditions	kg/m^3	lbm/ft^3
h	The height difference	m	ft
h	The thickness of the aquifer	m	ft
J	Productivity index	$Sm^3/d/bar$	
t	The time	$days$	$days$
B	The van Everdingen and Hurst water influx constant		
D	The diameter of the flow area	m	ft

L	The travelling length of the fluid	m	ft
P	The pressure	$Bara$	$Psia$
f	The Darcy friction factor		
g	The gravitational constant		
k	The permeability of the aquifer	m^2	md
n	The current time step	$days$	$days$
$n - 1$	The previous time step	$days$	$days$
u	The fluid velocity	m/s	ft/day
x	The volume flow rate exponent		
y	The viscosity function exponent		
ε	The pipe roughness		
ρ	The fluid density	kg/m^3	lbm/ft^3
$\gamma_{o,g}$	Specific gravity of oil, gas		
T	Temperature	K	R

Subscripts

O	Oil
TP	Two phase
g	Gas phase
l	Liquid phase
w	Water
m	Mixture

1 INTRODUCTION

Horizontal oil wells typically exhibit in time excessive production of gas and water, which results to the reduction of production time and overall oil recovery. The main causes of these challenges are usually premature water/gas breakthrough in the wellbore. According to Shi, et al., (2016) premature water/gas breakthrough is caused by water coning in the reservoir, which occurs due to many factors, but on this work the heterogeneity effect, the thin oil layer, and the heel to toe effect will be covered, since they can be mitigated with down-hole flow control devices (DFCs).

Heterogeneity effects occur in the reservoir with zones of different permeability. Higher permeable zones will allow fluid to flow easier than low permeable zones. Also, the movement of GOC and WOC will be higher in the higher permeable sections which causes water coning which results to earlier water/gas breakthrough in the wellbore and then excessive production of water, gas or both. The general results will be a reduction of oil production in the lower permeable sections, and hence decrease production time and cumulative oil production (Marzooqi, et al., 2010).

The thin oil layer effect occurs in reservoirs that have a small oil layer thickness thus the well is very close to the oil-water contact or gas-oil contact. In this type of reservoirs, usually producing high oil rates will cause the oil-water or gas-water interface to deform and eventually intersect with the wellbore (known as gas coning or water cresting). This will cause earlier water /gas breakthrough in the wellbore and then excessive production of water, gas or both. The excessive production of water and gas will result in the reduction of the production time and the cumulative oil production (Kabir, et al., 2004).

Heel to toe effect is the effect that occurs in the reservoir with a long horizontal well whereby there is a significant pressure drop along the horizontal part of the wellbore. These effects will cause most of the production in a wellbore to come from the heel and hinder oil inflow from other well sections. The gas oil contact (GOC) and water oil contact (WOC) move faster at the heel due to higher oil production and this will cause gas/water coning (earlier gas/water breakthrough) as seen by red and blue colour in Figure 1-1. Gas/water coning causes excessive production of water and gas in the wellbore and hinder the oil production from the lower productive sections as the results oil production time and cumulative oil production will be reduced (Sharma, et al., 2015).

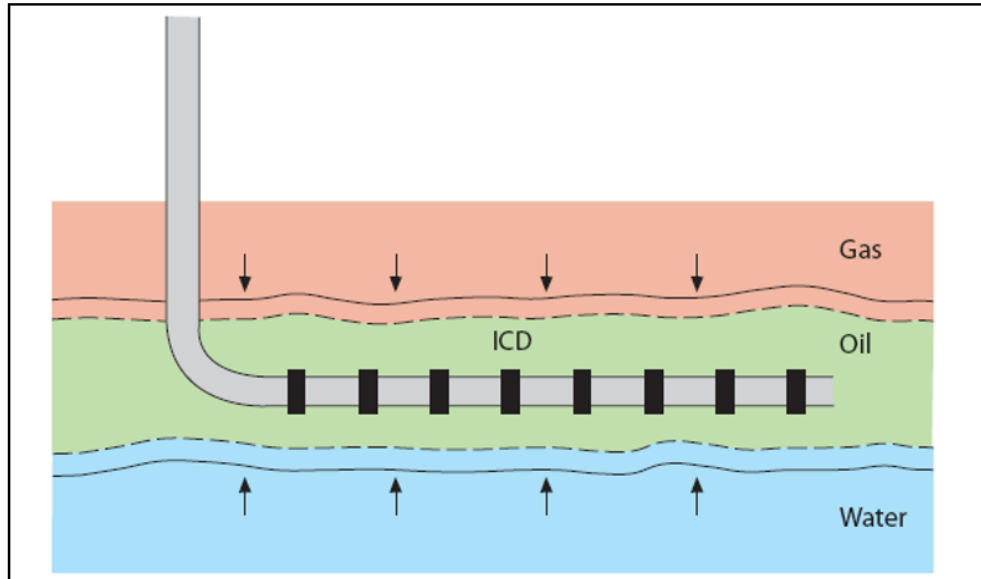


Figure 1-2: ICD installed in the horizontal well to balance inflow in the wellbore (Jovanov, 2016)

AICDs are devices used to choke the flow of low viscous fluids such as gas and water and favour the viscous fluid (oil). The AICDs combine properties of ICDs and fluid phase sensitivity (viscous sensitivity). This means before water/gas breakthrough AICDs are functioning like the ICDs, but after gas /water breakthrough AICDs add an extra restriction to unwanted fluid based on the viscosity. When AICDs are installed, the well performance and oil production can be greater after a gas breakthrough compared to conventional inflow control and open hole (Halliburton, 2017).

Another kind of Autonomous devices is called AICVs (Autonomous Inflow Control Valves), these devices are operated autonomously as AICDs, but they add one special property which other devices cannot do which is the ability to shutoff valve in the section which the unwanted fluid reached the target value (WC of 95%) and re-open when oil re-enter in the valve. The model (formula to model) of these devices are still under development.

The installation of DFCs in the horizontal well has brought many successes in different oil fields around the world such as reducing of the unwanted fluids (water and gas) production, increasing production time and cumulative oil recovery. A field pilot to test the advantages of DFC was carried out in the Gulf of Thailand, where the reservoir had a strong aquifer. Two wells A and B were perforated in the reservoir with the same properties, but with different completions, Well A was completed with Res flow ICDs and Well B was an open hole. The

production results show that Well A delays the water breakthrough by 50 days and increase of oil production by 50 % (Schlumberger, 2018).

Another study of DFCs was done in the Troll field, this field contains a reservoir with the thin layer of oil. The field was experiencing the problem of early gas breakthrough. When simulated models were run for the Troll field, the results show the completion with RCP valve increased the oil recovery by 20% higher than ICDs completion. The current production of oil after installation of RCP valve (AICD) in the Troll field shows higher oil recovery compared against the expected/simulated results ((Halvorsen, et al., 2012); (Halvorsen, et al., 2016)).

1.1 Problem description

Several researchers, including Halvorsen and his fellows in 2012 and 2016 studied the performance and effects of AICDs (self-regulating devices) on the reservoir containing a thin layer of oil. According to Halvorsen, et al., (2012) and Halvorsen, et al., (2016) completing a horizontal well with AICDs (RCP-Valve) in the Troll field reduces the GOR and increase the cumulative oil recovery by 20% higher than passive ICDs, however the researchers didn't address the performance of AICDs on restricting the water inflow in the wellbore.

The present work will focus on studying the flow performance of Autonomous ICDs (AICDs and AICVs) using numerical simulations and will quantify their performance and effects on the production from horizontal oil wells perforating the oil reservoir with an underlying aquifer.

1.2 Main objective

To evaluate the effects of inflow control strategies and technologies (DFCs) on the oil recovery factor of horizontal oil wells with an underlying aquifer using the numerical models.

1.3 Specific objectives

To compute the producing water cut with time and ultimate recovery factor of a horizontal well with an underlying aquifer and with open-hole completion, ICD, AICD and AICV for the following cases:

- I. Heterogeneous reservoir and heavy oil
- II. Heterogeneous reservoir and light oil
- III. Thin oil layer and heterogeneous reservoir
- IV. Homogeneous reservoir and heavy oil
- V. To optimize the performance of DFCs (ICDs, AICDs, and AICVs) and then compare the results.

1.4 Scope of the Thesis

There are many factors affecting oil production in the oil reservoir and also there are many ways of mitigating them, but in this work, the study of the performance and effects of Autonomous ICDs in comparison to passive ICDs in the horizontal well perforating the oil reservoir with an underlying aquifer was done. The study was concentrated in three devices ICD, AICD, and AICV and was done in four different environments, including the heterogeneous reservoir with the heavy oil, thin oil layer and low viscosity oil, and the

homogeneous reservoir with heavy oil. To include the aquifer effects in this model, the Fetkovich aquifer model was used. The work was done by using a numerical simulator called Eclipse in designing and running the models and Microsoft Excel in results analysis and evaluating some Eclipse input data, such as solution gas oil ratio, formation volume factors, and viscosity. This work excludes the study of other factors affecting the oil production such as variations of the well trajectory. Also, this study did not include the study of packer types.

2 LITERATURE REVIEW

The present study comprises of several parts including ICDs, AICDs, and AICVs completions. The performance of DFCs in the horizontal well will be modelled based on the pressure drop in the reservoir and wellbore. In this chapter the theoretical framework about pressure in the oil reservoir and production well, horizontal well (open hole), Inflow Control Devices (ICDs), Autonomous Inflow Control Devices (AICDs), and Autonomous Inflow Control Valves (AICVs) will be covered.

2.1 The reservoir pressure and the pressure along the well

2.1.1 Inflow performance relationship (IPR) for the oil reservoir

Drilling a horizontal well in the oil reservoir and opening it (to produce the oil) creates the pressure drop between the reservoir and the well. This pressure drop causes the fluid to flow from the higher pressure zone (reservoir) to the lower pressure zone (wellbore). When a well is producing in an undersaturated oil reservoir, the bottom hole pressure (P_{wf}) can be found by the IPR equation (1), where P_R is the reservoir pressure, J is the productivity index and q_o is the flowing rate at surface conditions, the equation is expressed in SI units.

$$P_{wf} = P_R - \frac{1}{J} q_o \quad (1)$$

The pressure drop in a reservoir is the indicator of energy loss created by the resistance of a fluid to flow. The resistance of the fluid flow depends on the rate of the fluid flow and a productivity index (J). The high fluid rate results in a higher pressure drop in the reservoir, so much energy is lost when the reservoir is produced at higher rates. Higher J will cause a lower pressure drop and hence lower energy losses in the reservoir.

The relationship between P_{wf} and q_o in the undersaturated oil reservoir is linear as shown in figure 2-1. Initially, the P_{wf} is low causing the maximum oil inflow to the wellbore, but when the P_{wf} increases, the inflow rate to the wellbore will be reduced.

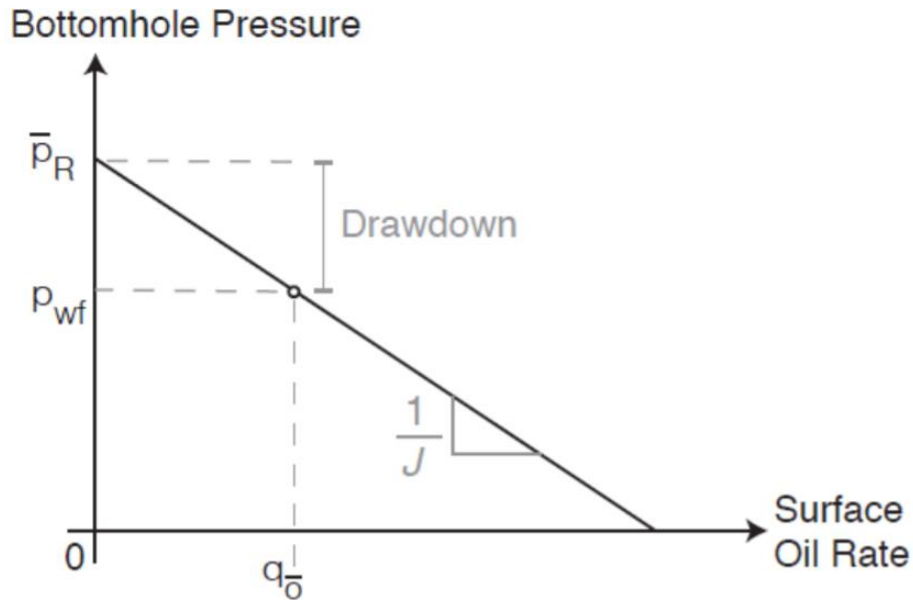


Figure 2-1: IPR for single phase oil flow (Håland, 2017)

The productivity index (J) depends on the fluid and reservoir properties including viscosity, permeability, formation volume factor and geometry of the reservoir. Productivity index is directly proportional to the permeability and inversely proportional to viscosity, this means an increase in permeability of rock increase the fluid productivity and reduce the pressure losses, whereas an increase in fluid viscosity reduces the productivity index and increases the pressure losses and the vice versa is true (equation (2)). The reservoir zones with high permeability produce more fluid than the zone with low permeability since high permeable zone provides lower fluid restriction (pressure loss is small). The productivity index (J) for a long horizontal well is defined in equation (2) (Asheim, 2017).

$$J = \frac{6\pi k_h h}{\mu B_o \left(\frac{\pi D}{2L_w} + \frac{3h}{L_w} \left(\ln \left(\frac{h}{2\pi r_w} \right) + S \right) \right)} \quad (\text{SI units}) \quad (2)$$

For solution gas drive reservoirs (saturated reservoir), bottom hole pressure can be obtained from the reservoir pressure by using Vogel equation (3). Vogel equation is applicable in the saturated oil reservoir, the relationship between pressure and flow rate for a saturated reservoir deviates from the linear relationship due to the presence of gas, they have a quadratic relationship as shown in figure 2-2. Figure 2-2 shows above the bubble point the relationship between the P_{wf} and q_o is linear (single phase oil flow), but when pressure drop below bubble point the relationship becomes quadratic.

$$\frac{q_o}{q_{o\max}} = 1 - 0.2 \frac{P_{wf}}{P_R} - 0.8 \left(\frac{P_{wf}}{P_R} \right)^2 \quad (3)$$

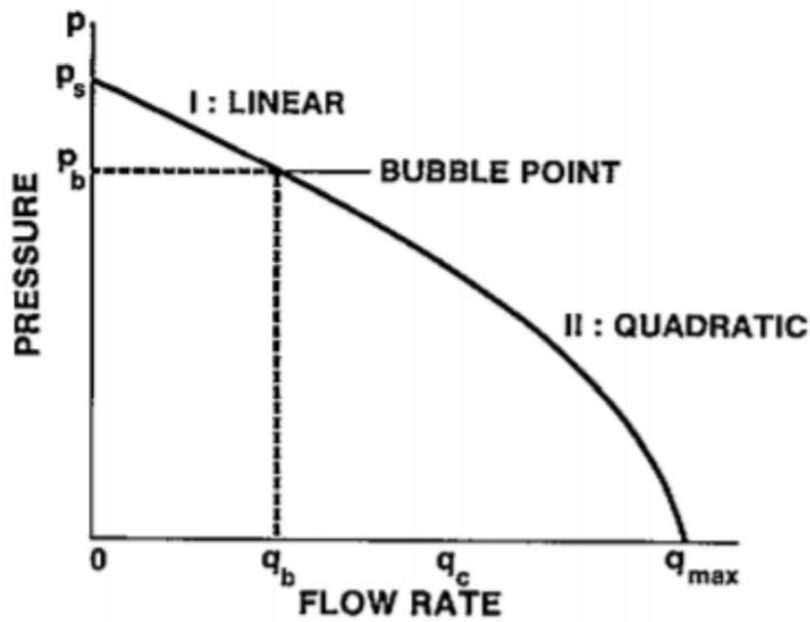


Figure 2-2: IPR for multiphase fluid flow (Håland, 2017)

Equation (3) is applicable in the vertical well, according to Ogunleye (2012) the equation can be developed to equation (4) when used for the horizontal well. Other researchers develop correlations including Cheng’s correlation, Wiggins’ correlation and Retnanto and Economide’s correlation which can be used for horizontal wells.

$$\frac{q_o}{q_{o\max}} = 1 - 0.45 \frac{P_{wf}}{P_R} - 0.55 \left(\frac{P_{wf}}{P_R} \right)^2 \quad (4)$$

According to IPR equations higher production rate will lead to a higher difference in pressure between the reservoir and sand phase, this will cause higher drawdown in the reservoir and earlier water /gas breakthrough is likely to occur. The variations in the reservoir permeability cause the variations in the fluid inflow in the wellbore, which also results in an earlier water/gas breakthrough in the zones with higher permeability.

2.1.2 Pressure drop in the fluids flowing into the wellbore

Fluid in the production tubing is experiencing a pressure drop caused by resistance created in the tube. The total pressure in the production tube can be the sum of the individual pressure drops including pressure drop due to gravitation, acceleration (or momentum) and friction as shown in equation (5).

$$dP_{\text{total}} = \rho g dh + \rho v dv + f * \frac{\rho u^2}{2D} * dL \quad (5)$$

When all parameters are substituted in equation (5), integration is done and the equation is rearranged, equation (6) will be formed for incompressible fluids such as oil and water.

$$P_1 + \frac{\rho v_1^2}{2} + \rho g h_1 = P_2 + \frac{\rho v_2^2}{2} + \rho g h_2 + \frac{1}{2} * f * \frac{\rho v^2}{D} * L \quad (6)$$

A friction factor (f) can be found depending on the types of flow regime as shown in equation (8) and (9). There are two main types of fluid flow, namely laminar flow and turbulent flow as they were explained in section 2.1.3.

For a long horizontal well with the same diameter, the velocity along the wellbore will be the same and there will be no change in vertical distance, so the equation (6) will be reduced to the equation (7). The pressure at the heel (P_1) will be equal to the pressure at the toe (P_2) minus the friction pressure losses along the wellbore, friction pressure losses in a fluid flowing along the wellbore from the toe to the heel are proportional to the length throughout wellbore. So the pressure at the heel will be the lowest along the horizontal section, then the pressure drop in the heel from the reservoir will be highest as seen in Figure 2-3. Frictional pressure loss along the wellbore from toe to heel will cause the heel to toe effect. This is the effect where due to the high pressure drop at the heel, most of the production will come from the heel and hence causing gas/water coning (Birchenko, et al., 2010).

$$P_1 = P_2 - \Delta P_{\text{friction}} \quad (7)$$

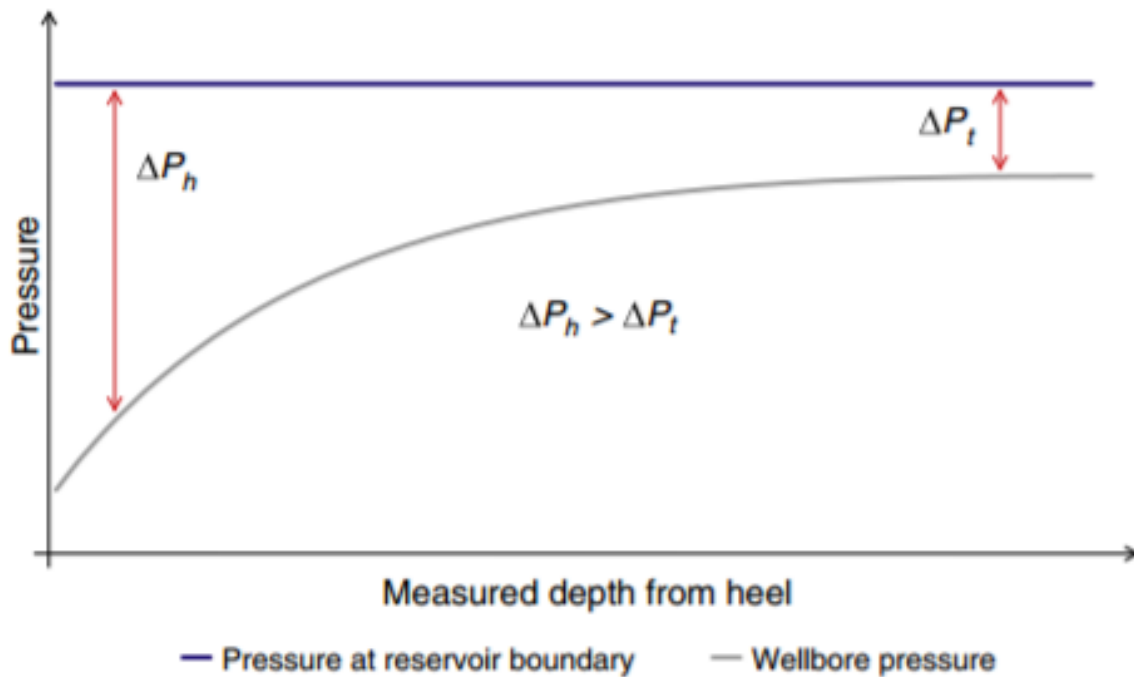


Figure 2-3: Pressure drop along the horizontal well (Birchenko, et al., 2010)

2.1.3 Flow of fluids

The movement of hydrocarbon fluid from the reservoir to the surface is divided into two types of flow, laminar flow and turbulent flow.

2.1.3.1 Laminar flow

Laminar flow is the type of flow regime which is smooth, steady and it is easy to recognize this kind of flow as shown in figure 2-4. The determination of friction factor in laminar flow can be done using the equation (8). The pressure drop of fluid flowing under laminar flow is depending on the density of a fluid.

$$f = \frac{64}{Re} \quad (8)$$

Where $Re = \frac{\rho V D}{\mu}$ in laminar flow Reynold (Re) number is less than 2000.

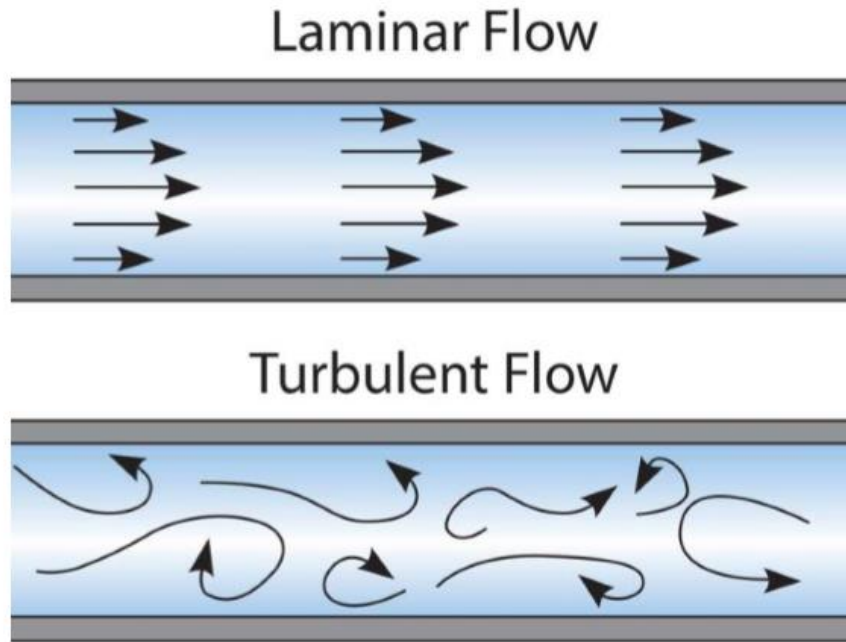


Figure 2-4: Laminar and Turbulent flow regimes (Håland, 2017)

2.1.3.2 Turbulent flow

Turbulent flow is the random and unsteady flow as shown in figure 2-4. The Reynolds number (Re) of turbulent flow is greater than 2300. The friction factor can be found empirically by a formula developed by Colebrook as seen in the equation (9) (Håland, 2017). The pressure drop in the fluid flowing under turbulent flow is depending on the density of a fluid.

$$\frac{1}{\sqrt{f}} = -2 \log \left(\frac{\epsilon}{3.7D} + \frac{2.51}{\text{Re}\sqrt{f}} \right) \quad (9)$$

The pressure drop of fluid flowing from the reservoir to the surface will depend on the type of flow as follows, the fluids in the reservoir have a laminar flow and the pressure drop is depending on the viscosity, on the wellbore (Production tubing) fluid flow in both laminar and turbulent flow, so the pressure drop is depending on both viscosity and density, the fluids in the DFCs have a turbulent flow and pressure drop is dependent on the density (Aadnoy, 2008).

2.1.4 Pressure drop for multiphase flow in a horizontal well

The production tubing in the oil fields normally contains oil, water, and gas, so the multiphase flow needs to be taken into account when calculating the flow rates and the pressure drop. According to Brill, (1987) during the early stage of the production, the wells are producing at high flow rates, which cause multiphase fluids to exist in the homogenous mixture. In

homogeneous mixture both fluids travel with the same velocity and the pressure equation in the production pipe can be modified as shown by equation (10).

$$P_1 + \frac{\rho_m v_{m1}^2}{2} + \rho_m g h_1 = P_2 + \frac{\rho_m v_{m2}^2}{2} + \rho_m g h_2 + \frac{1}{2} * f_m * \frac{\rho_m v_m^2}{D} * L \quad (10)$$

The density of the mixture (ρ_m) and velocity of the mixture (v_m) can be found using equation (11) and (12) respectively.

$$\rho_m = \rho_g \lambda_g + \rho_l \lambda_l \quad (11)$$

$$v_m = v_g + v_l \quad (12)$$

Where liquid volume fraction (λ_l) and gas volume fraction (λ_g) are $\lambda_l = \frac{q_l}{q_t}$ and $\lambda_g = \frac{q_g}{q_t}$

The friction factor of the mixture can be found with the same equations (7) and (8) but in determination of the Reynolds number, the velocity, viscosity, and density used will be of the mixture. Where the viscosity of the mixture can be found by using equation (13).

$$\mu_m = \mu_g \lambda_g + \mu_l \lambda_l \quad (13)$$

According to Asheim, (1986) pressure gradient equation for two phase flow with the slippage can be expressed with equation (14). The equation takes into consideration that the production pipe will have the same diameter (The velocity will be the same throughout the wellbore).

$$\frac{dP}{dx} = \rho_{TP} g_x + \frac{1}{2} * f_{TP} * \frac{\rho_m}{D} * v_m^2 \quad (14)$$

Where the density of mixture and two phases can be expressed by the equation (11) and (15) respectively.

$$\rho_{TP} = \rho_g (1 - Y_1) + \rho_l Y_1 \quad (15)$$

$$\text{Where } Y_1 = \frac{[(v_{sg} + a_1 v_{sl} - a_2)^2 + 4a_1 a_2 v_{sl}]^{0.5}}{2a_2} - \frac{v_{sg} + a_1 v_{sl} - a_2}{2a_2}$$

Frictional factor for two phases (f_{TP}) can be given by the equation (15).

$$f_{TP} = a_3 f_m * \frac{1}{F} \quad (16)$$

$$\text{Where } F = \frac{\rho_l}{\rho_m} * \frac{\lambda_l^2}{Y_1} + \frac{\rho_g}{\rho_m} * \frac{(1-\lambda_l)^2}{Y_1}$$

The constants of a_1 , a_2 , and a_3 can be found experimentally, where the error between the actual data and calculated data is found and it is supposed to be small.

2.2 Horizontal oil wells/ Open hole

Horizontal wells are the wells which extend along the reservoir in the horizontal direction to recover oil from the reservoir. The horizontal wells consist of two main sections vertical depth and horizontal sections (wellbore). The oil flows from the reservoir to the well in the horizontal section. The first part of the horizontal section is called the heel and the end part is called a toe as shown in Figure 2-5. The longest horizontal well drilled by Statoil Company in Statfjord field had a horizontal extension of 7288 m and true vertical depth of 2788 m (Jubralla, et al., 1996).

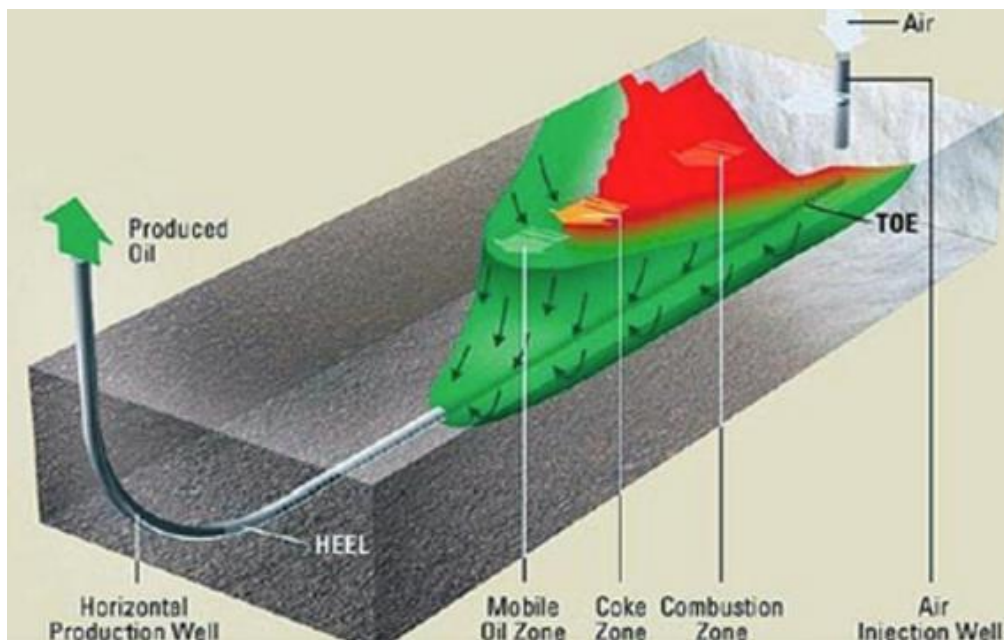


Figure 2-5: Perforating a reservoir with the horizontal well (Birchenko, et al., 2010).

2.2.1 The advantage of the horizontal well

Horizontal wells have a large coverage area of the reservoir than the vertical wells, which increase their productivity. The comparative study came out by (Berge, 2011) at Troll field indicated that the productivity index (J) of the horizontal well was 40 times the productivity index of the vertical well. Other advantages of horizontal wells include, they are usually quicker on recovering oil from the field, less cost and more effective than vertical wells. Also, they provide higher recovery from the oil reservoir, fewer disturbances to the surface since fewer wellheads may be required, they have the ability to monitor beneath contaminant sources such

as tanks, pits, and lagoons, increase the surface-area contact with contaminants, reduce cost of operating wells since few wells will be used (U.S. Department of Energy, 1998).

2.2.2 Factors affecting oil production in the open hole

2.2.2.1 Heterogeneity effect

These are the effects occur in the heterogeneous reservoir as shown in Figure 2-6. The heterogeneous reservoir has different zones with different properties including permeability. Reservoir with high permeability differences can lead to different oil inflow in the wellbore, which results to early water breakthrough to the zone with high production (high permeability). This will cause total production to come from some zones with high permeability and hinder oil production to the zones with low permeability as the results overall oil recovery will be reduced. When the heterogeneous reservoir is affected by heterogeneity effect and heel to toe effect, the heterogeneity effect dominates.

ICDs help in attaining uniform fluid influx into the wellbore through increasing the pressure drop in the higher permeability zones. Installation of ICDs result of the increase of the overall oil recovery ((Marzooqi, et al., 2010); (Jadhav, et al., 2017)).

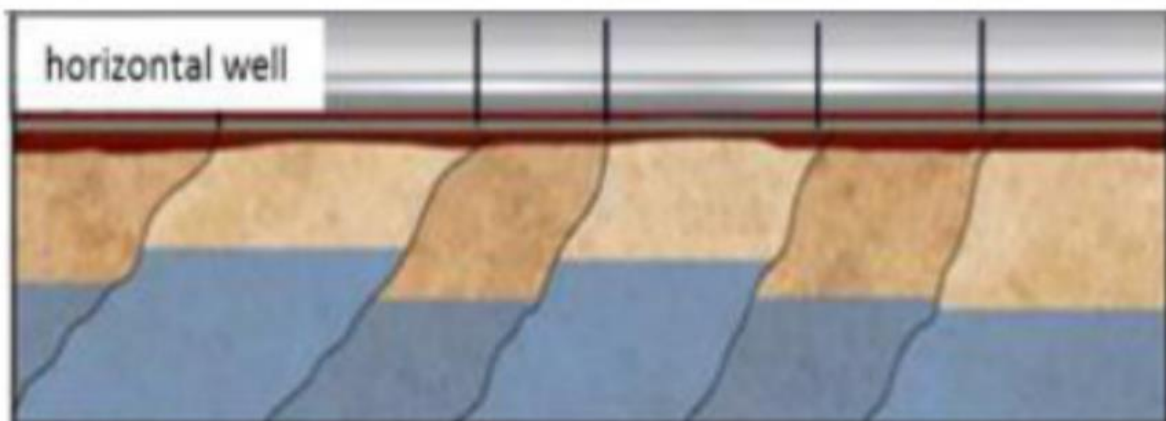


Figure 2-6: Reservoir heterogeneity (Marzooqi, et al., 2010)

2.2.2.2 Thin Oil Layers

Thin oil layer is the relative term, which depends on the cost of drilling well and accumulations of oil. In field with short drilling depth (lower cost), there is very thin oil layer, for example Onshore U.S.A, 20 feet is considered thin, whereas when the drilling depth increase large oil thickness is considered as a thin oil layer, for example Australia Bass Strait with 230 ft water

depth, 44 ft was considered thin, and in the Troll field (offshore Norway, 980 ft water depth), 79 ft was considered thin (Petrowiki 2017).

When a reservoir with thin oil layer is perforated with a horizontal well, the horizontal well will be close to both gas cap and aquifer which stimulates premature gas /water breakthrough (due to water coning). Water and gas coning in a thin oil reservoir depends on the well production rate, increasing in the production rate increase the risk of water/gas coning. ICDs balance the influx to the well, hence reducing the risk of earlier gas/water breakthrough (Kabir, et al., 2004).

2.2.2.3 Heel-toe effect

These are effects caused by the friction pressure drop along the wellbore, friction pressure drop along the wellbore cause differences in the inflow rates between the heel and the toe of the horizontal well. The difference in inflow rates between the heel and the toe can cause earlier water or gas (or both) breakthrough in the wellbore as shown in figure 1-1. Figure 1-1 shows a horizontal well perforating an oil reservoir with gas cap at the top (Red colour) and the aquifer at the bottom (blue colour), due to higher pressure losses in the wellbore the inflow rate at the heel will be higher compared against the toe causing WOC to move faster in the heel and then causing earlier water or gas breakthrough at the heel and hinder oil production at the toe (Birchenko, 2010).

The cumulative oil recovery is increasing with the increase in the horizontal well length, but due to the heel to toe effect, it will reach the length where the cumulative oil production is stopping to increase as shown in Figure 2-7. This variation of the cumulative oil production with the well length is depending on several factors, including permeability of the reservoir, the viscosity of the fluid, wellbore diameter and the drawdown pressure as shown in Figure 2-7 for permeability case (Ohaegbulam, et al., 2017).

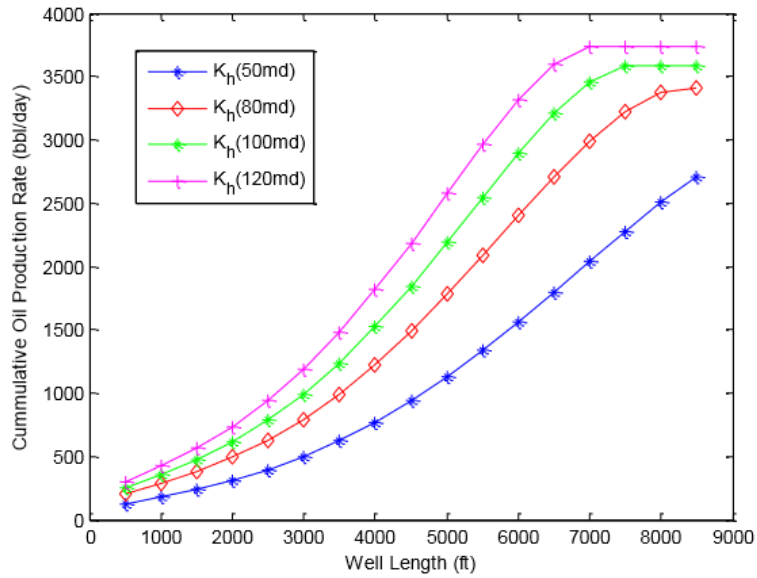


Figure 2-7: The variation of cumulative oil production with the well length (Ohaegbulam, et al., 2017)

The heel-toe effect dominates in the homogeneous reservoir (Darcy permeability) or in the well with small wellbore diameter, producing oil at a high flowing rate will cause high frictional pressure losses in the wellbore. To reduce this problem, it is advised to increase the diameter of the wellbore, use shorter wells or complete the well with inflow control devices (ICDs) (Sharma, et al., 2015).

2.3 Inflow control devices (ICDs)

ICDs are devices installed in a horizontal well to solve the challenge of excessive production of gas, water or both, which are caused by earlier water/gas breakthrough and also the ICD contains screen to control excessive sand production (Osman, et al., 1990). The ICDs provide the restriction or friction of fluid to pass through the channel, nozzle or orifice as shown in Figure 2-8, where the fluid from the annulus indicated with the red arrow is flowing to the orifice then to the production pipe. The restriction of fluid provided by ICDs causes the fluid pressure drop. The ICDs are installed in the well segments with lower pressure drops so as to add extra pressure drop and balance the pressure drops in all wellbore segment and then equalise the inflow along the wellbore.

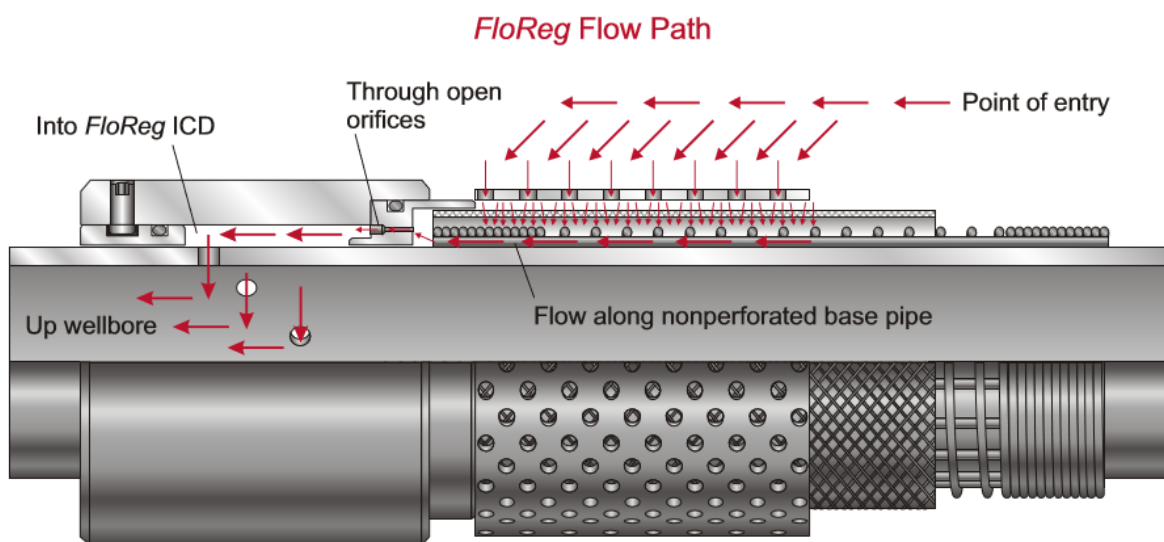


Figure 2-8: Schematic diagram of orifice ICD (Birchenko, 2010)

When ICDs are installed in the horizontal well, no any adjustment of the size of the nozzle, channel or orifice can be done. Due to that ICDs are sometimes called passive ICDs since they are not active and are not adjusted after their installation. An ICD is a passive system such that it cannot be controlled from the surface. But, over well life, reservoir conditions, and fluid properties change, while passive ICD completion remains static with less effective performance, so after gas /water breakthrough the ICD does not provide restriction anymore.

The flow regime through an ICD is turbulence, resulting in a quadratic relationship between velocity and pressure drop, this cause ICDs to be effective in reducing gas production. In situ gas viscosity is smaller than that of oil or water and density of gas is also smaller than that of oil and water, causing the velocity of gas to be the highest, since the pressure drop through the

restriction is proportional to the square of velocity, gas flowing through the ICDs experience higher restrictions than to oil and water (Birchenko, 2010).

2.3.1 Types of ICDs

There many types of ICDs which are used in the oil field depending on the manufacturer, and mechanism of performance. In this Thesis, the ICDs will be discussed based on their performance mechanism, including friction mechanism, restriction or combination of friction and restriction mechanism to generate pressure drop.

2.3.1.1 Channel-type (Helical channel) ICD

The channel-type ICD shown in Figure 2-9 is the type of ICD that uses surface friction to generate a pressure drop. The fluid flows through the channel type ICD by passing through the channel with a defined length, and then to the opening before entering the wellbore. The pressure drop in the channel type ICDs depends on the length of the channel and the diameter of the opening. The fluid will change direction when passing through these ICDs which will cause the pressure drop to be distributed along a longer channel path. This kind of ICD is supposed to have enough length, typically 120 inches to create enough pressure drop (Torbergsen , 2010).

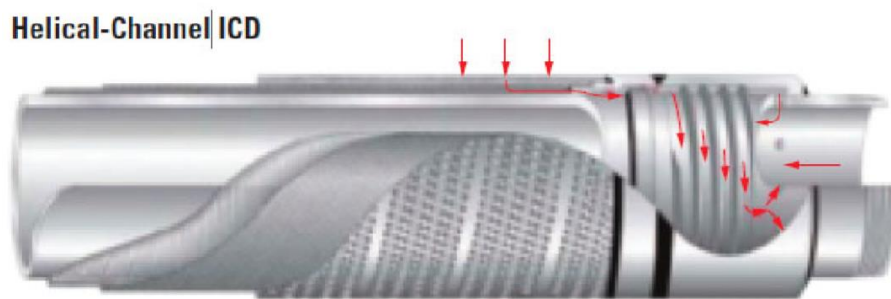


Figure 2-9: Helical-channel type ICD (Shevchenko, 2013)

The performance of channel type ICDs is explained based on the Poiseuille’s law, whereby the pressure drop of fluid passing through the channel type ICD is proportional to fluid viscosity and velocity as it is shown in Poiseuille’s equation (17).

$$\Delta P = \frac{128 \cdot \mu \cdot L \cdot Q}{\pi \cdot d^4} \quad (17)$$

According to Al-Khelaiwi, (2013) channel type ICDs are available in different ranges of pressure starting from 0.2, 0.4, 0.8, 1.6, 3.2 to 6.4 bars for a water with the flow rate of 26 Sm³/day/ICD joint.

The main advantage of channel type ICDs is that they generate lower flow velocities, hence reduce the erosion and plugging of equipment. While the disadvantage is that the restriction /pressure drop through the channel type ICD depends on the viscosities of the fluids, so when there is a big difference in viscosity between water and oil, the restriction of water will be reduced due to its lower viscosity hence the objective of reducing the water inflow will not be attained (Daneshy, et al., 2010).

2.3.1.2 Orifice/Nozzle type ICD

Nozzle type ICDs shown in figure 2-10 provide the fluid restriction to generate a desired pressure drop. Fluid is forced to pass through a small opening (orifices) in a pipe to generate flow resistance. The pressure drop is generated due to the generated flow resistance. These kind of ICDs are sensitive to the density and the square of the velocity of the fluid passing through the ICD as expressed by equation (18).

$$\Delta P = \frac{\rho * v^2}{2} \quad (18)$$

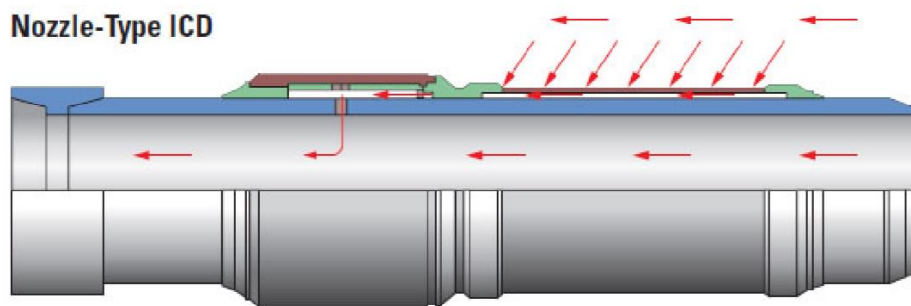


Figure 2-10: Nozzle type ICD (Shevchenko, 2013)

The advantage of Orifice/Nozzle type ICD is that they are simple to design and can be used in the reservoir which has a large variation in viscosity between water and oil, it can choke water easily since the pressure drop does not depend on the viscosity (Daneshy, et al., 2010). But the nozzle type ICDs are dependent on fluid velocity which makes them highly disposed to erosion from sand particles and less resistant to plugging (Fernandes, et al., 2009).

2.3.1.3 Tube and Hybrid channel types of ICDs

Figure 2-11 shows other types of ICDs, which are the tube-type and hybrid channel. Tube-type is the type of ICD which combine the restrictive and friction mechanism to create the pressure drop. The hybrid channel is the type of ICD which combine the restrictive, some friction and a tortuous pathway mechanism to create the pressure drop of the fluid flowing through the

device. These types of ICD combine the technology of Nozzle type ICD and channel types ICD in order to mix the advantages of all two types (Zeng, et al., 2013).

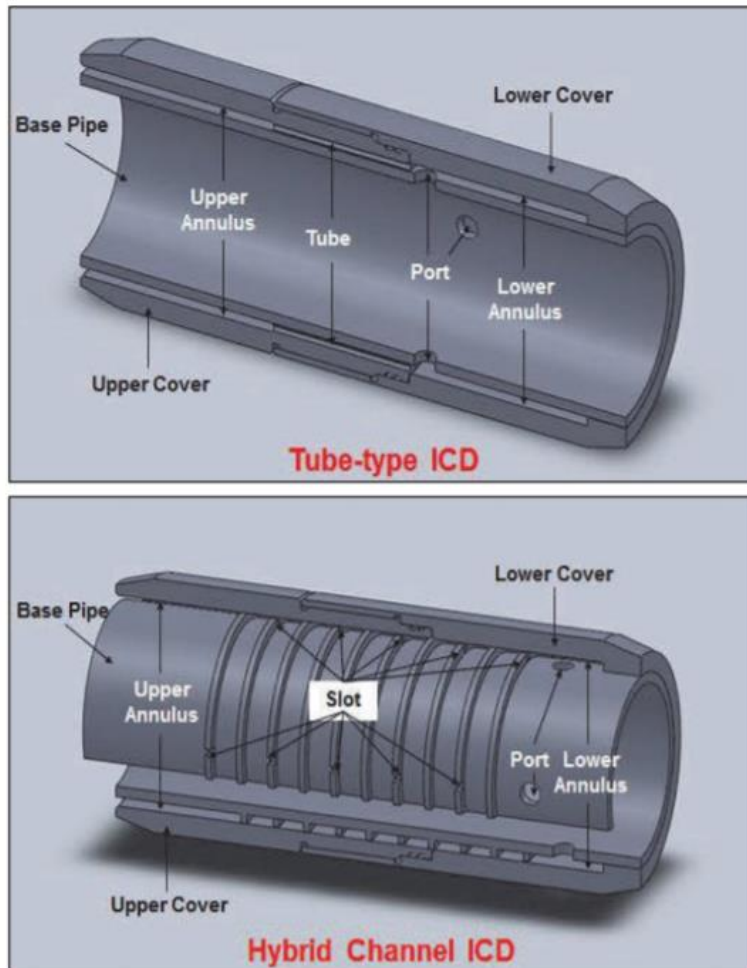


Figure 2-11: Section view of Tube type and Hybrid channel ICDs (Zeng, et al., 2013)

2.3.1.4 Performance curves of ICDs

Each type of ICD responds differently when fluid is flowing through it and they create different pressure drops. As shown in Figure 2-12 when water and oil with viscosity range from 4 cP to 200 cP are flowing through the ICDs the responses are different, for a fluid with a viscosity of 200 cP Tube and Helical channel types ICDs provide high pressure drop, while nozzle and hybrid type of ICDs provide the lowest pressure.

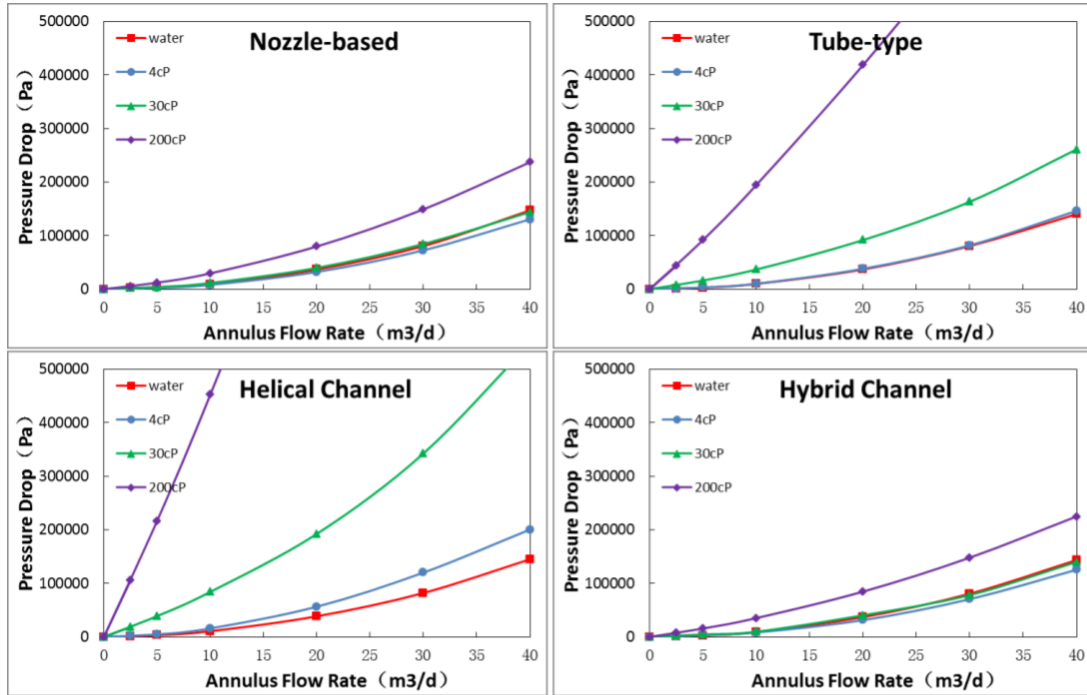


Figure 2-12: Pressure drop for different types of ICD (Zeng, et al., 2013)

2.3.2 Steps to design inflow control devices

According to Marzooqi, et al., (2010) ICDs can be designed in the oil horizontal well by the following steps:

- a. Selecting the type of ICD to be used

There are several types of ICD to be used in the completion of a horizontal well. The devices are selected depending on their performance and area of application. The properties which guide the proper selection of ICD are viscosity, density, erosion and flexibility of the ICD.

- b. Selecting ICD installation mechanism

Two mechanisms can be applied during the well completion time, constant strength (uniform strength) and variable strength mechanism. In uniform strength mechanism, ICD of the same strength (size) are installed throughout the wellbore. This kind of design is recommended in most of the area since it didn't bring bad results when ICD misplacement occurs since all ICDs have the same area (Strength).

The variable strength mechanism is the one which ICDs of different strength are installed. ICDs are installed in the location so as to compensate for the friction loss along the wellbore or to compensate for the heterogeneity effect. ICD with high strength is installed in the high

production zone in order to reduce the production and match with the low production zone. The variable strength ICD is designed by assuming no misplacement of ICD during installation.

c. Define minimum target rate

Based on the field experience minimum target rate is set. The target rate is not supposed to be high enough to cause suddenly drop of bottom hole pressure or too low to affect equalization effect. The target rate also should be designed based on the capacity of a separator.

d. Define the required pressure drop through ICD

According to Marzooqi, et al., (2010) optimum equalization is reached when pressure drop through the ICD is greater or equal to pressure drop through the reservoir. The ICDs can also be designed so that the pressure drop in the ICDs compensates the pressure losses along the wellbore (in homogeneous reservoir).

e. Determine the total number of ICD

The pressure drop versus ICD inflow curve, which is shown in figure 2-13 is used to predict the rate per ICD based on the designed pressure drop. In designing the ICD, there are two main designs of inflowing rate per ICD. The first design is to suggest the equal inflow rate for each ICD and the second design is to suggest u shaped inflow rate. The first design where each ICD contributes the same inflow rate to the total flowing rate, this design is good for controlling earlier water breakthrough. In the equal inflow rate design, the total number of designing ICD is taken by dividing the minimum target rate with flowing rate per ICD.

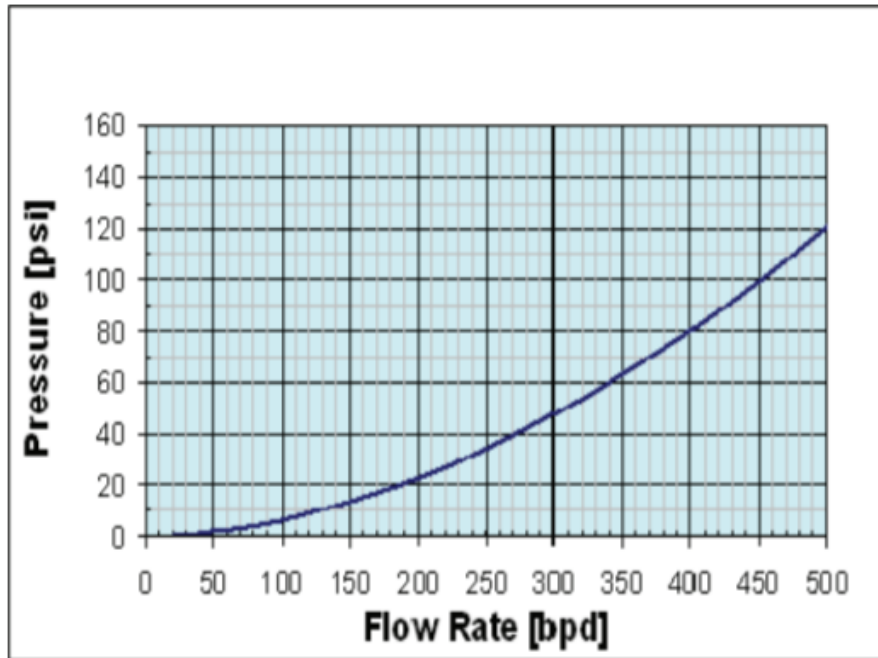


Figure 2-13: The variation of pressure drop with flow rate per ICD (Marzooqi, et al., 2010)

In the second design, the pressure drop of fluid passing through the ICD has to be designed so that the heel and the toe parts of wellbore contribute more inflowing rate compared against other parts of the wellbore as showing in figure 2-14. This design is facing a challenge of earlier water breakthrough, but results in higher total cumulative oil production when than the first design.

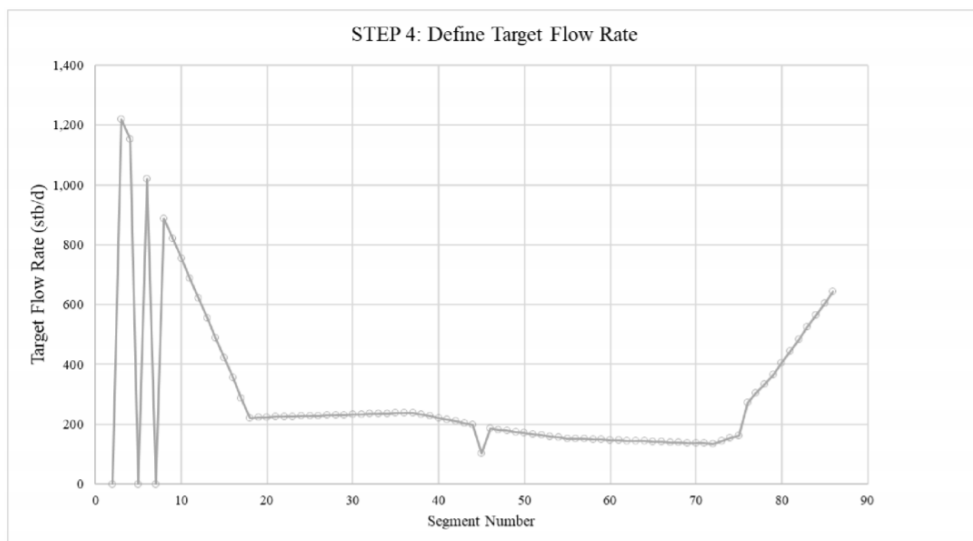


Figure 2-14: Inflow rate throughout the wellbore (Lim, 2017)

f. Optimal number of ICD and compartments by running a simulation

During simulation, heterogeneity will cause pressure drop through the ICD to vary. The actual number of ICD and compartments have to be found when running simulations.

2.4 Autonomous Inflow Control Devices (AICDs)

The AICDs are devices developed to solve the challenge of the passive ICDs completion, that they can't provide restriction of unwanted fluid after gas /water breakthrough in the wellbore. To provide more limitation of unwanted fluid (gas and water) along horizontal well, a new developed Autonomous ICD (AICD) has been proposed as shown in Figure 2-15. There is no need for intervention when AICD is installed. The AICD autonomously provides additional flow restriction to the unwanted fluid. The AICD valve chokes the flow of low-viscous fluids and favours the viscous fluid. When AICDs are installed, the well performance and the oil production after a gas/water breakthrough will be greater than conventional inflow control and open hole (Halliburton, 2017).

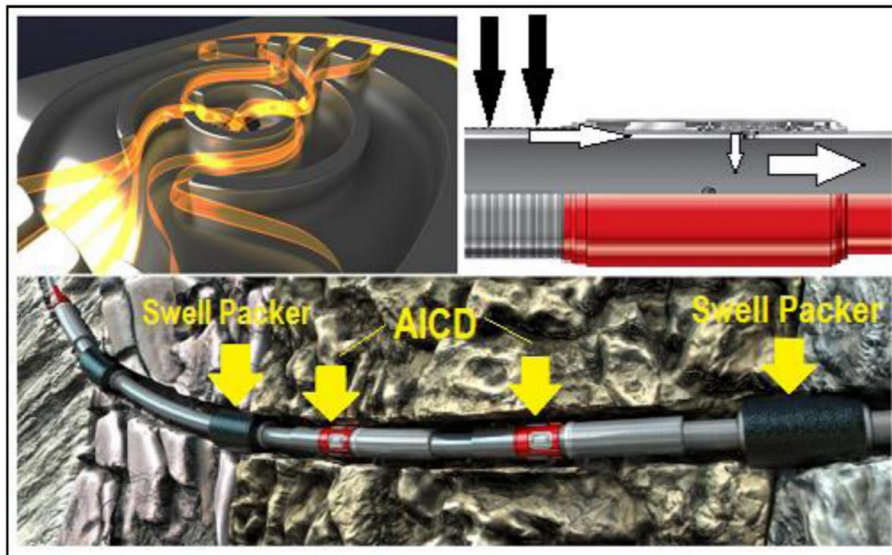


Figure 2-15: Horizontal well completion with Autonomous inflow control devices (AICDs)
(Halliburton, 2017)

The installation of AICDs in the well is incorporated with the installation of packers in the annulus as shown in Figure 2-15. Packers are used to separate annulus into sections with different properties and prevent fluid from flowing through the annulus. The use of the AICDs in heterogeneous reservoir creates different annulus pressures in sections between packers. The advantage of this will be a lower drawdown in sections with high permeability and the higher drawdown in sections with lower permeability.

2.4.1 Application of AICDs

The AICDs are installed during the well completion and they help a reservoir to produce for a long time. The AICDs are applicable in a well experiencing heel-toe effects, the earlier breakthrough of water/gas, reservoir heterogeneity, and water or gas challenges in horizontal or layered reservoirs (Halliburton, 2017).

2.4.2 Features of AICDs

The AICDs have many features including, they are operated autonomously, are not operated from the surface, before water/gas breakthrough AICDs function as a passive ICD while after gas/water breakthrough they have an additional restriction to unwanted fluids (gas and water), the installation of AICDs does not require intervention, each device works independently for accurate response to the reservoir, they allow injection of the reservoir, treating fluids and self-regulating depending on produced fluids (Halliburton, 2017).

2.4.3 Different technologies of AICDs

There are different technologies that have been termed as AICDs such Electrical resistivity (ER-AICD), a fluidic diode AICD and Rate controlled production RCP-AICD. All AICDs types are operated autonomous but their working mechanism differ, there are those which use resistivity theory, the moment of inertia theory, and Bernoulli principle (Ahmad, et al., 2016).

2.4.3.1 ER-AICD

The ER-AICD is the type of AICD which use the electrical resistivity mechanism depicted in Figure 2-16. The AICD has two flow paths, namely main flow path which most of the fluid is passing and secondary flow path. The secondary flow path contains a sensor which detects viscosity of the fluid and sends an electrical signal to a solenoid which has an electromagnetic effect to open the valve of the main flow path for highly viscous fluid such as oil and close valve of the main flow path for low viscous fluid such as water and gas. This technology chokes unwanted fluid (fluid with low viscosity which are water and gas) and favours the oil inflow in the wellbore.

The two main functions of ER- AICD are to identified fluid present according to viscosity and restrict unwanted fluid to the wellbore (Fripp, et al., 2013).

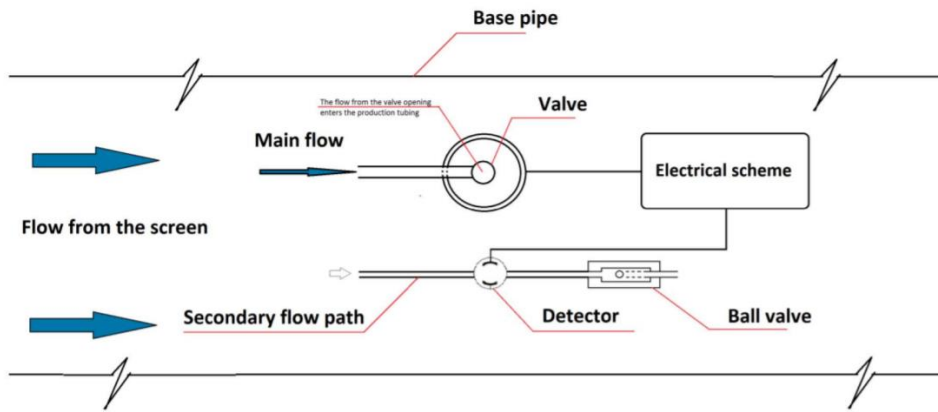


Figure 2-16: ER –AICD system mounted in the production pipe (Jadhav, et al., 2017)

2.4.3.2 Fluidic diode type AICD

The fluidic diode type AICD also is called Equiflow AICDs. This kind of AICD does not contain a movable part, it is functioning depending on the changes of fluid properties (James, et al., 2017). It is functioning by directing different fluids to different pathways depending on the properties of fluids.

Important fluids properties for the AICD to operate are density, viscosity and flow rate. The inertial forces are created by densities and flow rates of the flowing fluids, whereas viscosities and flow rates create the viscous forces. AICD is working by balancing inertia and Viscous forces in the fluids.

The flow of fluid is shown in Figure 2-17 c, the fluid enters the AICD through the entrance and leave the AICD through the hole in the centre of vortex bowl, then pass through the production tubing to the surface. As shown in Figure 2-17 a and b the flowing pathways depend on inertial forces and viscous forces, when viscous forces dominate, the fluids will pass to straight pathway and divergence pathway as shown in Figure 2-17 a but when inertial forces dominate, the fluids will path on straight path only as shown in Figure 2-17 b.

For oil, viscous forces dominate so oil is flowing in both straight and divergence path and AICD is set such that fluid which passes in both pathways will leave the AICD through the exit to the surface while fluid which passes in straight pass only will continue rotating in the AICD and being restricted to leave AICD. As the viscosity of the fluid increases, most of the fluid will pass through the divergence pathway hence reduce spinning of the vortex bowl and allowing more fluid to pass through the exit.

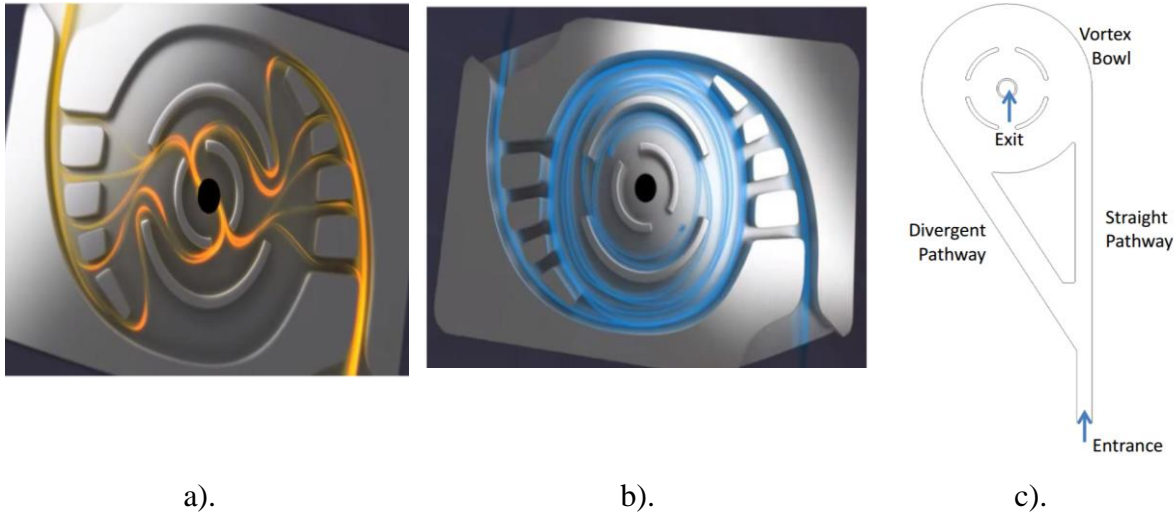


Figure 2-17: Fluidic diode type AICD. (a) Is the streamline for oil flow and (b) is the streamline for water and (c) Simplified model of AICD (James,et al., 2017; Fripp, et al., 2013)

Pressure drop through the Fluidic diode type AICDs

Halliburton developed the model explained the pressure drop of fluid flowing across the EquiFlow AICD. The pressure drop across the fluidic diode type AICDs can be given by the equation (19) (James, et al., 2017).

$$\Delta P = \frac{8K\rho_{\text{mix}}Q^2}{\pi^2 n^2 D_h^4} \quad (19)$$

2.4.3.3 RCP-AICD

Figure 2-18 shows the RCP-AICD, another kind of AICD used to restrict fluids of low viscous fluid such as water and gas. The AICD uses the Bernoulli principle which is expressed in equation (20). The low viscosity fluid is passing through AICD with the higher speed than high viscous fluid. The higher speed of fluid causes the pressure at the flowing side of the disc to be lower compared against the pressure on the other side of the disc (Stagnant pressure). The pressure difference on these two sides causes the disc to move towards the seats and reduce the flowing area. When the flowing area is reduced the unwanted fluid production (gas and water) will also be reduced. The flowing speed of the highly viscous fluid (oil) is low, so the pressure difference between two sides is not high enough to reduce the flow area and the oil production (Halvorsen, et al., 2012).

$$P_1 + \frac{\rho v_1^2}{2} = P_2 + \frac{\rho v_2^2}{2} + \Delta P_{\text{friction}} \quad (20)$$

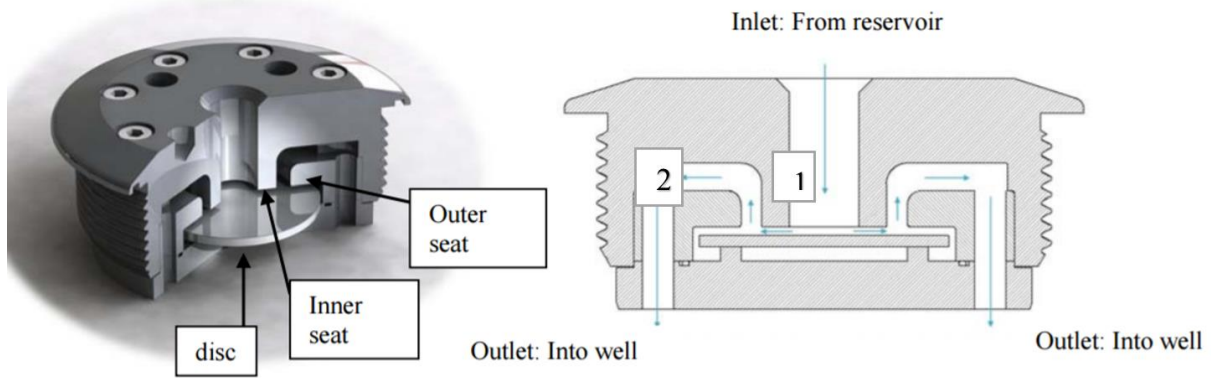


Figure 2-18: RCP valve (AICDs) (Halvorsen, et al., 2012)

Main parts of RCP-AICD

The RCP-AICDs contain three parts as shown in figure 2-18, which are:

- a) Outer seat
- b) Inner seat and
- c) Disc

Outer seat and inner seat create the flow path of fluid passing through the AICD whereas the disc is used to control the amount fluid passing through the production choke.

The pressure drop across the RCP-AICDs

When AICD is installed in the wellbore, the pressure drop of fluid passing through the AICD will depend on the density and viscosity of that fluid as shown in equation (21).

$$\Delta P = \left(\frac{\rho_{\text{mix}}}{\rho_{\text{cal}}} \right) * \left(\frac{\mu_{\text{cal}}}{\mu_{\text{mix}}} \right)^y * \rho_{\text{mix}} * K * q^2 \quad (21)$$

Where,

K is the base strength of the AICD, with a dimension of inverse area squared, and defined as:

$$K = a_{\text{AICD}} * q^{x-2}$$

Where, a_{AICD} is defined as the strength of the AICD

$$\mu_{\text{mix}} = \alpha_o \mu_o + \alpha_g \mu_g + \alpha_w \mu_w$$

$$\rho_{\text{mix}} = \rho_o \mu_o + \rho_g \mu_g + \rho_w \mu_w$$

2.4.3.4 Advantage and disadvantage of AICDs

There are many benefits of AICDs including facilitation of oil recovery, maximizing oil recovery, and reducing unwanted fluid production (delay water and gas production). These advantages were proved in different fields, including Ecuador, where the WC decreased by 34% and oil recovery increased by 16% and the UAE where the WC decreased by 47% and oil production increased by 400% after installation of EquiFlow-AICDs in the horizontal well (Halliburton, 2017). Also, installation of RCP-Valves in the Troll fields resulted in reduction of the GOR and increasing the cumulative oil recovery by 20% higher compared to passive ICDs ((Halvorsen, et al., 2012); (Halvorsen, et al., 2016)).

The main disadvantages of AICDs are: some type of AICD like ER-AICD are not working in the high temperature environment since they consist electronics devices and valves which are affected by temperature. Also, the installation of AICDs in the well with small pressure loss from the toe to the heel may lead to lower oil recovery compared to open hole (Jadhav, et al., 2017).

2.5 Autonomous Inflow control Valve (AICV)

The AICV is the special type of AICD with the ability to stop completely the inflow of unwanted fluid in the wellbore from the reservoir segment which reached the targeted amount of unwanted fluid (targeted water cut). Figure 2-19 shows the cross section view of AICV, the AICV was developed for the purpose of combining the benefits of AICDs and ICDs. The same to AICD, AICV is operated autonomously. It is used to equalize the inflow of fluid flowing to the wellbore, prevent unwanted fluid inflow into the wellbore and shut off the valve when unwanted fluid exceeding the specified amount (for example WC of 95%).

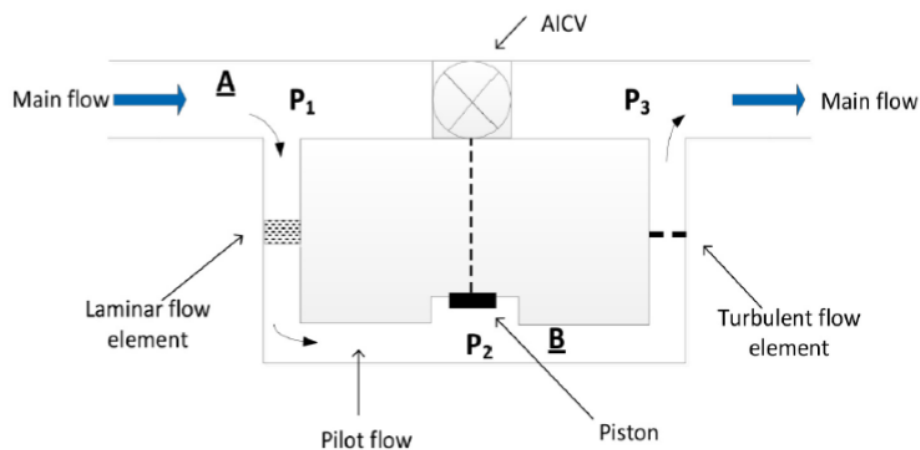


Figure 2-19: Cross section view of AICV (Nugraha, et al., 2016)

There are two flow paths in the AICV, pilot flow path, and main flow path. When fluid is passing through the AICV most of the fluid is passing through the main flow path and about 1% of the total flow is passing through the pilot path, both paths end in the outlet of the valve. The pilot path contains piston which is sensitive to pressure and is used to shut off liquid flow in the main flow path. As shown in Figure 2-19 in the pilot flow path there is laminar flow and turbulent flow elements. Pressure drop in the laminar flow element depends on the viscosity of fluid as shown in equation (22), when fluid with high viscosity (Heavy oil) is passing through the pilot flow path will be choked in laminar flow element resulting to lower pressure (P_2) in the fluid passing through the piston which will not be enough to trigger the piston (Figure 2-19). When low viscous fluid is passing through the laminar flow element will not be choked, hence fluid with enough pressure will flow and trigger the piston and shut off fluid inflow completely in the main flow. When fluid with high viscosity re-enters the valve, the main flow path will re-open. So AICV is a self-regulating and reversible valve. The pressure variations for fluids passing through the AICV is shown in Figure 2-20.

The pressure drop through the laminar flow element can be found using equation (22)

$$\Delta P = \frac{32 \cdot \mu \cdot v \cdot L}{D^2} \quad (22)$$

The pressure drop through the turbulent flow element can be found using equation (23)

$$\Delta P = C * \frac{1}{2} \rho v^2 \quad (23)$$

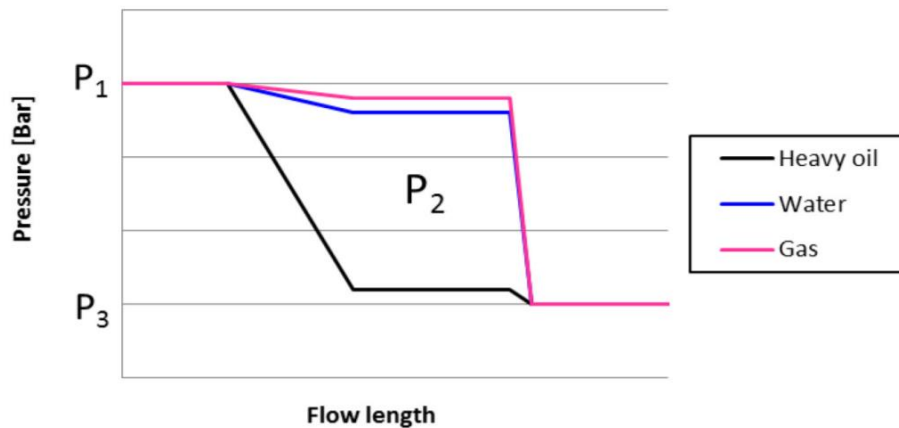


Figure 2-20: Pressures in the AICV (Mathiesen, et al., 2013)

2.5.1 Forces on the AICV

As shown in Figure 2-21 there are different kind forces acting on the AICV, The force F_1 ($P_1 \cdot A_1$) is the force caused by pressure P_1 at the upper part of piston acting downward, force F_2 ($P_2 \cdot A_2$) caused by pressure P_2 at the lower part of the piston acting upward. Also, there is friction force (F_r) acting in the opposite direction of the movement and F_3 acting on the outer part of the piston downward. The net force can be found as $F_1 - F_2 + F_3 \pm F_r$. When the net force is positive the piston will move in the open direction and when the net force is negative the piston will close the main flow.

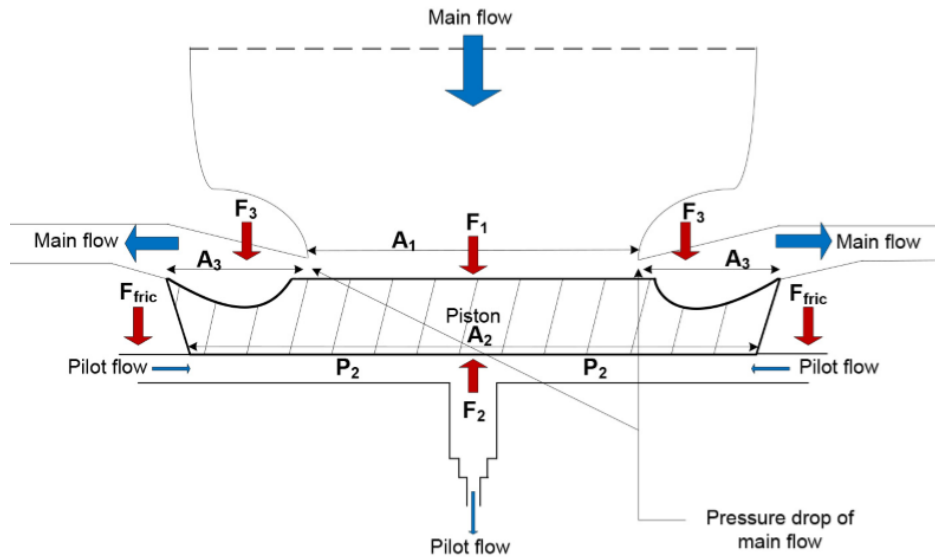


Figure 2-21: Forces acting on the AICV (Nugraha, et al., 2016)

2.5.2 The AICV features

There are several features of AICV such as:

- a) AICV is operated autonomous, that it is not controlled from the surface.
- b) It is simple with low risk of failure,
- c) It has the ability to shut off unwanted fluid (water and gas) completely.
- d) It is reversible when oil re-enters the valve it will open again.
- e) It can be installed in a new or old wells
- f) And it can be adjusted depending on a reservoir or fluid properties.

2.5.3 The advantage of AICVs

The AICV technologies have the advantage of increasing the chance of drilling the longer horizontal well, which leads to significant increase in oil production. Also, this technology reduces the unwanted (water and gas) fluid production, hence reducing the cost of handling them (separation and transportation). These advantages are proved by new research done by Elverhoy and his fellows in 2018, they modelled the horizontal well in the reservoir by the NETool simulator. The case which a reservoir containing a fluid with the viscosity of 10 cp showed that the installation of AICVs on the horizontal well resulted to the increase of the oil production from 22 sm³/d for the open hole to 38% and reduction of WC from 80% to 55%. Another case was done in the reservoir containing a fluid with the viscosity of 2 cp, where the installation of AICVs in the horizontal well reduced WC from 60% for the open hole to 29%,

this reduction is higher than the ICDs installation which reduced the WC from 60% to 52%. In this case, the AICVs installation increased the oil production by 75% (Elverhoy, et al., 2018).

2.6 Factors affecting the horizontal well completion

The success of well completion depends on many factors, including differences in reservoir permeability, the presence of fractures in the reservoir, differential pressure system in the pores, the closeness of water and gas contact, the properties of fluids and the kind DFC (Akbari, et al., 2014). The decision on the number of DFCs will depend on these factors. If the reservoir contains sections of different permeability, a decision can be to install at least one DFC on each section with a packer to separate the sections.

Reservoir sections with fractures have higher permeability than the sections which do not have a fracture, so DFCs are installed in the fracture to regulate the inflow with non-fracture sections. Also, there are pores with higher pressure than others, DFCs are installed to create a pressure drop in order to balance the pressure among all pores. The closeness of water and gas contact create a thin layer of oil. The thin layer of oil experience a gas and water coning, to overcome this problem DFCs are installed. DFCs reduce the flow rate which causes the GOC and WOC to move slowly and reduce the coning effect.

Completion design type also can affect the well completion, tailored design is the one which ICDs of different size/strength are recommended in the wellbore. During the installation period, ICDs can miss the target depth (TD), misplacement of ICDs can cause earlier water breakthrough. This situation is more likely to happen due to complications happening in the wellbore due to the tight hole, collapsed formation and hole stability problems. Due to this problem uniform design is recommended, in this design ICDs of the same size is recommended to be installed throughout the wellbore (Torbergsen, 2010). According to Al-Khelaiwi, (2013) the simulation results of the horizontal well completed with ICDs of different size didn't differ much compared to when a horizontal well is completed with ICDs of the same size.

There are several kinds of DFCs including ICDs, AICDs, ICVs and AICVs which react differently in the wellbore, there are those which provide friction and others which create resistance, so the well completion will depend on the type of DFCs. The successful completion is expected to increase the oil recovery and reduce water production.

2.7 The underlying aquifer/ Natural water drive

The aquifer is one among the drive mechanisms of the oil reservoir, other including the gas cap drive, solution gas drive, and compaction drive (Dake, 1998). The aquifer helps to maintain the reservoir pressure when the oil is produced, when the oil is produced the reservoir pressure is depleting causing the aquifer rock to compress, water in the aquifer to expand and overflow in the oil reservoir. The water helps to push oil to the production wells and hence increasing the oil recovery.

The ability of aquifer/water influx to improve the oil recovery depends on the size of the connection of the aquifer to the oil reservoir, the degree of aquifer and oil reservoir communication, and the amount of water that intrudes into the oil reservoir.

2.7.1 Water influx

The water influx (W_e) can be found by using equation (24), the sum of the pore compressibility (c_w) and fluid compressibility (c_f) is very small in magnitude (10^{-5} /Psia), so for the small aquifer, the effect of water influx is negligible. Equation (24) is valid when the initial water in place (W_i) is of the same magnitude as the reservoir since when the aquifer is very large there will be a time lag between the pressure drop in the reservoir and the changes in the aquifer. The changes in the aquifer are time dependent, this means when the reservoir is producing at a high rate the response of the aquifer will be small, which causes its effect to be small in the production of oil (Dake, 1998).

Another important parameter in the aquifer is permeability. Permeability is the ability of a porous rock to allow fluid to flow through it, permeability is supposed to be high enough to allow water influx to move to the reservoir, otherwise large pressure differential is required. When the permeability is very low the effect of the aquifer will be ignored (Ahmed, 2005).

$$W_e = (c_w + c_f)W_i\Delta P \quad (24)$$

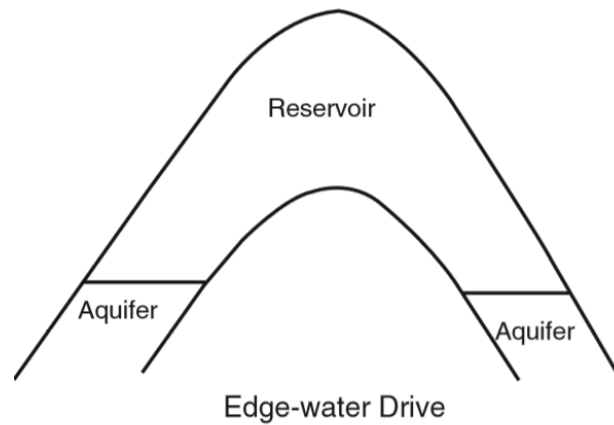
2.7.2 Classifications of aquifer

The aquifer can be classified based on many factors, including the location of the aquifer from the reservoir, the strength of the aquifer, flow geometries and flow regimes.

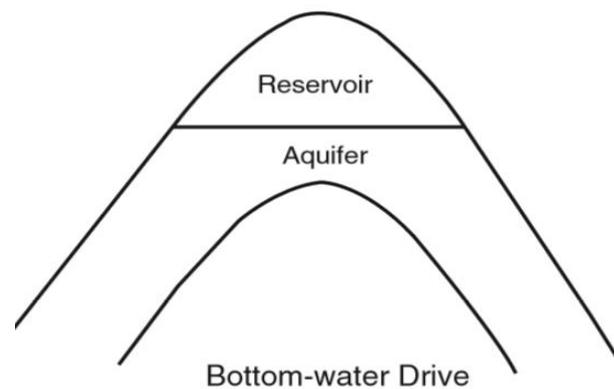
- a) The strength of the aquifer is the measure of how the aquifer diminishes the pressure drop in the reservoir. There are three types of aquifer based on its strength, namely strong aquifer/active water drive, partial aquifer/partial water drive, and weak aquifer. The strong

aquifer is the one which water influx is equal to the reservoir fluid withdraw whereas in the partial and weak aquifer the water influx is less than the reservoir fluids withdraw.

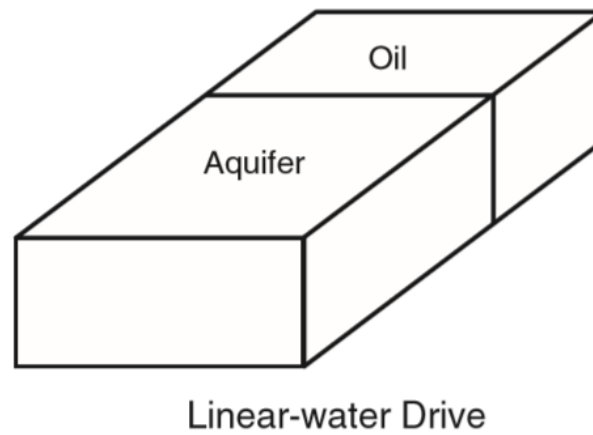
- b) Linear water drive, Edgewater drive, and bottom water drive are types of aquifer based on the location from the reservoir (Figure 2-22). Linear water drive is the one which the flow of water to the reservoir is linear. Edge water drive is the one which water moves to the edge of the reservoir as a result of oil/fluid production and pressure drop at the reservoir aquifer boundary. Bottom water drive is the large aquifer found underneath the reservoir, it is found in a gentle slope reservoir. The flow from this aquifer is radial flow and this aquifer has significant vertical flow.



a).



b).



c).

Figure 2-22: Types of aquifer based on the location from the reservoir (Ahmed, 2005)

- c) There is aquifer which changes in the reservoir cannot be felt in the outer boundary of the aquifer called infinite aquifer and other which changes in the reservoir affect the outer boundary of the aquifer called finite aquifer/finite system.

2.7.3 Aquifer models

Modelling of the aquifer contains many uncertainties since few wells are drilled through the aquifer to get information like porosity, permeability, thickness, and fluid properties, more uncertain arise on the area and geometry of the aquifer.

Several models have been developed to approximate the water influx based on the assumption that describes the properties of the aquifer. These models include pot aquifer, Schilthuis steady state, Hurst modified steady state, van Everdingen and Hurst unsteady state (edge-water drive and bottom water drive), Carter Tracy unsteady state, and Fetkovich method (radial aquifer and linear aquifer) (Ahmed, 2005).

2.7.3.1 The pot aquifer model

This is the model that describes aquifer based on the definition of compressibility. When oil/gas is produced, the pressure drop will be created in the reservoir and will cause water to expand and move into the reservoir. The pot aquifer model can be expressed mathematically by the compressibility equation (25). Equation (25) can be converted to the equation used to find the volume of water influx which is shown in equation (24).

$$c = \frac{1}{V} * \frac{\partial V}{\partial P} = \frac{1}{V} * \frac{\Delta V}{\Delta P} \quad (25)$$

Where c is the compressibility, v is the initial volume in place, ΔV is the volume change, and ΔP is the pressure drop in the reservoir.

2.7.3.2 The Schilthuis steady state model

This model is for the aquifer that is flowing under steady flow condition, the rate of water influx can be expressed by Darcy's equation (26), whereby C_w is rate of water influx (bbl/day), k is permeability of the aquifer (md), h is thickness of the aquifer (ft), r_a is the radius of the aquifer (ft), r_e is radius of the reservoir (ft), t is the time (days), W_e is the cumulative water influx (bbl), p_i is the initial reservoir pressure (psi), and p is the pressure at the oil water contact at time t (psi).

$$\frac{dW}{dt} = c_w = \left[\frac{0.00708kh}{(\mu_w \ln(\frac{r_a}{r_e}))} \right] (p_i - p) \quad (26)$$

2.7.3.3 The Hurst modified steady-state equation

This model is the modification of the Schilthuis steady-state model, it was modified by Hurst in 1943. The model considers the increase of (r_a) as the time increases when the aquifer is drained. This means the ratio of radius ($\frac{r_a}{r_e}$) will be time dependent. Based on this model the cumulative water influx (W_e) can be found by using equation (27), where constant (C) and (a) can be found graphically from slope and y-intercept respectively as shown in figure 2-23.

$$W_e = C \sum_0^t \left[\frac{\Delta P}{\ln(at)} \right] \Delta t \quad (27)$$

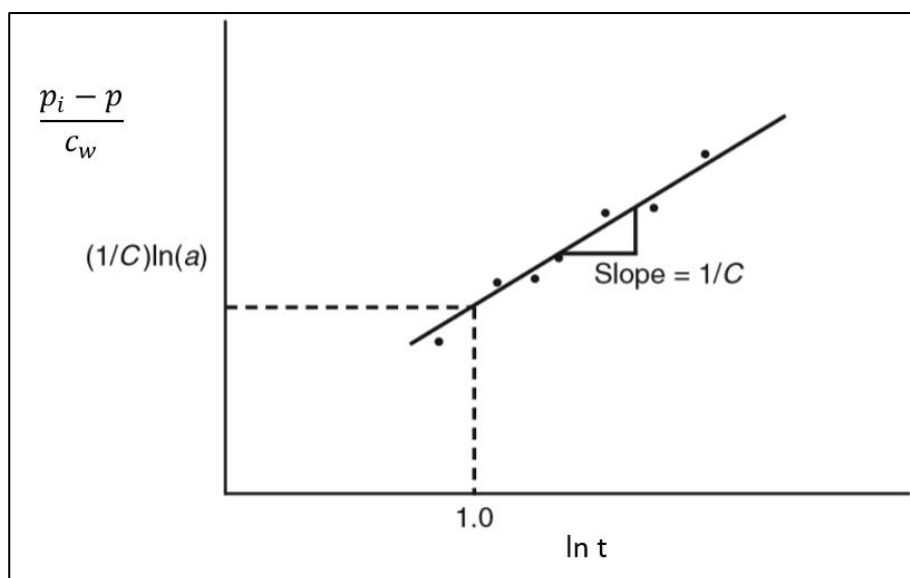


Figure 2-23: Determination of constant C and a graphically (Ahmed, 2005)

2.7.3.4 The van Everdingen and Hurst unsteady-state model

This model is designed based on the transient flowing condition and the pressure drop can be modelled by dimensionless diffusivity equation (28). This equation can be solved by Laplace transformation and can be used to find the water influx in a system, including edge-water drive system (radial system), bottom water drive system, and linear water drive system. The pressure drop designed in this model can be used to find water influx given by equation (29) (for linear water drive).

$$\frac{\partial^2 P_D}{\partial r_D^2} + \frac{1}{r_D} \frac{\partial P_D}{\partial r_D} = \frac{\partial P_D}{\partial t_D} \quad (28)$$

$$W_e = B_L \sum [\Delta P_n \sqrt{t - t_n}] \quad (29)$$

2.7.3.5 The Carter and Tracy water influx model

This model assumes there is a constant water influx rate over each finite time interval, this model does not need the use of superposition. The cumulative water influx at any time can be found directly from the previous time as shown in equation (30). Where B is the van Everdingen and Hurst water influx constant as defined by Equation (31), t_D is the dimensionless time as defined by Equation (33), n is the current time step, n - 1 is the previous time step, ΔP_n is total pressure drop ($P_i - P_n$) in psi, P_D is the dimensionless pressure, P_D' is the dimensionless pressure derivative.

$$(W_e)_n = (W_e)_{n-1} + [(t_D)_n - (t_D)_{n-1}] * \left[\frac{B \Delta P_n - (W_e)_{n-1} (P_D')_n}{(P_D)_n - (t_D)_{n-1} (P_D')_n} \right] \quad (30)$$

$$B = 1.119 \phi c_t r_e^2 h \quad (31)$$

$$P_D = \frac{370.529\sqrt{t_D} + 137.582t_D + 5.695(t_D)^{1.5}}{328.834 + 265.488\sqrt{t_D} + 45.2157t_D + (t_D)^{1.5}} \quad (32)$$

$$t_D = 6.328 * 10^{-3} \frac{kt}{\phi \mu_w c_t r_e^2} \quad (33)$$

The dimensionless pressure derivative can be approximated by using equation (34).

$$P_D' = \frac{E}{F} \quad (34)$$

Whereas,

$$E = 716.441 + 46.7984(t_D)^{0.5} + 270.038t_D + 71.0098(t_D)^{1.5}$$

$$F = 1296.86(t_D)^{0.5} + 1204.73t_D + 618.618(t_D)^{1.5} + 538.072(t_D)^2 + 142.41(t_D)^{2.5}$$

For dimensionless time greater than 100 the P_D and P_D' can be found using equation (35) and (36) respectively.

$$P_D = \frac{1}{2}[\ln(t_D) + 0.80907] \quad (35)$$

$$P_D' = \frac{1}{2t_D} \quad (36)$$

2.7.3.6 The Fetkovich model

This model is applicable to finite aquifer of radial and linear geometry. Water influx in this model is found based on the productivity index, hence the water influx is proportional to the pressure drop. The Fetkovich theory is as simple as the Carter–Tracy technique. In this theory, the transient period is not considered, but still producing excellent results compared to the methods discussed above.

In the Fetkovich model, the incremental water influx can be found using the equation (37).

$$(\Delta W_e)_n = \frac{W_{ei}}{p_i} [(\bar{p}_a)_{n-1} - (\bar{p}_r)_n][1 - \exp(-\frac{Jp_i\Delta t_n}{W_{ei}})] \quad (37)$$

Where $(\bar{p}_a)_{n-1}$ is the average aquifer pressure at the end of the previous time step and $(\bar{p}_r)_n$ is the average reservoir boundary pressure which are found by using equation (38) and (39) respectively.

$$(\bar{p}_a)_{n-1} = p_i(1 - \frac{(W_e)_{n-1}}{W_{ei}}) \quad (38)$$

$$(\bar{p}_r)_n = \frac{(\bar{p}_r)_n + (\bar{p}_r)_{n-1}}{2} \quad (39)$$

3 ADVANCED WELL COMPLETIONS

3.1 Introduction

This part covers all the methods which were used in this Thesis to attain the objectives of the Thesis. Several issues were covered in this chapter, including The reservoir modelling, Modelling of DFCs, Results, and Discussions.

3.2 The reservoir modelling

The reservoir was modelled by using Eclipse simulator, the reservoir contained 20 blocks horizontal in the x-direction, 20 blocks horizontal in the y-direction and 10 layers in the z-direction (3 layer with oil and 3 layer with aquifer as shown in Figure 3-1 while other four layer which were not assigned oil or aquifer and are not shown in the figure). Each block had a length of 500 ft in the x-direction, 50 ft in the y-direction, and thickness of 50 ft (z-direction) as shown in Figure 3-1. The reservoir contained the oil layer, the aquifer, and the horizontal oil well (PRODUCER on Figure 3-1) which perforated in 15 grid blocks, and with the horizontal length of 7500 ft.

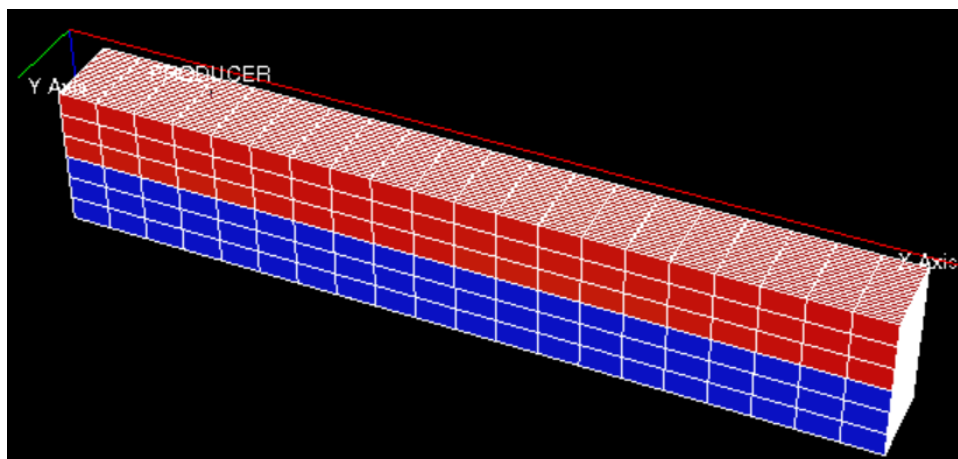


Figure 3-1: Horizontal well perforating in the oil reservoir

3.2.1 The Reservoir properties

The reservoir models used in this Thesis were divided into two groups, heterogeneous reservoir models and homogeneous reservoir model. In the heterogeneous reservoir models, the reservoir was divided horizontally into four zones with a permeability of 5000 mD, 500 mD, 3000 mD, and 1000 mD as shown in Figure 3-2. In the homogeneous reservoir, the reservoir permeability was set to permeability of 2000 mD throughout the reservoir. The reservoir also had a porosity of 0.3 and rock compressibility of $2.0E-5$ /psia.

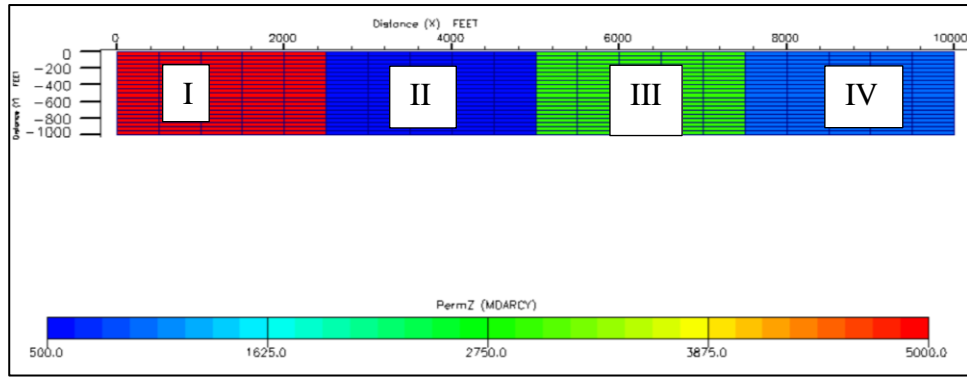


Figure 3-2: Permeability in the heterogeneous reservoir along the x-direction

3.2.2 The reservoir fluids (PVT data on Eclipse simulator)

The reservoir models were designed with two kinds of fluids, oil and water. When the reservoir is producing the reservoir pressure decrease and the oil starts to form the gas, so the properties of gas were also defined. Table 3-1 shows common fluid properties which were used in all reservoir models.

Table 3-1: Fluids properties found in the reservoir models

Fluid properties	Density of light oil at surface conditions (lbm/ft ³)	54.29
	Density of heavy oil at surface conditions (lbm/ft ³)	60.53
	Density of gas at surface conditions (lbm/ft ³)	0.06054
	Density of water at surface conditions (lbm/ft ³)	64.79
	Initial reservoir pressure (Psia)	5000
	Bubble point pressure (Psia)	4014.7
	Minimum BHP (Psia)	1000
	Reservoir temperature (°C)	60

The fluid properties showing in Table 3-1 were used to develop other reservoir fluid properties which depend on the reservoir conditions (P, T) and fluid densities, those properties include solution gas-oil ratio (Rs), viscosity of oil (μ_o), formation volume factor (B_o), viscosity of gas

(μ_g), and formation volume factor of gas (B_g). When the reservoir is depleted these parameters are also changing so in this section the variations of these parameters with pressure will be shown.

3.2.2.1 Solution gas oil ratio (R_s)

Solution GOR is defined as the amount of gas that dissolves in the reservoir oil (in standard conditions), the value of R_s depends on the density of gas and oil at surface conditions and the pressure and temperature in the reservoir. In this work equation (40) suggested in Guo, 2016 was used to model R_s and Figure 3-3 and Figure 3-4 show the value of R_s found at various reservoir pressures and the reservoir temperature of 60 °C which was used in the reservoir models for heavy and light oil respectively.

$$R_s = \gamma_g * \left[\frac{P}{18} * \frac{10^{0.0125(API)}}{10^{0.00091T}} \right]^{1.2048} \quad (\text{field units}) \quad (40)$$

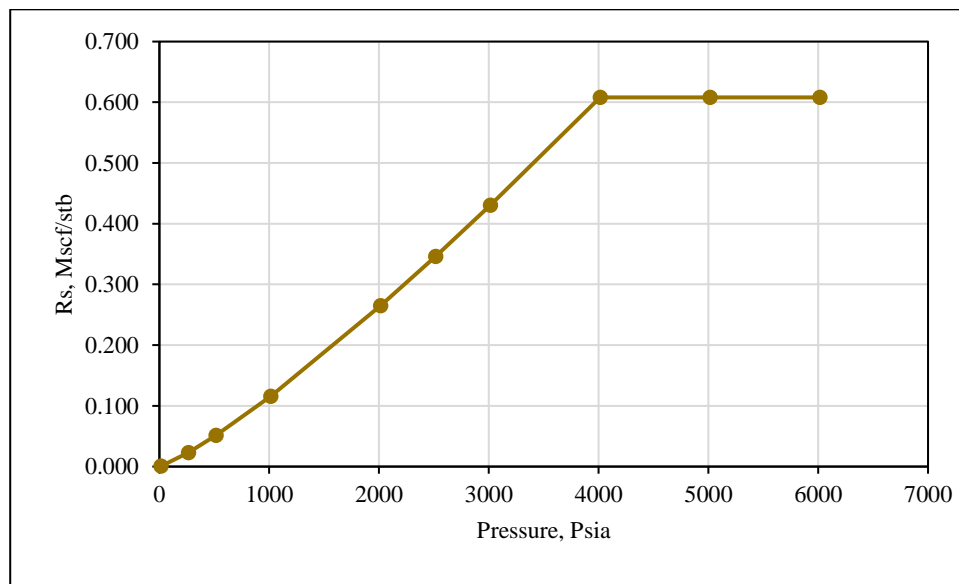


Figure 3-3: Solution GOR for heavy oil reservoir models

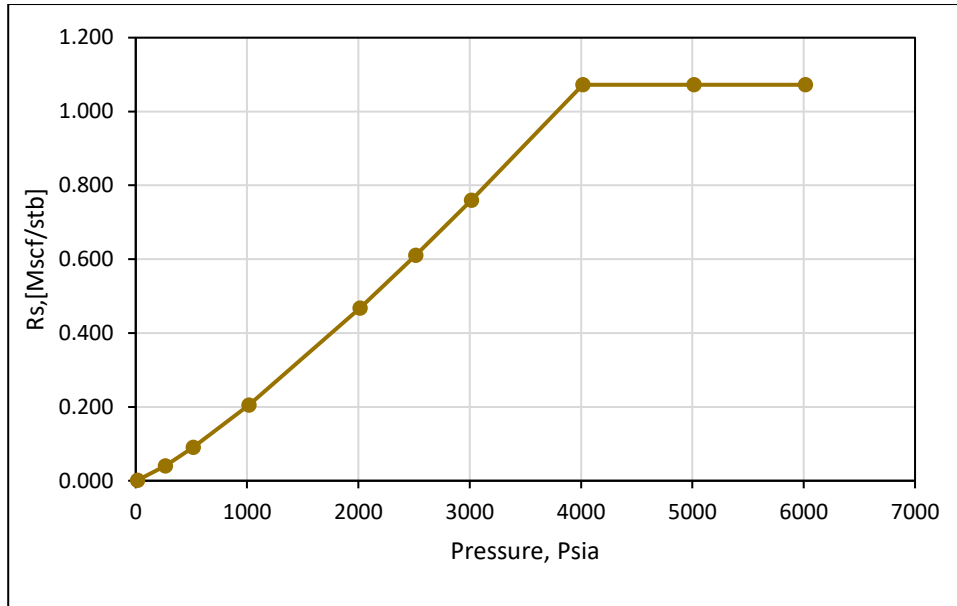


Figure 3-4: Solution GOR for low viscous oil reservoir models

3.2.2.2 Viscosity of oil

The viscosity is the resistance of a oil to flow. The viscosity is measured in the laboratory, but during modelling there are various correlations which can be used to model the oil viscosity. In this work Standing correlation as shown by equation (41) and (42) were used to model the oil viscosity at various pressures and at the reservoir temperature of 60 °C for saturated oil and unsaturated oil respectively, the constants (a, b and μ_{od}) are defined in Appendix 1 (Guo, 2016).

$$\mu_{ob} = 10^a * \mu_{od}^b \quad (\text{field units}) \quad (41)$$

$$\mu_o = \mu_{od} + 0.001(P - P_b)(0.024\mu_{od}^{1.6} + 0.38\mu_{od}^{0.56}) \quad (\text{field units}) \quad (42)$$

Where μ_{od} is the viscosity of dead oil (cp), μ_{ob} is the viscosity of the saturated oil and μ_o is the viscosity of the unsaturated oil.

The viscosity of oil in the reservoir found by using equation (41) and (42) were changing with pressure as shown in Figure 3-5 and Figure 3-6 for the heavy oil reservoir and light oil reservoirs respectively.

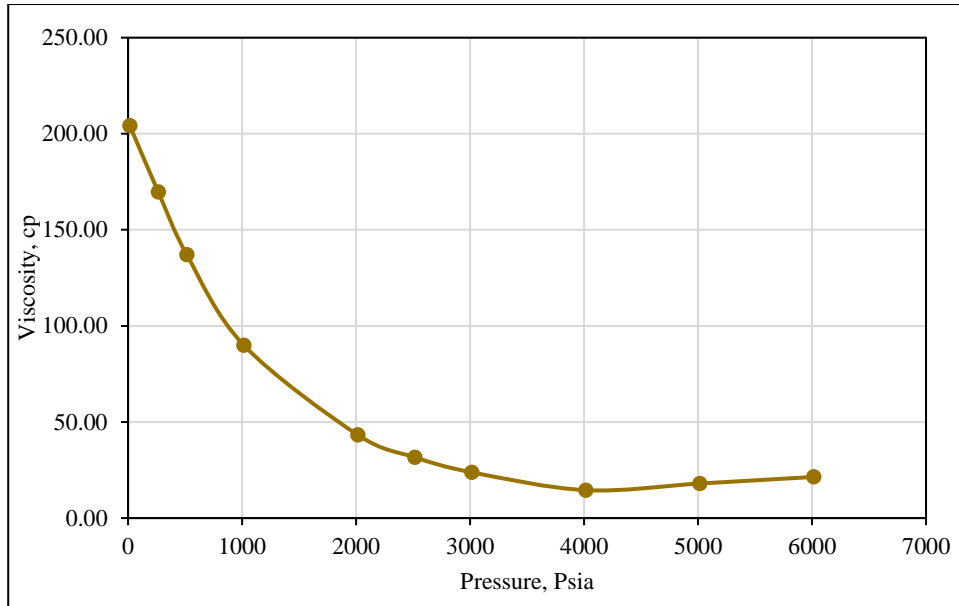


Figure 3-5: Variation of the viscosity of oil with the pressure in the heavy oil reservoir models

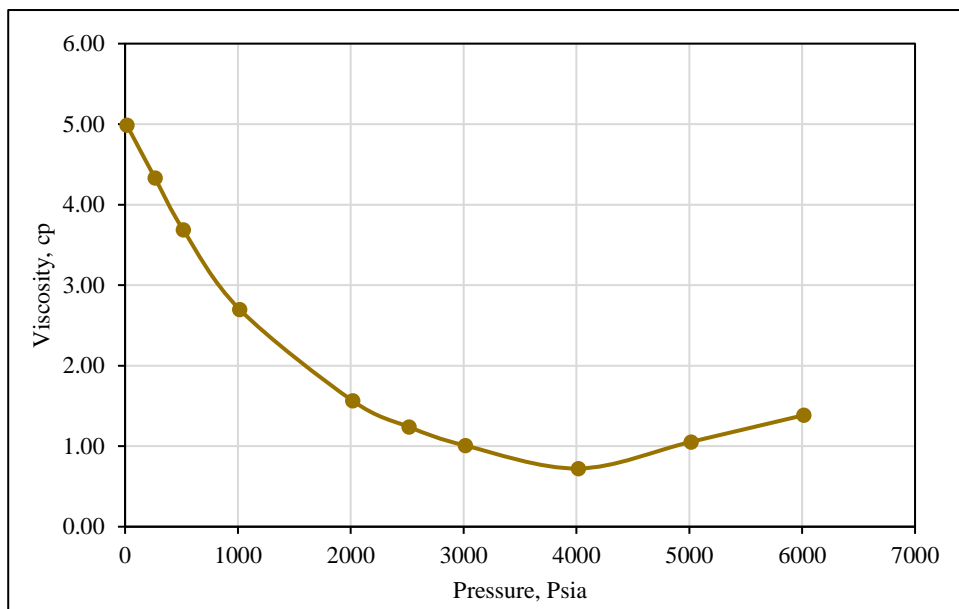


Figure 3-6: Variation of the viscosity of oil with the pressure in the low viscous oil reservoir models

3.2.2.3 Formation volume factor of oil (B_o)

Formation volume factor of oil (B_o) is the ratio of the volume of oil in the reservoir to the volume of oil in the surface. The value of B_o depends on the specific gravity of gas and oil as shown by standing correlation in equation (43) and (44) for B_o below saturation pressure and above saturation pressure respectively which were used to model B_o in this work.

$$B_o = c_B + 0.952 \cdot 10^{-3} \left(\left(\frac{\gamma_g}{\gamma_o} \right)^{0.5} R_s + 0.401 T - 103 \right)^{1.2} \quad (\text{SI units}) \quad (43)$$

Where $c_B = 0.972$

$$B_o = B_{ob} e^{-c(p-p_b)} \quad (\text{SI units}) \quad (44)$$

The variation of B_o and pressure in the heavy oil and low viscous oil reservoir models are shown in Figure 7-1 and Figure 7-2 in Appendix 1.

3.2.2.4 The viscosity of gas (μ_g) and formation volume factor of gas (B_g)

The gas viscosity is the resistance of gas to flow, in many laboratories gas viscosity is approximated by using correlations such as Carr et al. correlation, Lee-Gonzalez gas viscosity correlation, and Dempsey correlation since they do not have the equipment to measure it. In this work the viscosity of gas was modelled by using the Lee-Gonzalez gas viscosity correlation as showing in equation (45) since it is a more effective correlation with the accuracy of 2 to 4% for specific gravity of gas (γ_g) less than 1 and is used by most PVT laboratories, whereby M_g is molecular weight, μ_g is the viscosity of gas in cp, ρ_g is the gas density in g/cm^3 , and T is the temperature in °R (Whitson & Brule, 2000).

$$\mu_g = A_1 * 10^{-4} \exp(A_2 \rho_g^{A_3}) \quad (45)$$

$$\text{Where } A_1 = \frac{(9.379 + 0.01607 M_g) T^{1.5}}{209.2 + 19.26 M_g + T},$$

$$A_2 = 3.448 + \frac{986.4}{T} + 0.01009 M_g,$$

$$\text{and } A_3 = 2.447 - 0.2224 A_2.$$

Formation volume factor of gas (B_g) is the ratio of the volume of gas in the reservoir to the volume of gas at the surface, In this work, the B_g was modelled by using equation (46) which was derived from the ideal gas equation.

$$B_g = \frac{0.02827(ZT)}{p} \quad (\text{field units}) \quad (46)$$

The variation of the gas viscosity and the formation volume factor of gas with a pressure which were found by using equation (45) and equation respectively are showing in Figure 3-7 and Figure 3-8. These parameters were used as PVT data in the reservoir model.

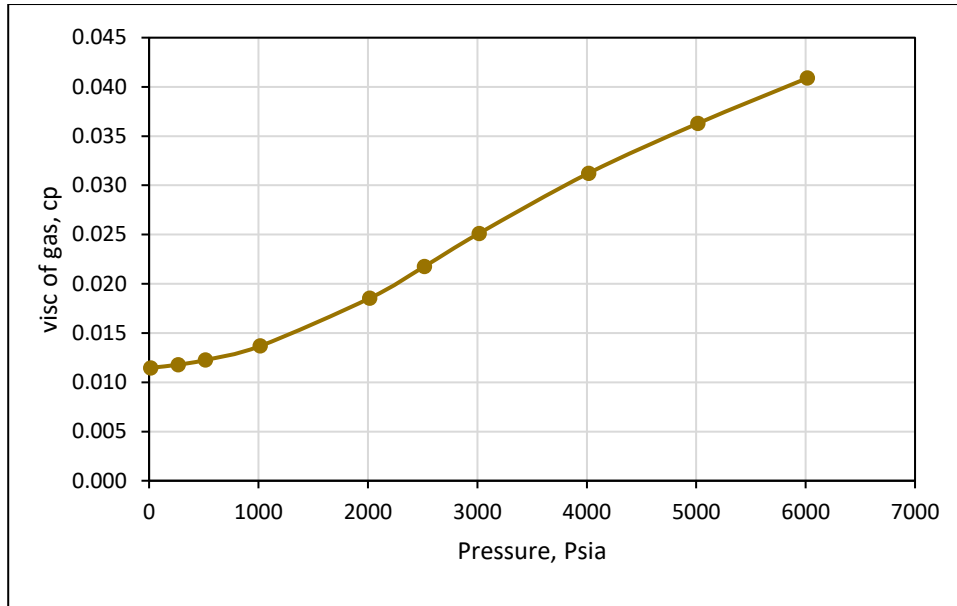


Figure 3-7: Variation of the viscosity of gas (μ_g) with the pressure in the reservoir

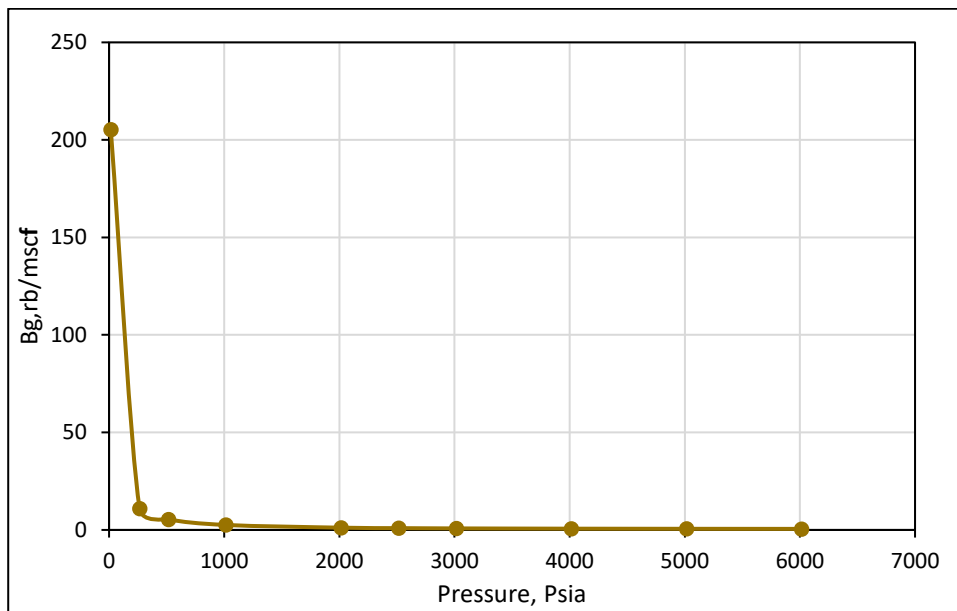


Figure 3-8: Variation of the formation volume factor of gas (B_g) with the pressure in the reservoir

3.2.3 Reservoir models used in this Thesis

The study of Autonomous ICDs was done in four reservoir models which represent the majority of oil fields present in the world, those models were different depending on the properties of the reservoir, fluid properties, and the thickness of the oil layer as shown in Table 3-2. Model 1 represented the heterogeneous reservoir comprised with heavy oil, model 2 represented the

heterogeneous reservoir with a thin layer of oil, model 3 represented heterogeneous reservoir with a low viscosity fluid (oil), and the model 4 represents a homogenous reservoir with the heavy oil.

Table 3-2: Reservoir models used

Reservoir model	1	2	3	4
Reservoir type	Heterogeneous reservoir	Heterogeneous reservoir	Heterogeneous reservoir	Homogeneous reservoir
Oil viscosity[cP] at pressure of 1000 Psia	90	90	2.7	90
Oil thickness [ft]	150	100	150	150

3.2.4 The Aquifer

In order to maintain the reservoir pressure when oil is produced, the reservoir needed to be supported by the strong aquifer. The presence of the aquifer has helped to increase the oil production since water from the aquifer push the water to the production well. The reservoir was modeled with the fetkovich aquifer model with a volume of 2.0E13 ft³. The fetkovich model was selected since it has a property of approaching a pseudo steady-state condition quickly in the aquifer and the pressure felt uniform throughout the reservoir (Schlumberger, 2015).

3.3 Modelling of DFCs

The fluid flowing from the reservoir to the wellbore experiencing two kinds of pressure losses, pressure losses in the reservoir (ΔP_r), and frictional pressure losses in the wellbore (ΔP_f). The DFCs were introduced in the wellbore as shown in Figure 3-9 to add an extra pressure drop (ΔP_{ICD}) in the zones with low total pressure drop so as to balance the inflow in the wellbore.

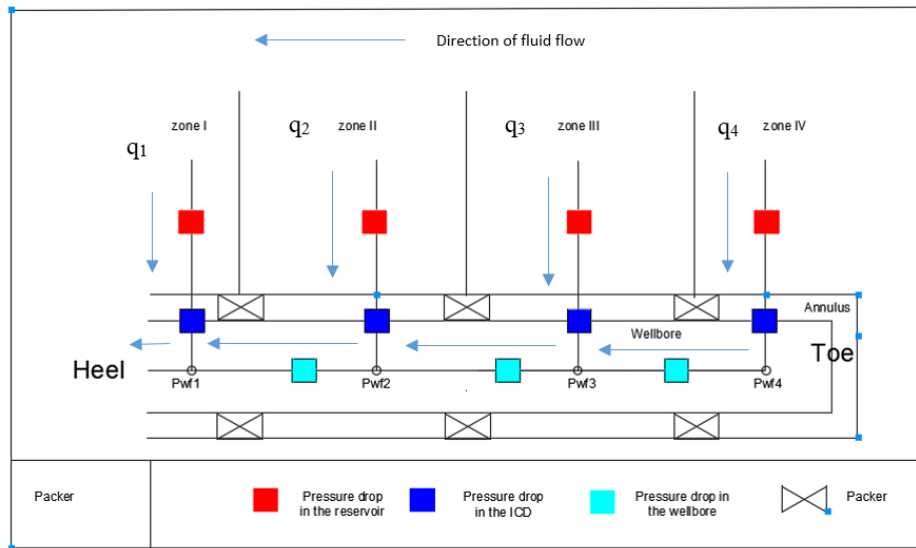


Figure 3-9: Sketch of the reservoir model which shows the pressure losses from the reservoir to the wellbore

The modelling of DFCs in the horizontal well on this work was performed considering the following assumptions:

1. The reservoir was the undersaturated reservoir, contain only liquids (oil and water).
2. Fluids were incompressible.

3.3.1 The number of DFCs in the horizontal well

In this work, the horizontal well perforated a reservoir in 15 grid blocks and had a horizontal length of 7500 ft from the toe to the heel. According to Iversen, et al., (2017) DFCs are installed at every 40 ft (length of DFC), so the number of DFCs throughout the wellbore were supposed to be 187, but only 15 modified DFCs (one in each block) with the rate given by equation (47) were suggested.

According to Eltahir, et al., (2014) the accuracy of results is increasing when the modified DFCs are used in the Eclipse 100 simulator and their effects are the same to the DFCs (which are suggested according to their length) installed in the wellbore (in the real field).

The main reason for reducing the number of DFCs on this work was that its implementation needed the refinement of grid blocks in the reservoir which increased the number of blocks. But in Eclipse 100 reservoir simulator, many blocks lead to complexity of simulations which is caused by increasing reservoir and well calculations, usually this lead to convergence problems, crashing due to rounding problems, increasing the simulation period and interrupt simulations.

The reduction of the number of DFCs was done by combining the effect of several DFCs to a single equivalent DFC. The modified DFC model had the same results compared to the previous model (Group of DFCs). According to Eltaher, et al., (2014) the inflow through the single modified DFC (q_{DFC}) can be approximated by the equation (47).

$$q_{DFC} = q_{cell} * \frac{L_{DFC}}{L_{tubing}} \quad (47)$$

3.3.2 Modelling of the ICDs

The nozzle ICDs model was designed depending on the reservoir properties, two different approaches were used, for the heterogeneous reservoir and homogeneous reservoir as explained in section 3.3.2.1 and section 3.3.2.2.

3.3.2.1 Modelling of the ICDs in the heterogeneous reservoir

The modelling of the ICDs in the heterogeneous reservoir was influenced by the heterogeneity effect. This is because, between the two factors affecting oil production in the heterogeneous reservoir, which are heel to toe effect and heterogeneity effect, the heterogeneity effect dominates (Marzooqi, et al., 2010). Due to that, the pressure losses in the wellbore were assumed to be very small and they were not included in the calculations. This means the bottom hole pressures were constant (ΔP_{wf1} , ΔP_{wf2} , ΔP_{wf3} , and ΔP_{wf4} were the same).

The ICDs were introduced into the wellbore to add extra pressure drop in the reservoir sections with higher permeability. That section had a higher inflow rate, so the extra pressure drop was added to increase the pressure drop and reduce the inflow rate in order to create even fluid inflow in the wellbore.

The orifice was designed by following the procedures:

1. The size of ICDs was found by equating the ΔP across all sections (zones) as depicted in figure 3-9, ΔP was found by adding pressure losses in the reservoir and pressure losses in the ICD as shown in equation (2).

$$\Delta P = \Delta P_{ICD} + \Delta P_r \quad (48)$$

2. The wellbore at the reservoir section with the lowest permeability (500mD) was open (No ICDs), so the ΔP was equal to pressure losses in the reservoir as shown in equation (49).

$$\Delta P = \Delta P_{rl} \quad (49)$$

3. The orifice size was designed by equating pressure drop in the reservoir section with lowest permeability (ΔP_{rl}) and pressure drop (ΔP) in other sections as shown in equation(50).

$$\Delta P_{rl} = \Delta P_{ICD} + \Delta P_r \quad (50)$$

According to Schlumberger, (2015) the pressure drops across the ICDs can be expressed based on the ICD type. The nozzle ICD was selected since they have good performance in the reservoir which has a large variation in viscosity between water and oil, the pressure drop of the nozzle ICD was found by using equation (51).

$$\Delta P_n = \frac{1}{2} * C_u * \frac{\rho V_c^2}{C_v^2} \quad (51)$$

Where ΔP_n is the pressure drop in the nozzle ICD, ρ is the density of the fluid, V is the velocity of the fluid passing through the nozzle ICD, C_u is the unit conversion factor explained in Table 3-3 and C_v is a dimensionless flow coefficient for the valve.

Table 3-3: Conversion factor (C_u) when finding the pressure drop across the ICDs (Schlumberger, 2015)

Unit system	C_u	Density	Velocity	Pressure
METRIC	1.0E-5	kg/m ³	m/s	bars
FIELD	2.159E-4	lb/ft ³	ft/s	psi
LAB	9.869E-7	gm/cc	cm/s	atm
PVT-M	9.869E-6	kg/m ³	m/s	atm

In the undersaturated oil reservoir, the flow rate in the reservoir can be found from reservoir pressure drop as shown in equation (52). This equation helped to find the pressure drop across the reservoir as shown in equation (53).

$$q = J(P_r - P_{wf}) \quad (52)$$

$$\Delta P_r = \frac{q}{J} \quad (53)$$

Where J is the productivity index for long horizontal well defined in equation (2) (Asheim, 2017)

Equation (50), (51), and (53) were combined to form an equation (54) which was used to find the cross sectional area of the nozzle type ICDs (ft^2). Where k is the permeability (mD) (k_{hl} is the permeability of the reservoir section with lower permeability, and k_{ho} is the permeability of the reservoir in other sections), h is the reservoir thickness (ft), $L_{wl/o}$ is the horizontal well length in section with lower permeability and in other sections (ft), D is the thickness of reservoir (ft) and r_w is the radius of the well (ft), ρ is the fluid density (lbm/ft³), q is the inflow rate (ft³/s), μ is the viscosity of fluid (cP), and B_o is the formation volume factor.

$$A = 5.48e - 8 * \sqrt{\frac{\pi h \rho q B_o}{\mu n^2 \left(\frac{\pi D}{2} + 3h \left(\ln \left(\frac{h}{2\pi r_w} \right) + S \right) \left(\frac{1}{k_{hl} L_{wl}} - \frac{1}{k_{ho} L_{wo}} \right) \right)}} \quad (54)$$

The cross sectional area of the ICDs was found in Excel using equation (54). Table 3-4 shows parameters used to model ICDs (red) and cross sectional areas found after modelling ICDs for reservoir model 1 (black), other results are found in Appendix 9. The diameter of ICDs depend on the length of perforation and permeability of the reservoir in that section.

Table 3-4: The designed diameter and cross sectional area of the ICDs in the reservoir model

1

Sections		I	II	III	IV
	units				
k	[mD]	5000	500	3000	1000
h	[ft]	150			
ρ_o	[lb/ft ³]	60.53			
q_o	[stb/day]	225			
B_o		1.08			
n		4			
μ_o	[cp]	90			
D	[ft]	1000			
L_w	[ft]	1000	2500	2500	1500
r_w	[ft]	0.5			
s		0			
A	[ft ²]	1.24E-04	0.00	1.17E-04	2.62E-04
d	[ft]	1.26E-02	0.00	1.22E-02	1.83E-02

3.3.2.2 Modelling the ICDs in the homogeneous reservoir

The ICDs in the homogeneous reservoir was modelled by equating the pressure drop in the ICD at the location with lower friction pressure losses and the friction pressure losses along the wellbore from the ICD point to the point experiencing higher friction losses as shown in

equation (55), for example the pressure drop in the ICD (installed in the heel) have to be equal to the friction pressure losses along the wellbore from the toe to the heel.

$$\Delta P_{ICD} = \Delta P_{fl} \quad (55)$$

$$\Delta P_{fl} = \frac{1}{2} * f * \frac{\rho v^2}{D} * L \quad (56)$$

The diameter of the nozzle type ICD as the function of distance from the toe was found by equating the friction pressure loss along the wellbore (equation (56)) and the pressure drop in the nozzle ICD (equation (51)), the diameter of nozzle type ICD found is shown in equation (57). Equation (57) depends on the distance from the toe (l), fanning friction factor of the production pipe (f), the diameter of the pipe (D) and the number of nozzles per ICD (n). The equation was valid for nozzle type ICD installed in the long horizontal well with high friction pressure losses.

$$d(l) = \left(\frac{1}{n} * \sqrt{\frac{3D^5}{fl}} \right)^{0.5} \quad (57)$$

Equation (57) can be used for field and SI units.

The parameters used to find the diameter of ICDs were wellbore diameter (D) of 0.5 ft, frictional fanning factor (f) was assumed to be 0.02 and 4 number of nozzles per ICD (n). The diameter of ICDs found by using the equation (57) at different blocks is shown in Table 3-5. The diameter was decreasing from the toe to the heel in order to increase the pressure drop which compensates the frictional pressure losses along the wellbore. This results trend resemble the trend found in Al-Khelaiwi , (2013) for ICDs design in the heel to toe effect.

Table 3-5: The designed diameter and area of the ICDs in the homogeneous reservoir

	d	d	A	Comments
Blocks	[ft]	[mm]	[ft2]	
1	0.08	24	4.91E-03	Heel
2	0.08	24	5.08E-03	
3	0.08	25	5.49E-03	
4	0.09	26	5.73E-03	
5	0.09	27	6.01E-03	
6	0.09	27	6.34E-03	
7	0.09	28	6.72E-03	
8	0.10	29	7.19E-03	

9	0.10	30	7.76E-03	
10	0.10	32	8.50E-03	
11	0.11	33	9.51E-03	
12	0.12	36	1.10E-02	
13	0.13	40	1.34E-02	
14	0.16	47	1.90E-02	
15	open	open	open	Toe

3.3.3 Modelling of AICDs and AICVs

According to Bernoulli's equation, the flow rate exponent for liquid flowing through the nozzle or orifice is 2. ICD and AICV/D were modelled by using equation (58), where the value of base strength (K) for ICD and AICV/D can be found using equation (59).

$$\Delta P = K * \rho * q^2 \quad (58)$$

And,

$$K = \begin{cases} \frac{C_u}{2C_v^2 A_c^2} & \text{ICD} \\ \left(\frac{\rho}{\rho_{cal}}\right) * \left(\frac{\mu_{cal}}{\mu}\right)^y * a_{AICV} & \text{AICV/D} \end{cases} \quad (59)$$

To the author's knowledge, there is no published model for the AICV available in the literature, so the AICV modelling were done based on method developed in Eltaher, et al., (2014). Two main assumptions helping in modelling AICV were:

- The pressure drop across the AICD/AICV is found by using equation (21)
- The performance of AICD/AICV is independent on the fluid flow regime upstream of the AICD/AICVs.

The AICDs and AICVs functions were designed based on the experimental data, which were presented in Mathiesen, et al., (2011) and Mathiesen, et al., (2016). The design was done by tuning RCP function to fit the data. The design of AICDs/AICVs functions was done by following the methods developed in Eltaher, et al., (2014). The model of AICD/AICV was designed depending on the data presented in form of the curves as shown in Figure 3-10 and Figure 3-12 and fluid properties such as viscosities and densities. Equation (58) and (59) were used to find the strength of AICD/AICV ($a_{AICV/D}$) and viscosity function exponent (y) used in the AICD/AICV function.

Below are the procedures suggested by Eltaher, et al., (2014) which were used to find the strength of AICD/AICV ($a_{AICV/D}$) and viscosity function exponent (y) which were used in the AICD/AICV function. These methods were based on the single-phase flow in the devices.

- a) Proper performance curves were selected for water and oil (Figure 3-10 and Figure 3-12), the water was used as the calibration fluid so its curve was selected first in order to find the strength of AICD/AICV ($a_{AICD/V}$).
- b) The pressure drop was found as the function of the flowing rate. The performance curve was digitized with web-tool WebPlotDigitizer to get the numerical values and then the Excel sheet was used to approximate the pressure drop from the flowing rate as shown in Appendix 3, Appendix 4, Appendix 5, and Appendix 6 for AICDs completion in heavy oil reservoir, AICVs completion in heavy oil reservoir, AICDs completion in low viscous oil reservoir, and AICVs completion in low viscous oil reservoir respectively.
- c) After calculating the pressure drop from the water performance curve. The value of K was found by substituting the pressure drop, fluid density and flowing rate of water into equation (58).
- d) For oil/water system the calibration fluid was water. That caused the density and viscosity of the fluid to be equal to density and viscosity of calibration fluid, so the value of K was equal to $a_{AICV/D}$ when all parameters are substituted into equation (59).
- e) From the oil performance curve of AICD/AICV the pressure drop was calculated, then the calculated pressure drop, oil density and flowing rate were substituted into equation (58) to find the value of K. The new value of K, $a_{AICV/D}$, density, and viscosity of oil were substituted into equation (59) to find the viscosity exponent (γ).
- f) When the value of the viscosity function exponent (γ) and constant $a_{AICV/D}$ were found, equation (58) was used in modelling AICD/AICV in the well completion.

3.3.3.1 The AICD model

The AICDs were modeled based on the experimental data suggested in Mathiesen, et al., (2011) as shown in Figure 3-10 and Figure 3-11 for heavy oil (90 cp) and low viscous oil (2.7 cp) respectively. The data were presented in graphical form, so the web-tool WebPlotDigitizer helped in extracting numerical values as shown in Appendix 2.

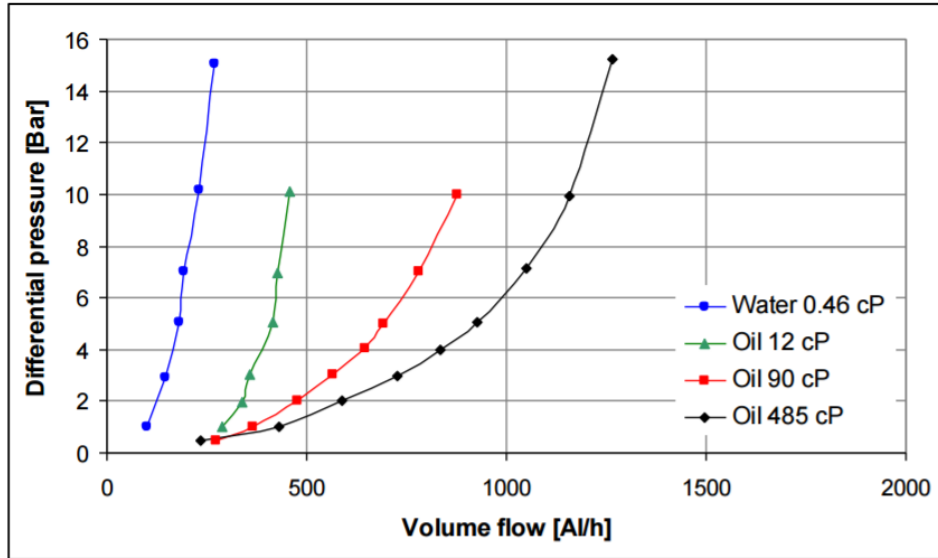


Figure 3-10: Performance curve for AICDs (Mathiesen, et al., 2011)

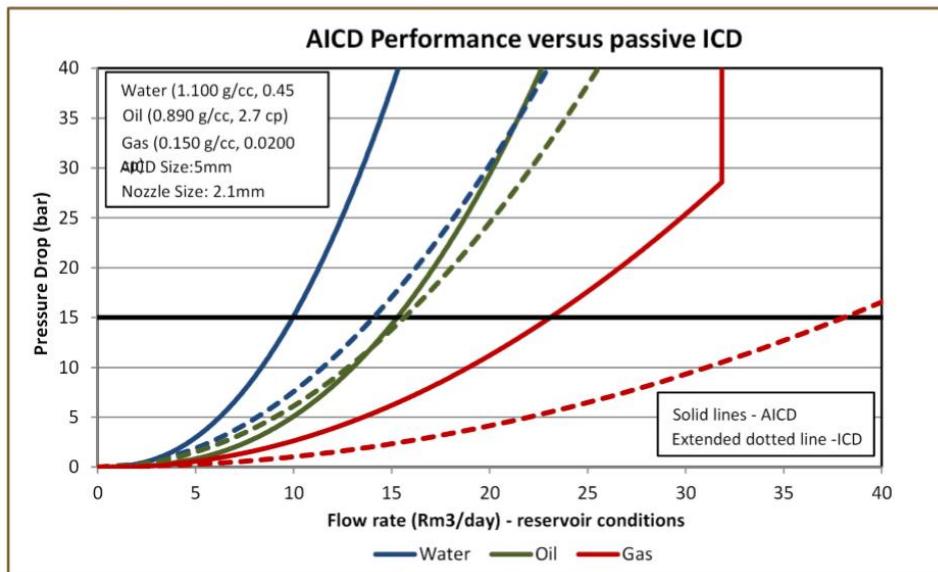


Figure 3-11: Performance curve for AICDs ((Halvorsen, et al., 2016))

Table 3-6 shows the parameters used in modelling the AICDs, these parameters were found by using procedures developed by Eltahir, et al., (2014) as shown in Appendix 3 and Appendix 5. The table includes the parameters for heavy oil (90 cp) and low viscous fluid (2.7 cp), also the parameters were used as the AICDs inputs in the Eclipse simulator.

Table 3-6: Parameters used in AICDs completion

AICDs parameters	Value	Values	Units
μ_o	90	2.7	cp
a_{AICD}	9.333E-5	2.136E-5	psi/((lb/ft ³)(rft ³ /day) ^x)
μ_{cal}	1.45	1.45	cp
ρ_{cal}	64.79	64.79	lb/ft ³
x	2.0	2.0	
y	0.79	0.39	

3.3.3.2 The AICVs model

The AICVs were modeled based on the experimental data presented in Mathiesen, et al., (2016). Two performance curves of AICVs shown in Figure 3-12 and Figure 3-13 were selected for heavy oil and low viscous oil respectively, then the methods developed by Eltaher, et al., (2014) were used to find the AICVs' parameters.

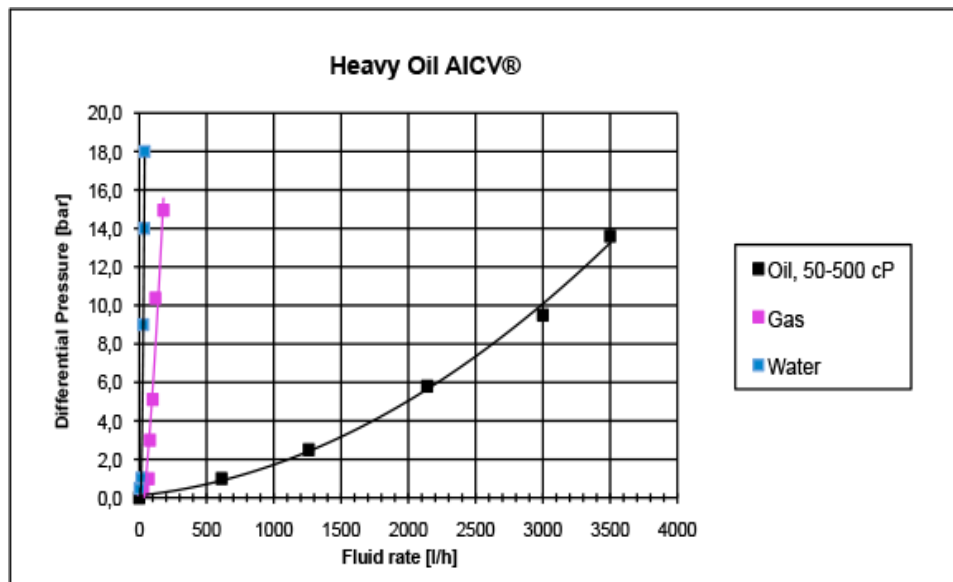


Figure 3-12: Fluids performance curve of AICV for heavy oil (Mathiesen, et al., 2016)

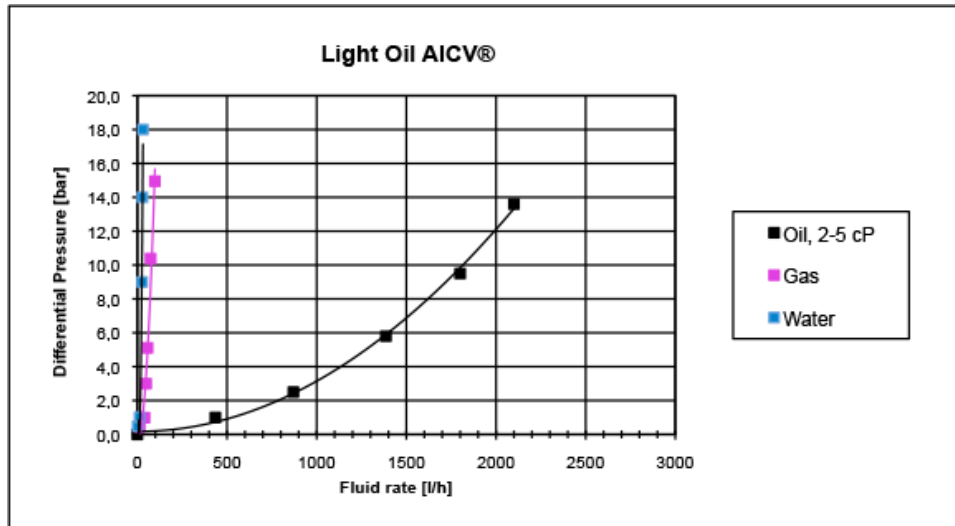


Figure 3-13: Fluids performance curve of AICV for low viscous oil (Mathiesen, et al., 2016)

Table 3-7 shows the parameters of AICVs found by using the method developed in Eltaher, et al., (2014) as shown in Appendix 4 and Appendix 6 for heavy oil and light oil respectively. These parameters were used as the AICVs' inputs in Eclipse simulator.

Table 3-7: Parameters used in AICVs completion

AICVs SIZE	Values	Values	Units
μ_o	90	2.7	cp
a_{AICV}	6.8502E-4	9.0393E-4	psi/((lb/ft ³)(rft ³ /day) ^x)
μ_{cal}	1.45	1.45	cp
ρ_{cal}	64.79	64.79	lb/ft ³
x	2.0	2.0	prop
y	1.31	3.97	prop

3.4 Pressures and saturation distribution in the reservoir

Pressures and saturation in the reservoir grid blocks are solved by different methods including IMPES, AIM, and fully implicitly solution methods. In this work fully implicitly method was used, this method use iterations methods such as Newtonian iteration to find pressures and saturation in the grid blocks. The method was selected because it is the stable method and is used in the difficult problems including coning studies.

After modelling and defining of the reservoir and DFCs parameters, the models (Reservoir coupled with horizontal well completed with DFCs) were run for 50 years (since there were

minimum oil rate) but it was constrained to WC of 95% since the field was assumed to be operated economically at WC below or equal to 95 %.

3.5 Results

3.5.1 Results for model 1

3.5.1.1 The oil recovery factor

In the heterogeneous reservoir with the fluid of viscosity of 90 cp and three layers of oil each with 50 ft thick (Reservoir model 1), the horizontal well with AICDs completion had the ultimate oil recovery of 46.42% which was 0.32% higher than open hole, while the ICDs and AICVs completion had 3.1% and 1.11% respectively lower RF than open hole completion (Figure 3-14).

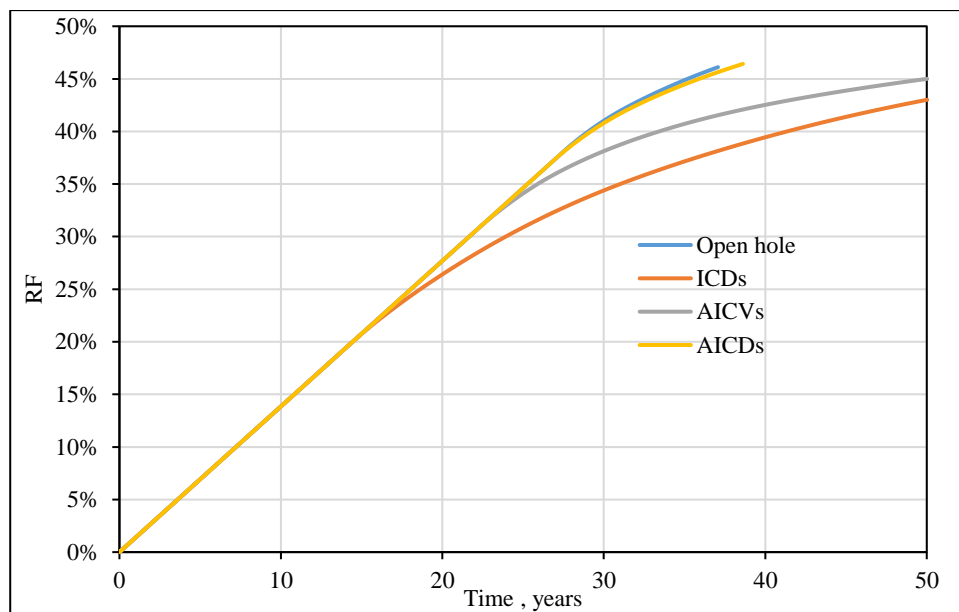


Figure 3-14: The oil recovery factor in the reservoir model 1

3.5.1.2 The performance of DFCs

The performance of DFCs in the horizontal well perforating the reservoir model 1 is shown in Figure 3-15. The high amount of water (WC) was controlled by a well completed with ICDs followed by a well completed with AICVs which was not expected since AICVs has the ability to shut off unwanted fluid completely when entered in the valve. This also shows that the restriction provided by ICDs was higher than expected due to the smallest size of orifice designed.

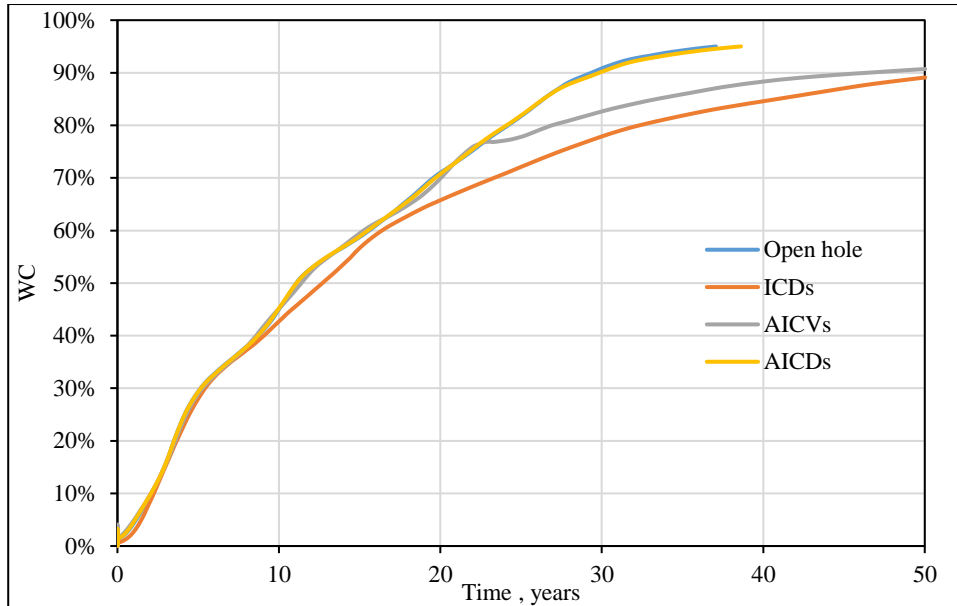


Figure 3-15: The WC in the reservoir model 1

3.5.2 Results for model 2

3.5.2.1 The oil recovery factor

The oil recovered in the heterogeneous reservoir contained an oil with viscosity of 90 cp and two layers of oil each with 50 ft thick is shown in Figure 3-16, where the horizontal well completed with AICVs had the RF of 42.81%, followed by the horizontal well completed with AICDs (42.5%). The same to model 1, the ICDs completion provided lower RF compared to the open hole.

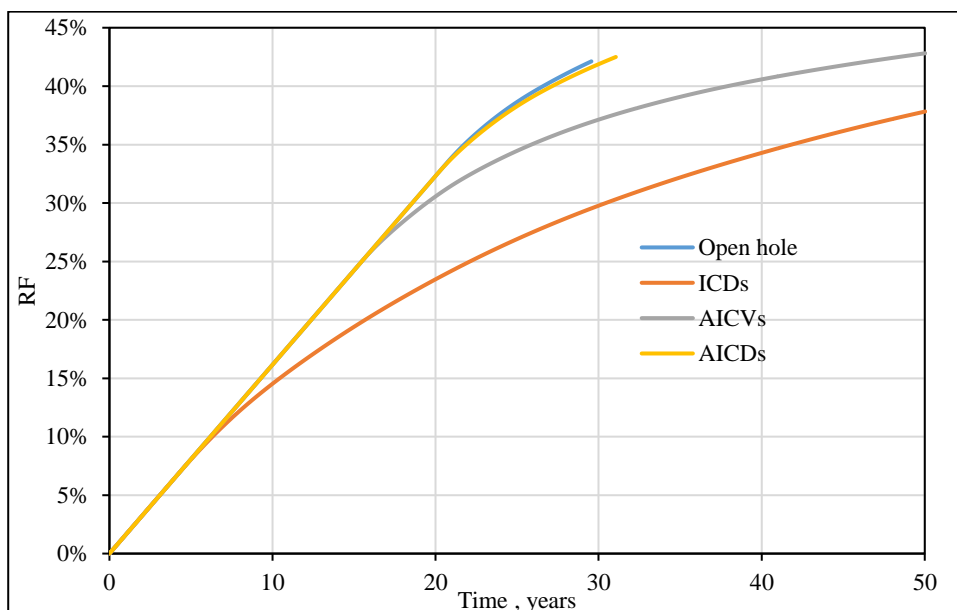


Figure 3-16: The oil recovery in the reservoir model 2

3.5.2.2 The performance of DFCs

The performance of DCFs in the horizontal well perforating the reservoir model 2 is shown in Figure 3-17, whereby the ICDs completion resulted to lowest WC compared to other case, this means the ICDs completion provided higher restriction than the expected one. The performance of AICVs was expected since it controlled higher amount of water than AICDs due to its property of shutting off valve when unwanted fluid exceed the specified amount.

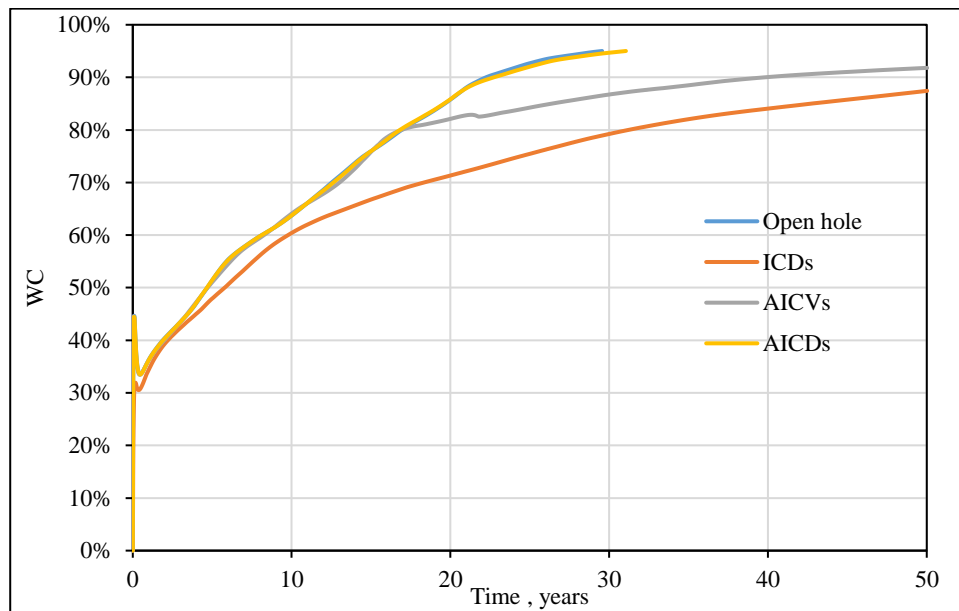


Figure 3-17: The WC in the reservoir model 2

3.5.3 Results for model 3

3.5.3.1 The oil recovery factor

Figure 3-18 shows the oil recovery factor by the heterogeneous reservoir with low viscous fluid (2.7 cp) and three layers of oil each with 50 ft thick. The horizontal well completed with AICVs had the highest oil recovery (58.66%), followed by AICDs completion with oil recovery of 58.5% but the well completed with ICVs had a lower RF compared to open hole which was not expected, so the optimization of the devices was needed.

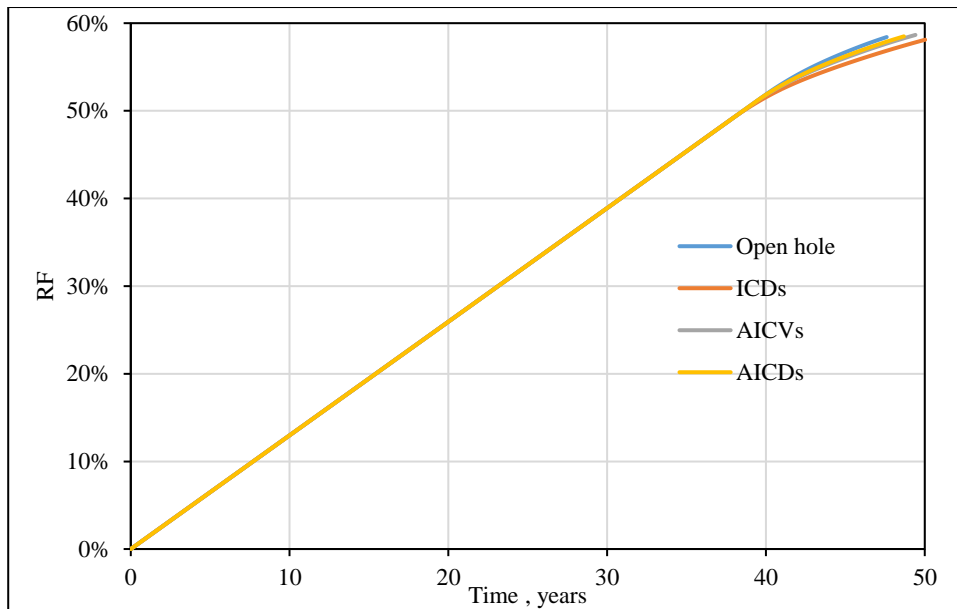


Figure 3-18: The oil recovery in the reservoir model 3

3.5.3.2 The performance of DFCs

The performance of DFCs in the reservoir model 3 is shown in Figure 3-19, where the WC in the horizontal well completed with ICDs was smaller compared to other case and it took long time (50 years) to reach the targeted WC of 95 %, followed by a well completed with AICVs (49.4 years), AICDs (48.7 years), and then open hole (47.6 years).

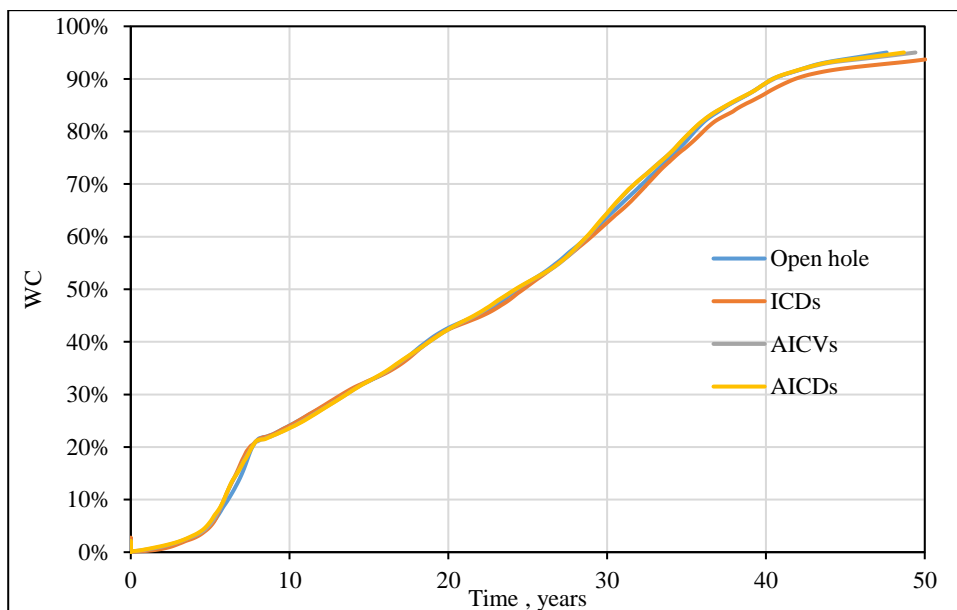


Figure 3-19: The WC in the reservoir model 3

3.5.4 Results for model 4

3.5.4.1 The oil recovery factor

In the homogeneous reservoir with a permeability of 2000 mD, oil with viscosity of 90 cp and three layers of oil each with 50 ft thick, the oil recovery by the horizontal well completed with AICVs is 40.46%, the RF due to AICDs completion was 41.17%, and the RF due to ICDs completion was 41.25%, both were lower than the open hole with a RF of 41.25% (Figure 3-20).

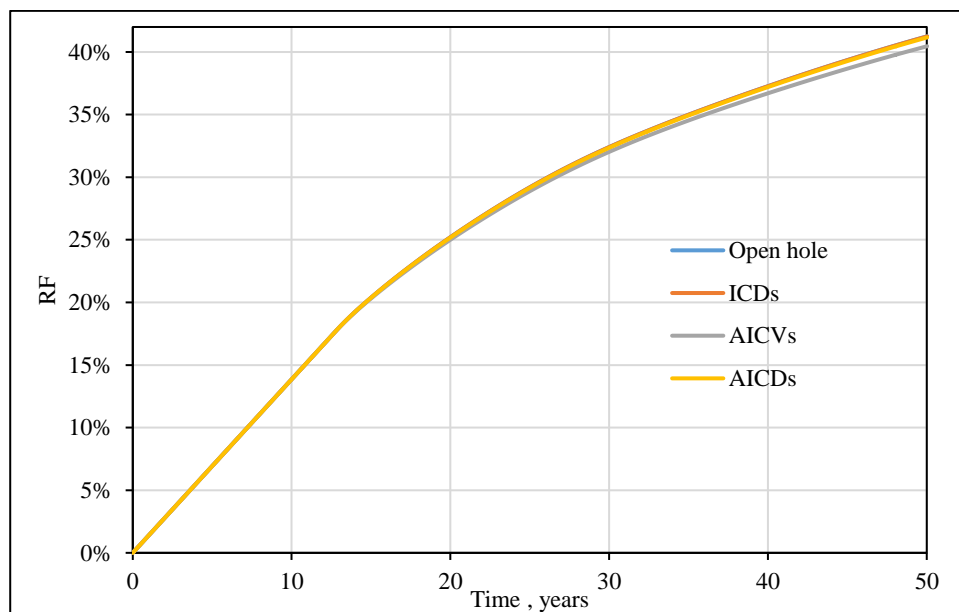


Figure 3-20: The oil recovery in the reservoir model 4

3.5.4.2 The performance of DFCs in model 4

Figure 3-21 shows the performance of ICDs, AICDs, and AICVs in the homogeneous reservoir, whereby the WC for all four cases were almost the same and the production time was also the time.

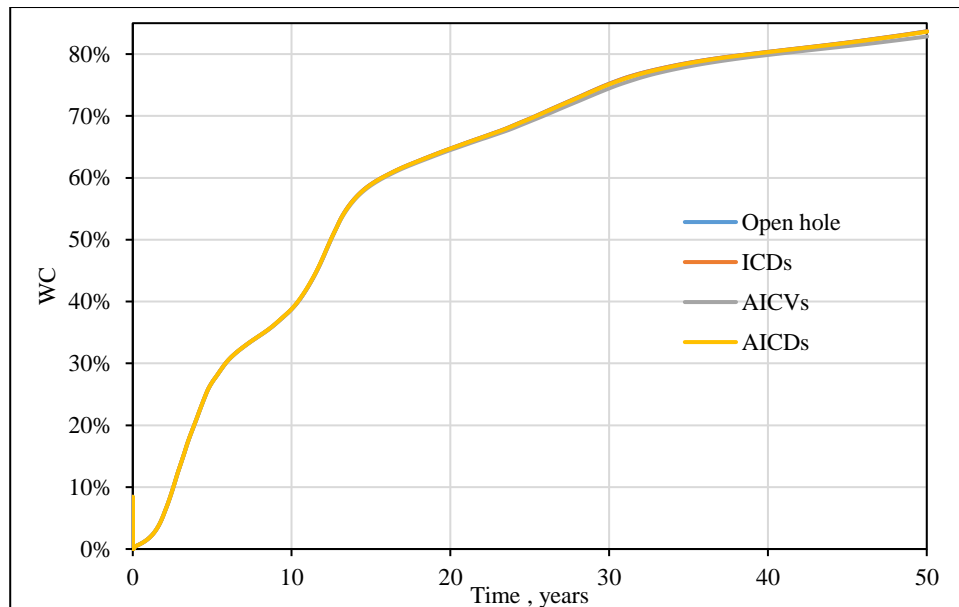


Figure 3-21: The WC in the reservoir model 4

3.6 Discussions

According to Elverhoy, et al., (2018), Halvorsen, et al., (2012), and Halvorsen, et al., (2016) the completion of horizontal well with Autonomous ICDs (AICDs and AICVs) increase the amount of oil recovered when compared against passive ICDs, and AICVs completion increase the amount of oil recovered when compared against the AICDs completion due to its behaviour of shutting off the valve when unwanted fluid exceeds the maximum specified amount of unwanted fluid (for example WC of 95% in this work) in each segment.

In the reservoir model 1, producing with the AICDs completion results to higher RF (0.32%) compared against the open hole which agreed with the literature, but producing with AICVs and ICDs completion did not agree with literature since they produced less oil (ICDs completion 3.1% and AICVs completion 1.11% less than open hole completion) compared to the open hole. This could be due to the high restriction provided by AICVs and ICDs to both water and oil, so the size of ICDs (cross-sectional area) and AICVs strength were supposed to be adjusted so as to reduce the restriction and then increase the ultimate RF.

In the reservoir model 2 and 3, producing with AICDs and AICVs completions increased the ultimate oil recovery when compared against the open hole which was expected since autonomous devices controlled amount of unwanted fluid (water and gas) even after water breakthrough and AICVs has an additional property of shutting

off unwanted fluid in the zones reached a targeted amount of unwanted fluid in the valve (for example 95 % WC). Producing with ICDs completions resulted to the lower ultimate oil recovery when compared against open hole completion which was not expected since the addition of ICDs in the horizontal well added the pressure drop in the segment with lower pressure drop and then balance the inflow in the wellbore which finally increase the ultimate oil recovery. So this could be due to the smaller size of ICDs designed, which created higher pressure drop than required as the results of high fluid restriction in the wellbore,

And in the reservoir model 4, producing with all inflow control devices resulted to decrease of ultimate oil recovery when compared against the open hole completion which did not agree with the literature. This implies that inflow control devices are not working properly in the homogeneous reservoir or the heel to toe effects are not significant in this case. But optimization of the devices was needed for further analysis.

In all models, the results were partially agreed with the literature, so optimization of the devices were required for all four cases so as to increase the performance and oil recovered by the devices.

4 OPTIMIZATION

When all parameters used in the DFCs are defined (Modelled), the DFCs were in coupled in the reservoir model by the Eclipse simulator and then run to obtain the results. The results were then taken to Microsoft Excel for analysis and optimization. The optimization of these parameters was done for all four cases so as to obtain the maximum oil recovery.

4.1 The optimization of the cross sectional area of ICDs

The optimization of the cross sectional area of the ICDs was done so as to reach the maximum oil recovery. The optimization of cross sectional area of the ICDs was done in the constant strength (uniform strength) mechanism, where the same size of ICDs was used throughout the wellbore. The variations of the cumulative oil production with the cross sectional area of ICDs were developed by running the model in the Eclipse simulator with several cross sectional areas of the ICDs. The diameter of the ICDs were supposed to be less than the diameter of the wellbore (Constrain). The numerical method (Bracketing search method) with the Golden ratio search was used in this work.

The Golden ratio search method was applied to the unimodal function ($f(x)$) on point $[a, b]$, the method was done by developing two internal points $[d, c]$ as shown in Figure 4-1 such that $a < c < d < b$ and the intervals $[a, c]$ and $[d, b]$ were supposed to be symmetrical as shown in equation (60). The value of c and d was obtained by using equation (61) and (62) respectively. The function $f(d)$ and $f(c)$ were large compared to $f(a)$ and $f(b)$.

$$b - d = c - a \quad (60)$$

$$c = a + (1 - l)(b - a) \quad (61)$$

$$d = b - (1 - l)(b - a) \quad (62)$$

Where, the golden ratio $(l) = \frac{-1+\sqrt{5}}{2}$

When $f(d) > f(c)$, the maximum occurred in $[c, b]$, and a was replaced with c and continued the search in $[c, b]$. When $f(c) \geq f(d)$, the maximum occurred in the subinterval $[a, d]$ and b was replaced with d and the search continued in the new subinterval $[a, d]$. The method continued until when the difference between $f(c)$ and $f(d)$ is very small ($1e - 5$) as shown by the MATLAB code in Appendix 7.

The method was applied to the function (y) which was found by developing the Trendline which fit the data of variations of cumulative oil production and cross sectional area of ICDs as shown in Figure 4-1. Trendline development and curve fitting were done in Microsoft Excel software. Then the code which defines the algorithms of the Golden ratio search method was written and run in MATLAB as shown in Appendix 7.

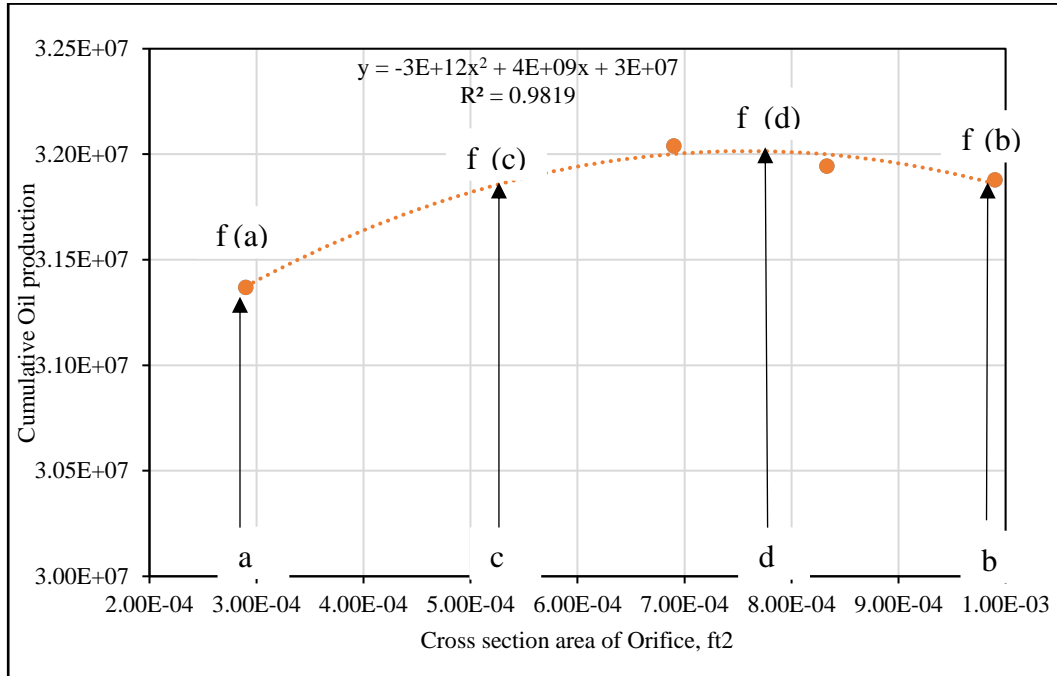


Figure 4-1: Trend line of cumulative Oil production versus cross sectional area

Table 4-1 shows the optimal cross sectional areas of ICDs found by using the Golden ratio method for four cases which differ according to reservoir conditions, reservoir oil viscosities and the thickness of the oil layer.

Table 4-1: Optimal cross sectional area of ICDs for different cases

Model	1	2	3	4
Area [ft ²]	6.68E-04	9.90E-04	1.70E-03	9.90E-03

4.2 The optimization of the strength of AICD/Vs (a) and Viscosity function exponent (y)

The optimization of the AICD strength ($a_{AICD/V}$) and viscosity function exponent (y) were done to obtain maximum oil recovery. By using Eclipse simulator several points were developed by running the model at different values of AICDs strength ($a_{AICD/V}$) and viscosity function exponent (y) starting from the designed one. So the variations of cumulative oil production with these two parameters were presented in microsoft excel. By using the microsoft

excel the trend line for the curve of cumulative oil production against (a) and another trendline for cumulative oil production against (y) were developed as shown in Figure 4-2 and Figure 4-3.

The Function for variation of cumulative oil production and the parameters ($a_{AICD/V}$ and y) was found by combining the two trendline equations with the weighted average method as shown in equation (63).

$$Y = w * A + (1 - w) * B \quad (63)$$

Whereby w is the weight average constant, A is the trend line equation for the first relationship, and B is the trend line equation for the second relationship.

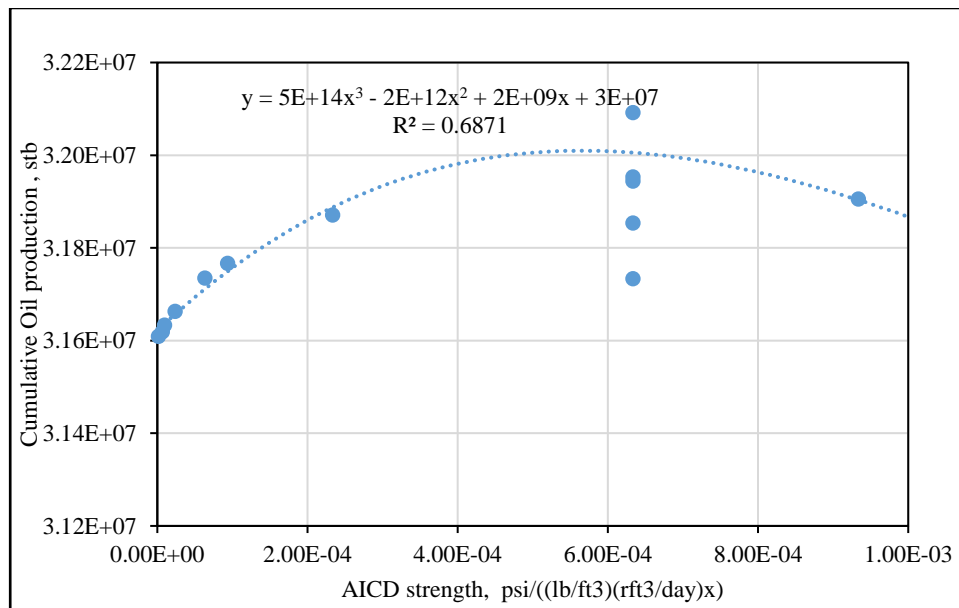


Figure 4-2: Cumulative oil production against AICDs strength for the horizontal well completed with AICDs

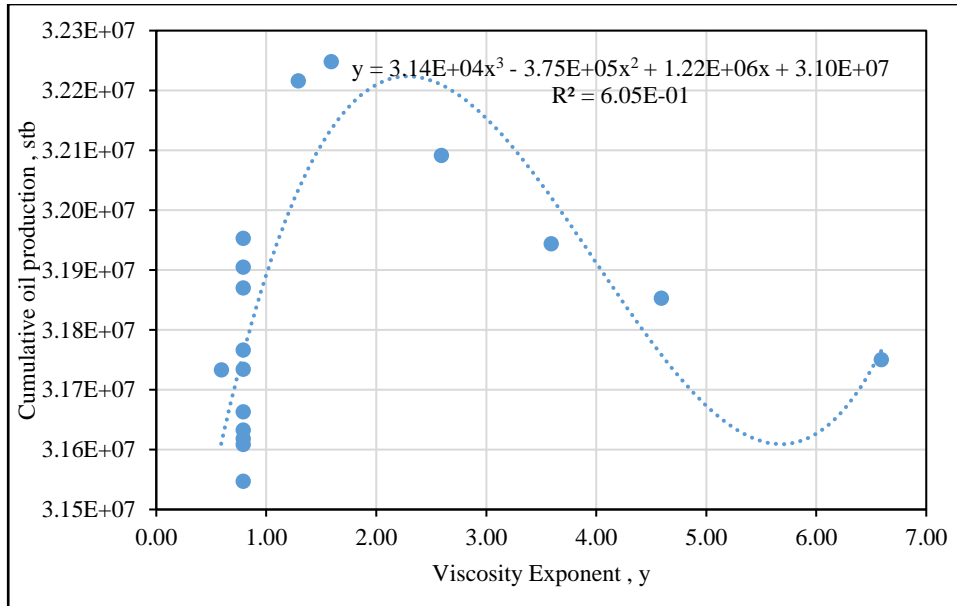


Figure 4-3: Cumulative oil production against AICDs strength for the horizontal well completed with AICDs

The value less than 1 was suggested for (w), and then the cumulative oil production was found by using the equation (63) in Excel software. The error of these results and the actual results from Eclipse was found. The solver was used to adjust the weight average constant (w), so as to minimize the total absolute error between results predicted by the proposed formula and actual results from Eclipse, and the constraint was the value of (w) to be between 1×10^{-4} and 0.9 as shown in Figure 4-4.

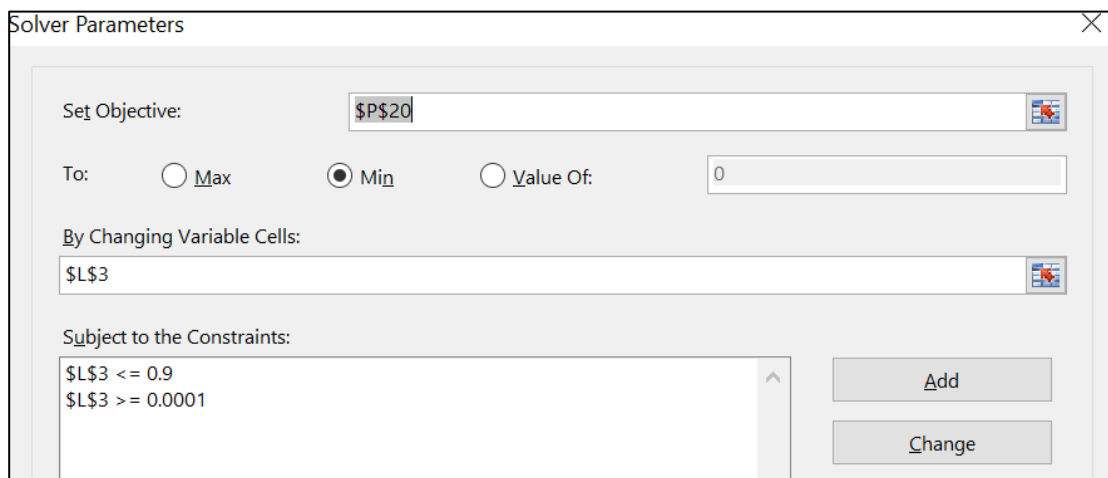


Figure 4-4: Solver for adjusting the w

The value of (w) was found when the total absolute error is small (for example error of 0.54%). The value of w was then substituted into equation (63) to obtain the required equation, for

example equation (64). Then that equation was regarded as the equation used to determine cumulative oil production from the strength of AICD/V ($a_{AICD/V}$) and viscosity function exponent (y) for model 1.

$$F = 1 * 10^{-4} * (-6.59 * 10^{19}a^4 + 1.21 * 10^{17}a^3 - 6.60 * 10^{13}a^2 + 9.09 * 10^9a + 6.09 * 10^7 + (1 - 1 * 10^{-4}) * (5.33 * 10^4y^3 - 5.64 * 10^5y^2 + 1.91 * 10^6y + 5.97 * 10^7)$$

(64)

Where a is the AICD strength ($a_{AICD/V}$) and y is the viscosity function exponent.

The first and second derivative method was used to optimize the value of y and $a_{AICD/V}$, whereby the first derivative was used to define the critical point and the second derivative was used to define the maximum point. The critical point was found by equating the partial gradient ($\frac{\partial F}{\partial a}, \frac{\partial F}{\partial x}$) to zero. The maximum point was found when the second derivative was less than 0.

During Optimization, the parameter $a_{AICD/v}$ and y for AICDs and AICVs were changing and common values brought the highest cumulative oil production for both cases, since they have the same function used in the same reservoir with the same fluid properties. This means AICDs and AICVs had the same results after optimization.

The optimum value of the strength of AICD/Vs ($a_{AICD/V}$) and viscosity function exponent (y) for different models including heterogeneous reservoir, homogeneous reservoir, low viscous fluid reservoir, and high viscous fluid reservoir are shown in Table 4-2.

Table 4-2: The optimization of the strength of AICDs (a) and Viscosity function exponent (y)

Model	1	2	3	4
$a_{AICD/V}$ [psi/((lb/ft ³)(rft ³ /day) ^x)]	9.33E-05	9.24E-05	9.14E-05	5.33E-07
y	3.0	4.93	0.79	0.79

4.3 Thesis process

The process of this work involved designing and defining the input of reservoir and DFCs models, running the open hole and the well completed with DFCs with the Eclipse simulator, and then optimizing DFCs' defined parameters to obtain maximum oil recovery as shown in Figure 4-5.

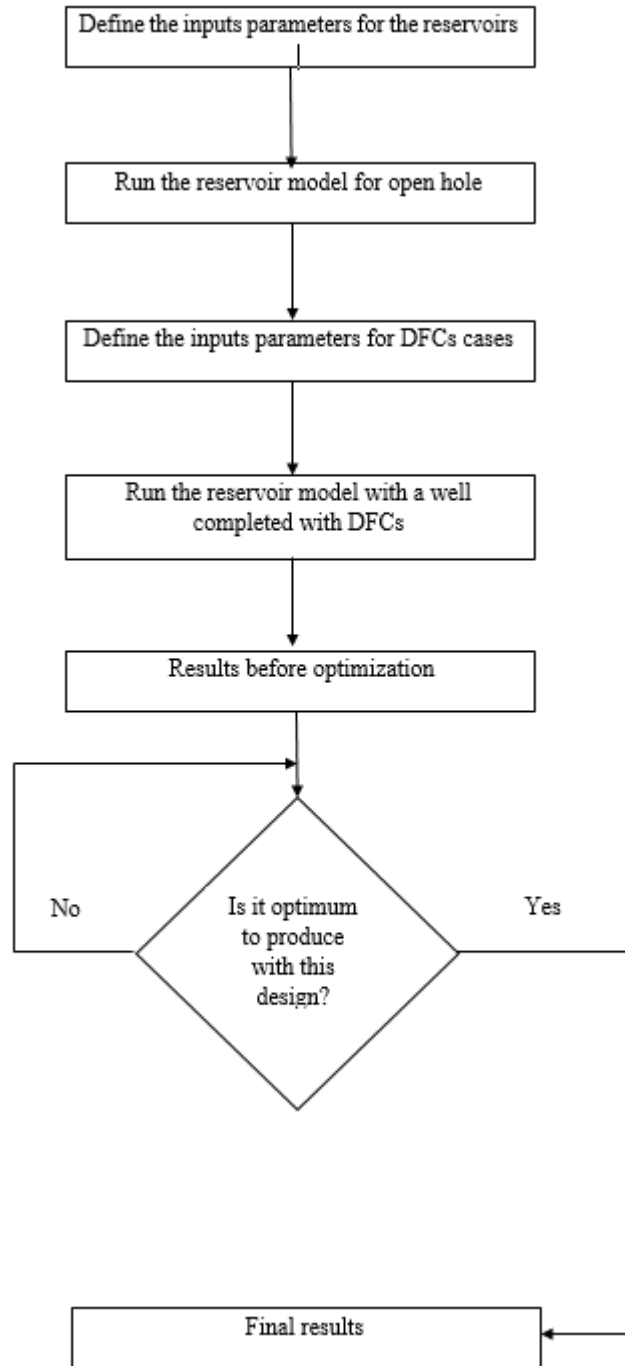


Figure 4-5: Procedure to model DFCs

4.4 Economic evaluation

To evaluate the viability and feasibility of completing the horizontal well with DFCs (ICDs and AICDs), an economic evaluation was done. This evaluation was done by comparing the revenue obtained from the increased oil due to ICDs and AICDs completion and the cost of the devices as shown in equation (65). The oil price and cost of ICDs used to evaluate the Net revenue are shown in Table 4-3, the effect of the discount rate and inflation was not taken into considerations. Also, it was assumed that the cost of installing AICDs is the same as the cost of installing ICDs.

$$\text{Net revenue} = P * \Delta q - C_{DFCs} \quad (65)$$

Where P is the oil price, Δq is the oil increased due to DFCs installation, and C_{DFCs} is the cost of installing DFCs.

The sensitivity analysis on the oil price was done so as to overcome the uncertainty of the oil price which is changing regularly, so the oil price was increased and decreased by 40% as shown in Table 4-3.

Table 4-3: Parameters for economic evaluation

Name	Unit	Value	References
Oil price per bbl	USD	67.18	(Oilprice.com, 2018)
Cost of ICD per 25 ft joint ICD	USD	28,000	(Nnakaihe, et al., 2017)
Price variation (Uncertainty)		40%	assumed

4.5 Results

The AICDs and AICVs completions use the same function and were applied in the same reservoir, the adjustment of AICD/Vs parameters in both cases caused the results of AICDs and AICVs completions to be equal after optimization in all models. This means AICDs results represented both AICDs and AICVs completions.

4.5.1 Results for model 1

4.5.1.1 The oil recovery factor on model 1

Figure 4-6 shows the results of model 1, this was the heterogeneous reservoir with a permeability distribution shown in Figure 3-2, the reservoir was comprised with the oil with the viscosity of 90 cp, and there were three layers of oil each with 50 ft thickness.

The Figure 4-6 shows that the ICDs and AICDs completions increased the production duration when compared to the open hole (ICDs completion increased 7.5 years and AICDs completion increased 1.9 years). Also, the AICDs completion had the ultimate oil recovery factor (RF) of 46.84%, which is 0.73% higher than the open hole. While the ICDs completion had the RF of 46.44%, which is 0.33% (433,000 Stb of oil) higher than the open hole. So the increase of RF by the AICDs completion was higher compared to ICDs completion.

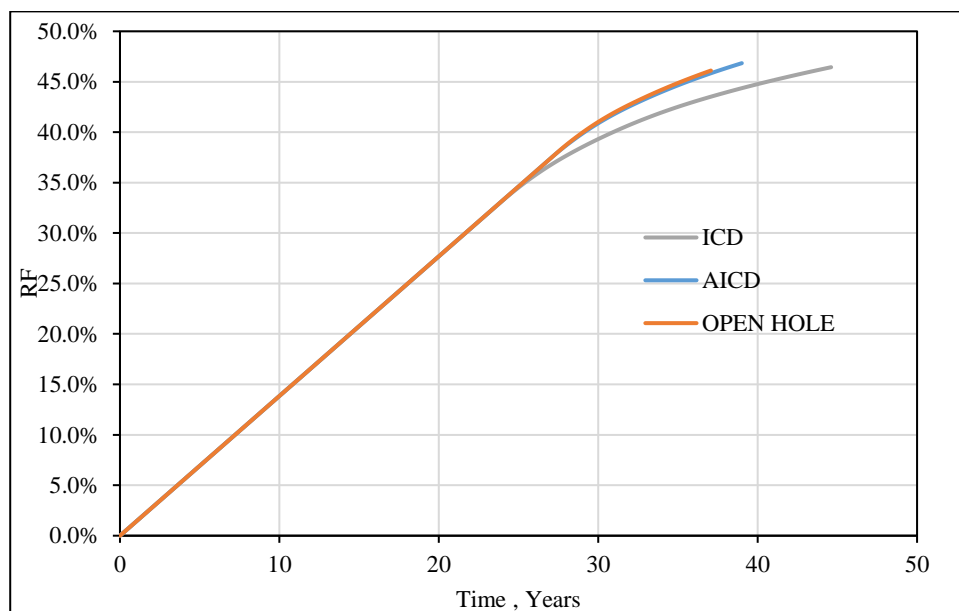


Figure 4-6: Oil recovery factor by horizontal well perforating a heterogeneous reservoir with 150 ft oil thickness (oil viscosity is 90 cp).

4.5.1.2 Economic impact of DFCs on the horizontal well for model 1

The economic analysis of the increased oil in relation to the cost of DFCs was done to see economical gain of installing DFCs. The installation of ICDs in the horizontal well resulted to increase the revenue by USD 20.9 million compared to the open hole whereby the installation of AICDs in the horizontal well resulted to increase revenue by USD 56.9 million as shown in Figure 4-7.

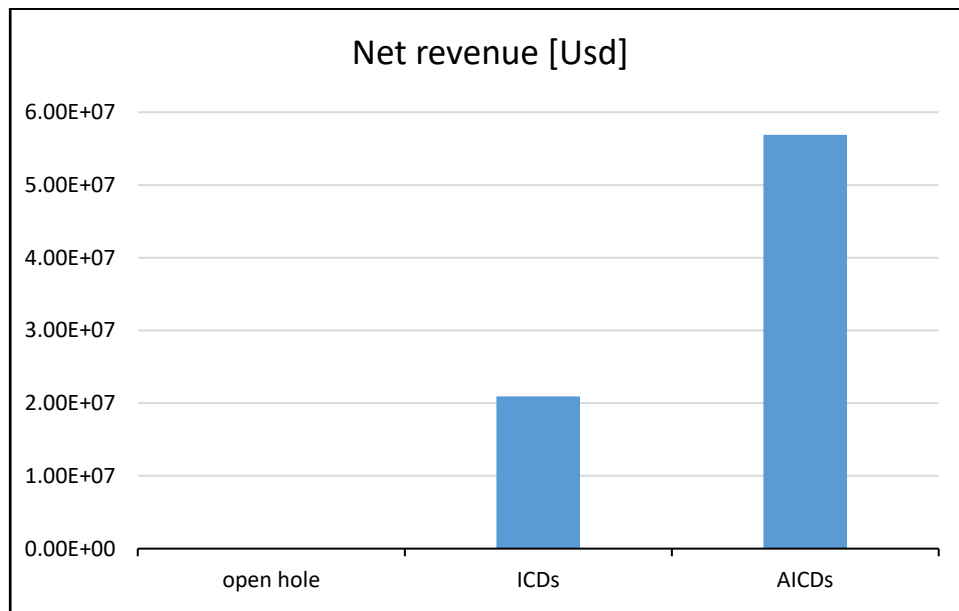


Figure 4-7: Net revenue of the increased oil for model 1

4.5.1.3 The performance of DFCs on model 1

The performance of DFCs was expressed by the restriction of water inflow in the wellbore. Figure 4-8 shows the results of produced water (WC) for model 1 whereby the open hole, a well completed with ICDs and a well completed AICDs had the same WC before 24 years. Also, the figure shows after 24 years the open hole was producing the higher amount of water compared to horizontal wells completed with ICDs and AICDs, for example, after 30 years open hole had a WC of 90.87%, a well completed with AICDs had a WC of 89.96% and a well completed with ICDs had a WC of 88.56%. The open hole reached the targeted WC of 95% after 37.1 years, followed by the horizontal well completed with AICDs (39 years), and horizontal well completed with ICDs had the longest time to reach the targeted WC of 95% (44.6 years).

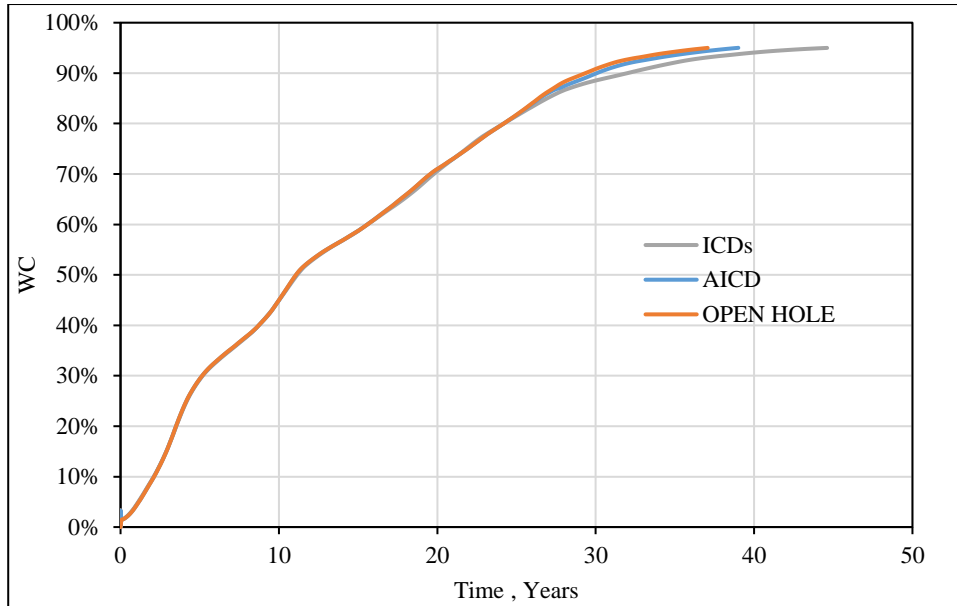


Figure 4-8: WC in the wellbore perforating the heterogeneous reservoir with a 150 ft oil thickness (Viscosity of 90 cp).

4.5.2 Results for model 2

4.5.2.1 The oil recovery factor on model 2

Figure 4-9 shows the results of model 2. Model 2 was a heterogeneous reservoir with the permeability distribution shown in Figure 3-2. The reservoir contained oil with the viscosity of 90 cP and two layers of oil with the thickness of 50 ft each (Thin oil layer).

Initially, both open hole, a well with ICDs completion, and a well with AICDs completion had the same RF, but after 18.6 years the RF started to differ. The horizontal well completed with AICDs had the RF 43.0 %, which was an increase of 0.9% of oil when compared against the open hole. The ICDs completion had the RF of 42.26%, which was an increase of 0.14 % when compared against the open hole. The production time of horizontal well completed with ICDs is higher compared to AICDs completion and open hole as shown in Figure 4-9.

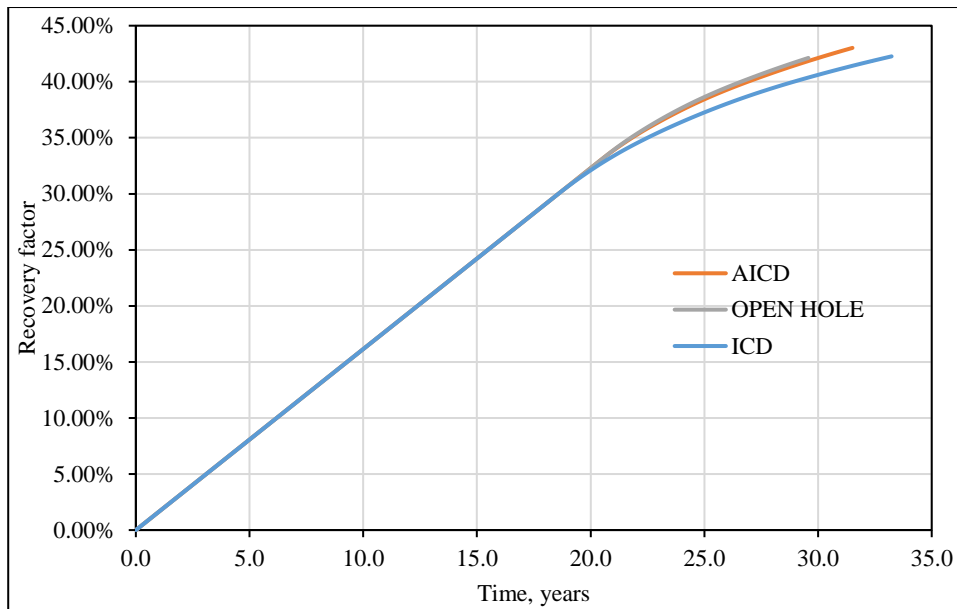


Figure 4-9: Oil recovery factor by horizontal well perforating a heterogeneous reservoir with 100 ft oil thickness (oil viscosity is 90 cP).

4.5.2.2 Economic impact of DFCs on the horizontal well for model 2

Figure 4-10 shows the incremental revenue after installation of DFCs, the ICDs completion in model 2 resulted to increase revenue by USD 2.41 million when compared against the open hole, whereas the AICDs completion resulted in the increase of revenue by USD 60.2 Million when compared against the open hole.

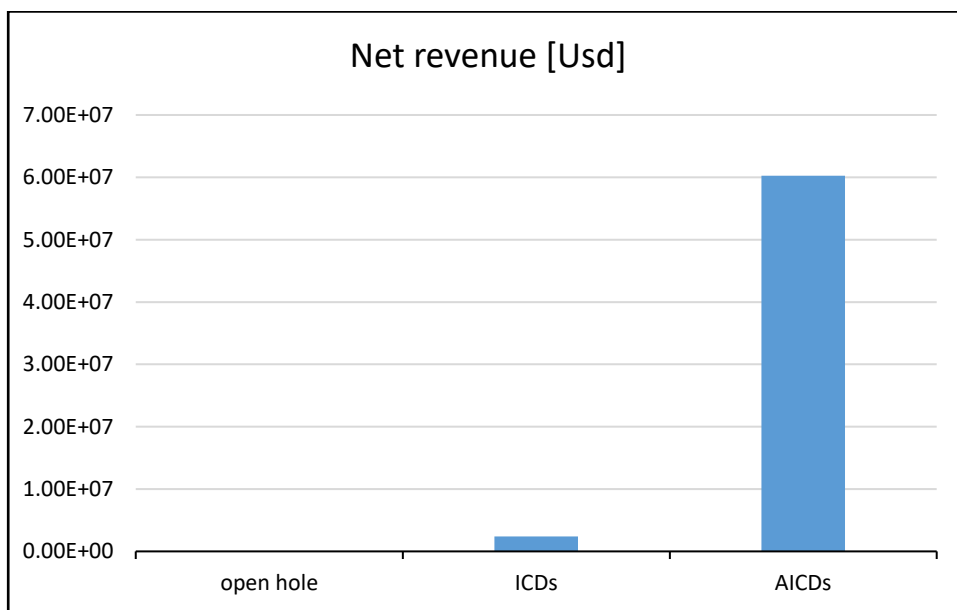


Figure 4-10: Net revenue of the increased oil for model 2

4.5.2.3 The performance of DFCs on model 2

Figure 4-11 shows the WC in the wellbore which represent the performance of ICDs and AICDs in the wellbore. After 20 years the open hole was producing the highest amount of water, followed by a well completed with AICDs and then a well completed with ICDs, for example, after 25 years open hole had a WC of 92.7%, a well completed with AICDs had a WC of 91.89%, which was a reduction of 0.8% WC, and a well completed with ICDs had a WC of 91.11%, which was a reduction of 1.59% WC.

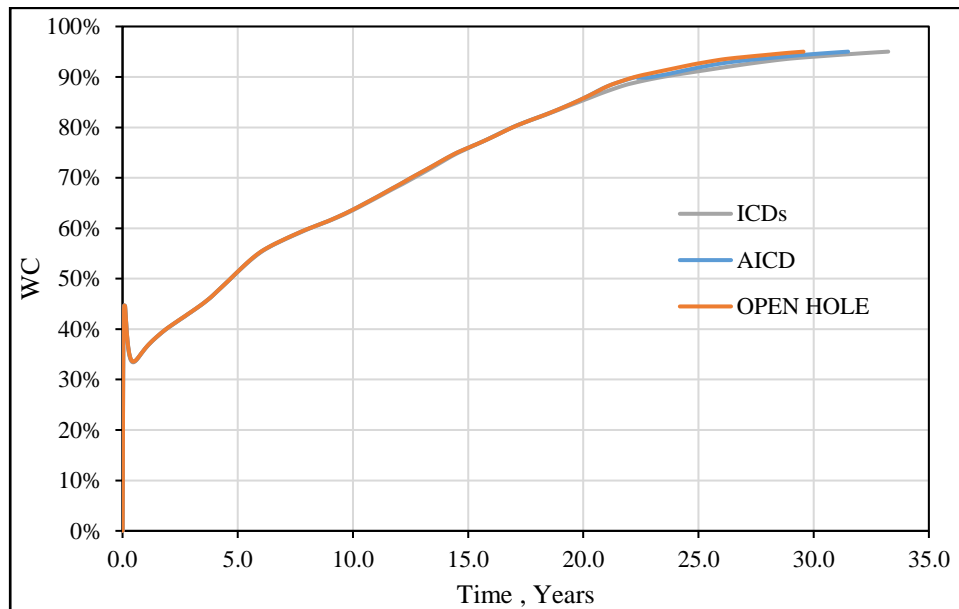


Figure 4-11: WC in the horizontal well perforating the heterogeneous reservoir with a 100 ft oil thickness (viscosity of 90 cp).

4.5.3 Results for model 3

4.5.3.1 The oil recovery factor on model 3

Model 3 was the heterogeneous reservoir with the permeability distribution shown in Figure 4-12. The reservoir contained the fluid with the viscosity of 2.7 cp and three layers of oil each with 50 ft thick. In model 3, a horizontal well completed with AICDs had the RF of 58.61% which was an increase of 0.2% when compared against the open hole, whereby the ICDs completion increased the ultimate oil recovery by 0.21% when compared against the open hole completion. Also, in this case, producing with the ICDs completion had the longest time (33.2 years) when compared against other cases as shown in Figure 4-12.

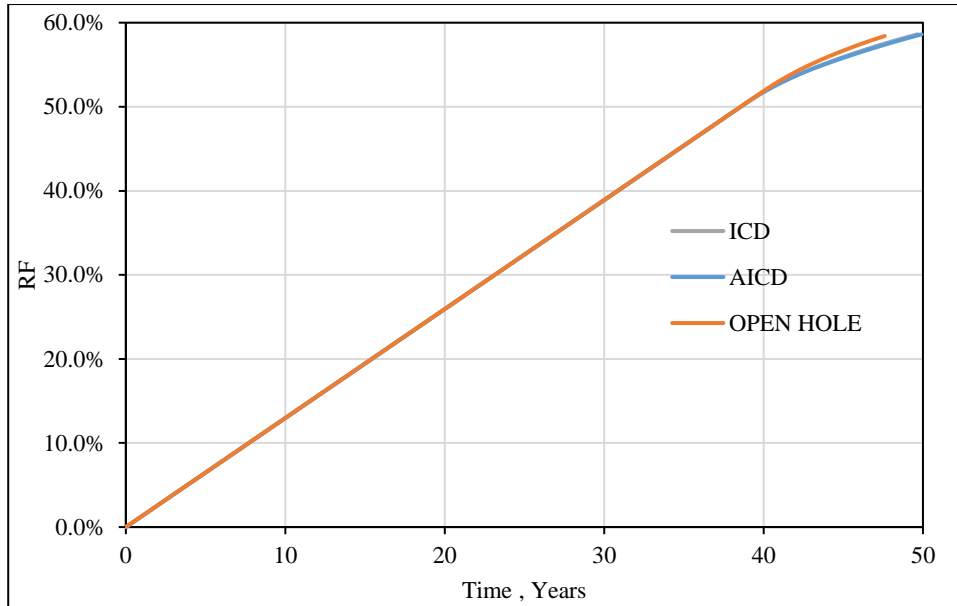


Figure 4-12: Oil recovery factor by horizontal well perforating a heterogeneous reservoir with 150 ft oil thickness (oil viscosity is 2.7 cP).

4.5.3.2 Economic impact of DFCs on the horizontal well for model 3

Figure 4-13 shows the results for model 3, where the installation of ICDs in the horizontal well resulted to the increase of revenue by USD 10.9 million when compared against the open hole, whereas the installation of AICDs resulted to the increase of revenue by USD 10.4 million when compared to the open hole.

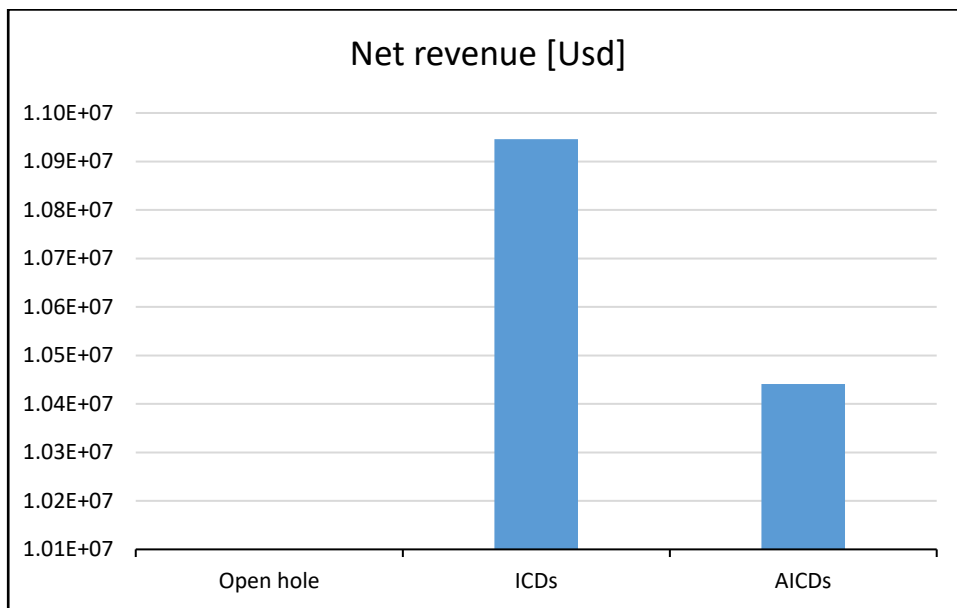


Figure 4-13: Net revenue of the increased oil for model 3

4.5.3.3 The performance of DFCs on model 3

Figure 4-14 shows the variation of WC in the wellbore for model 3, whereby the open hole reached a targeted WC (95%) after 29.6 years, a well completed with ICDs reached a targeted WC after 33.2 years, and a well completed with AICDs reached a targeted WC after 31.5 years. Also, the figure shows the variations in WC for all three cases was small, for example after 29.6 years the open hole had a WC of 95%, the well completed with ICDs had a WC of 93.89% and the well completed with AICDs had a WC of 94.37%.

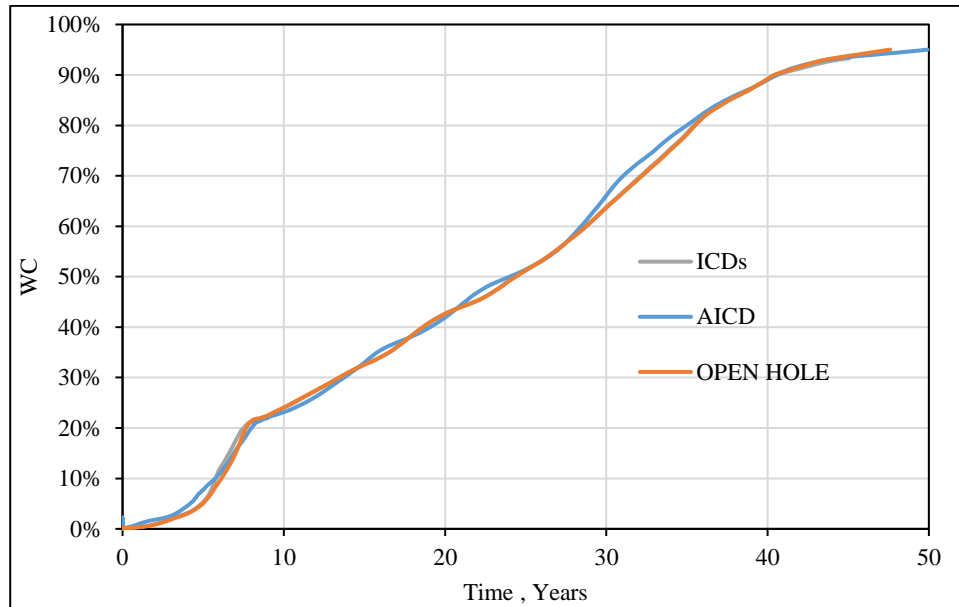


Figure 4-14: WC in the horizontal well perforating the heterogeneous reservoir with a 150 ft oil thickness (viscosity of 2.7 cP).

4.5.4 Results for model 4

4.5.4.1 The oil recovery factor on model 4

Model 4 was the homogeneous reservoir with the permeability of 2000 mD, contained the oil with the viscosity of 90 cP, and with three layers of oil with the thickness of 50 ft each. Graphically the results are not clearly separated but a completion with AICDs had the RF of 50.26% which was an increase of 0.03% (44,100 Stb of oil) when compared to open hole whereas the horizontal well completed with ICDs had a recovery factor of 50.25% which was an increase of 0.02% (27,400 Stb of oil) when compared to open hole as shown in Figure 4-15.

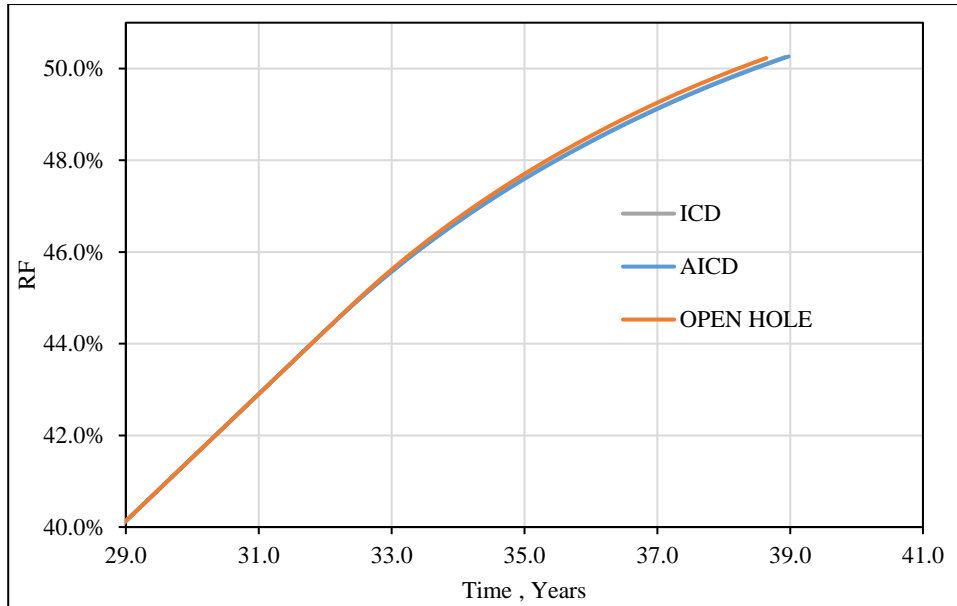


Figure 4-15: Oil recovery factor by horizontal well perforating a homogeneous reservoir with 150 ft oil thickness (Oil viscosity is 90 cP)

4.5.4.2 Economic impact of DFCs on the horizontal well for model 4

Figure 4-16 shows the economic analysis for model 4, whereby the installation of ICDs in the horizontal well perforated the oil reservoir resulted in the decrease of the revenue by USD 6.54 million when compared to the open hole. The AICDs completion resulted in a decrease of the revenue by USD 5.41 million when compared to the open hole.

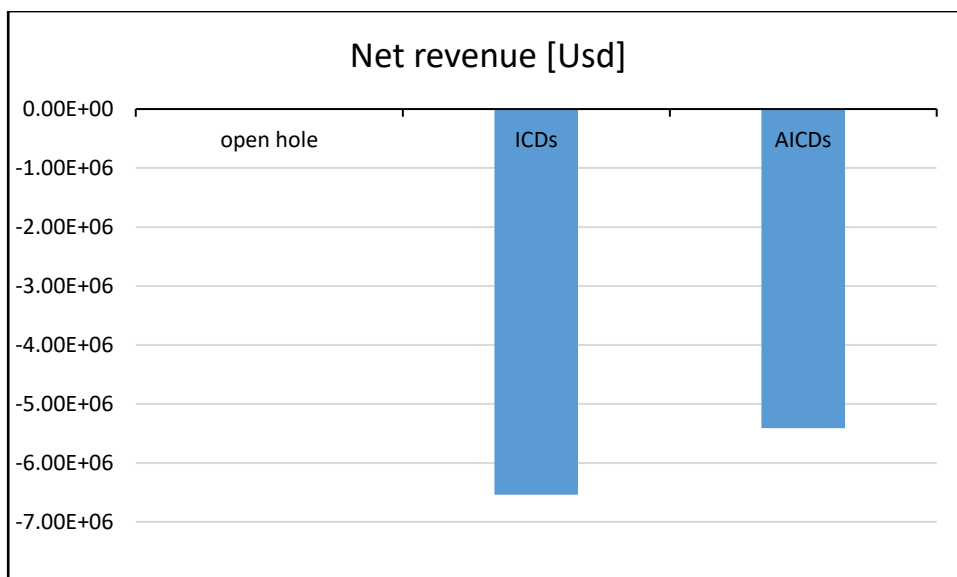


Figure 4-16: Net revenue of the increased oil for model 4

4.5.4.3 The performance of DFCs on model 4

Figure 4-17 shows the WC in the wellbore for model 4, the open hole reached a targeted WC after 38.6 years, a well completed with ICDs reached a targeted WC after 38.9 years, and a well completed with AICDs reached a targeted WC after 39 years. There was small different in WC between the open hole and wells completed with ICDs and AICDs.

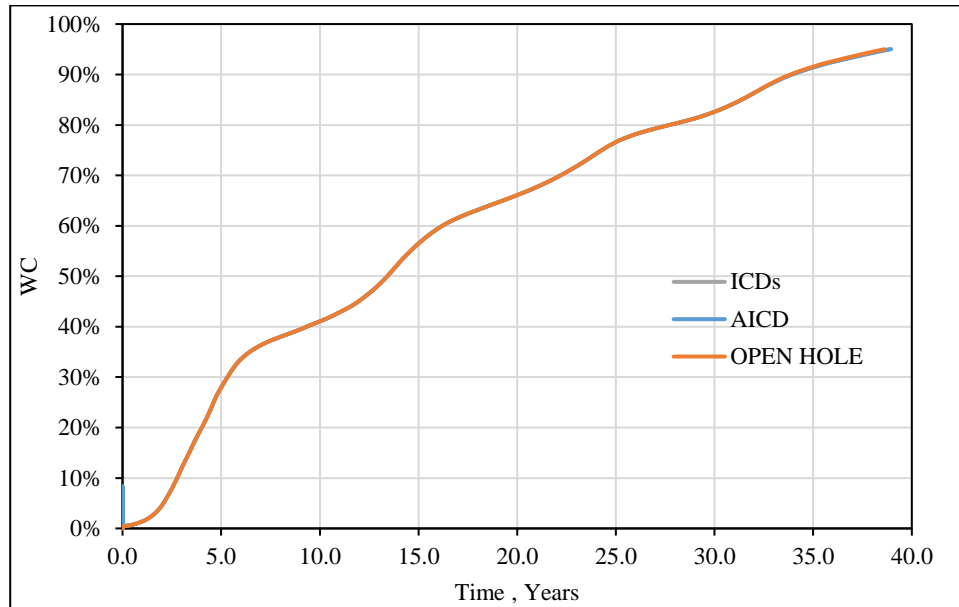


Figure 4-17: WC in the horizontal well perforating in the homogeneous reservoir with a 150 ft oil thickness (Viscosity of 90 cP).

4.6 Sensitivity analysis of the oil price

The economic evaluation of this work was done at the oil price of USD 67.8 per Bbl. Due to the regular changes in the oil price sensitivity analysis was done by varying the oil price by +/- 40% as shown in Figure 4-18. In model 1, 2, and 3 the change of oil price by +/-40% affected the net revenue, but the net revenue remained positive except for ICDs completion where the decrease of oil price by 40% resulted to negative net revenue, this means the installation ICDs and AICDs in the horizontal well remained economically significant even after increasing or decreasing the oil price by 40%. In the model 4, when the oil price increased or decreased by 40% the net revenue was lower than the cost of installing ICDs and AICDs so the net revenue became negative as shown by red colour in Figure 4-18. This means the installation of ICDs and AICDs in the homogeneous reservoir (model 4) does not have the economic benefit.

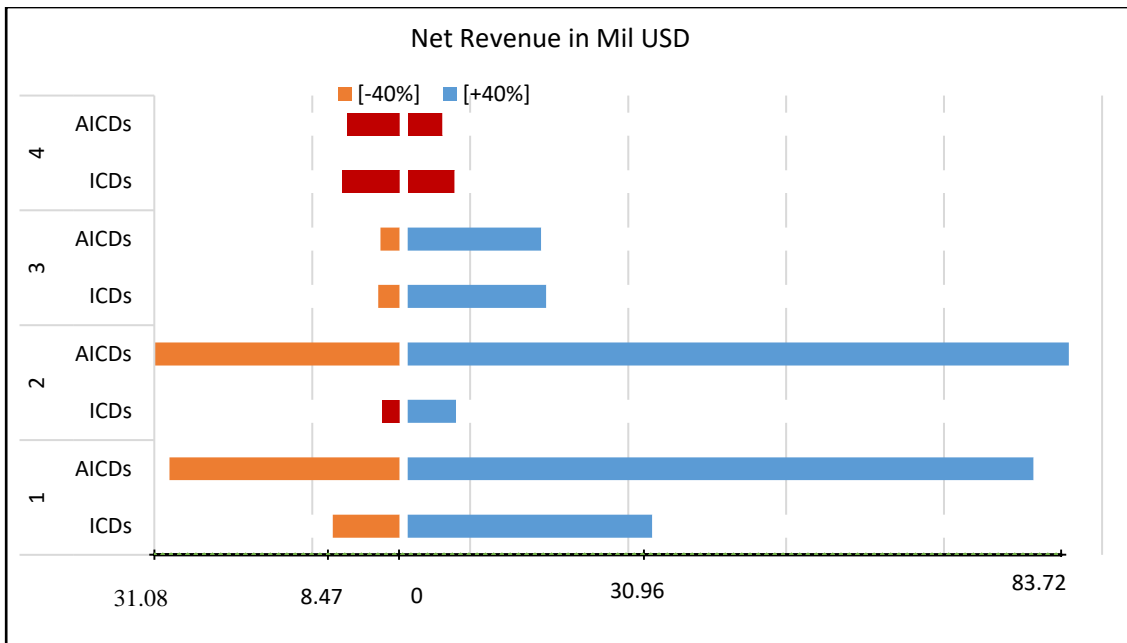


Figure 4-18: Sensitivity analysis of the oil price

4.7 Discussions

The results of this work on all reservoir models agreed with the results in other literature such as Marzooqi, et al., (2010), Halvorsen, et al., (2012) and Halvorsen, et al., (2016) that the installation of DFCs in the horizontal well perforating the oil reservoir improve the oil recovery, maximize oil recovery, reduce unwanted fluid production (water and gas), and increase the production time. The DFCs were installed in the horizontal well, the oil recovery and production time increased, therefore the installation of DFCs in the horizontal well causes the oil recovery and the production time to increase.

Also, the results show the oil recovery by the horizontal well completed with AICDs was greater compared against the horizontal well completed with passive ICDs when perforating the heavy oil reservoir (model 1, 2, and 4), which comply with the results presented by Halvorsen, et al., (2016). These could be due to the ability of AICDs to control unwanted fluids (water and gas) inflow in the wellbore even after water breakthrough as the results of more oil recovery. ICDs are passive devices so after water breakthrough they do not provide a further restriction to unwanted fluids. Therefore AICDs completion increases more oil compared to ICDs completion.

In low viscous oil reservoir (model 3), the installation of nozzle ICDs in the horizontal well increased more oil (0.01%) when compared against the RCP valves (AICDs) completions. This is due to the fact that the performance of RCP valve depends on the viscosity of the flowing

fluid (AICD favours high viscous fluid and restrict low viscous fluid) (Halvorsen, et al., 2016) whereas in the low viscous oil reservoir the different in viscosities between water and oil is small which causes difficult to control the water inflow in the wellbore, but the performance of nozzle ICDs do not depend on the viscosity of the flowing fluid (Daneshy, et al., 2010), which causes its performance to be better in low viscous oil reservoir.

The installation of ICDs and AICDs increased the investment cost, but the results show that the oil increased due to ICDs and AICDs completions had higher revenue compared to the cost of the devices for the heterogeneous reservoirs (model 1, 2, and 3) while in the homogeneous reservoir the cost was high compared to the increased oil revenue (model 4). This means the installations of ICDs and AICDs in the horizontal well perforating the heterogeneous oil reservoir has the economic benefits. The increase and decrease of the oil price by 40% proved the economic advantage of ICDs and AICDs in the horizontal well perforating the heterogeneous reservoir (model 1, 2, and 3) except for ICDs completion in the thin oil layer reservoir where decrease of oil price by 40% caused the devices to be uneconomical (negative incremental revenue). These results comply with the results of Nnakaihe, et al., (2017) that the installation of ICDs adds higher profit compared to the open hole, however the installation of AICDs added the highest profit when compared against open hole and the ICDs completions in the heavy oil reservoir (high viscosity fluid).

5 CONCLUSIONS AND RECOMMENDATIONS

5.1 CONCLUSIONS

Four reservoir models have been run in the Eclipse simulator for different completions including the open hole, ICDs completion, AICDs completion, and AICVs completion. The AICDs and AICVs completions had the same results after optimization since they use the same function and in the same oil reservoir (all reservoir and fluid properties were the same), however, in the real field the AICVs completion increases more oil when compared to the AICDs completion due to its ability of shutting off valve when unwanted fluid enters into the valve (AICV).

The installation of DFCs (ICDs, AICDs, and AICVs) in the horizontal well increases the oil recovery (RF) significantly, however the installation of Autonomous ICDs (AICDs and AICVs) in the horizontal well perforating the heavy oil reservoir increase more oil when compared against the passive ICDs, this had been proved by the results of the three reservoir models including:

The heterogeneous reservoir contained the heavy oil (90 cp) and the thick layer of oil (150 ft), whereby producing with AICDs completion increased the RF by 0.73% when compared against the open hole completion, while producing with the ICDs completion increased the RF by 0.33% when compared against the open hole.

The heterogeneous reservoir contained the heavy oil (90 cp) and the thin layer of oil (100 ft), whereby producing with AICDs completion increased the RF by 0.9% when compared against the open hole completion, while producing with the ICDs completion increased the RF by 0.14% when compared against the open hole completion.

The homogeneous reservoir contained oil with the viscosity of 90 cp and 150 ft oil layer, whereby producing with AICDs completion increased the RF by 0.03% when compared against the open hole completion, while the ICDs completion increased the RF by 0.02% when compared to open hole completion. The increase in recovery factor was very small even its incremental revenue was negative, this may indicate that the heel to toe effect are not significant when compared to the heterogeneity effect.

But, in the low viscous oil reservoir the results were different, whereby in the heterogeneous reservoir contained the oil with the viscosity of 2.7 cp and oil thickness of 150 ft, producing with the AICDs completion increased the RF by 0.2% when compared to open hole completion,

which was lower when compared to the nozzle ICDs completion which increased the RF by 0.21% when compared to open hole completion, these results indicate that the performance of nozzle ICDs is better than RCP- valve in the low viscous fluid reservoir.

Also, the completion of the horizontal well with ICDs and AICDs reduce the WC in the wellbore, however the AICDs completion reduces less WC compared to the ICDs completion as it was seen in three reservoir models including:

The heterogeneous reservoir contained the heavy oil (90 cp) and the thick layer of oil (150 ft) in which after 30 years the AICDs completion reduced the WC by 0.9% when compared against the open hole, whereas the ICDs completion reduced WC by 2.31% when compared against the open hole.

The heterogeneous reservoir contained the heavy oil (90 cp) and the thin layer of oil (100 ft) in which after 25 years open hole had a WC of 92.7%, a well completed with AICDs had a WC of 91.89%, which was a reduction of 0.8% WC, and a well completed with ICDs had a WC of 91.11%, which was a reduction of 1.59% WC.

The heterogeneous reservoir contained the oil with the viscosity of 2.7 cp and 150 ft oil layer thickness in which after 29.6 years a well completed with AICDs reduced WC by 0.63% when compared against the open hole, whereas a well completed with ICDs reduced WC by 1.11% when compared against the open hole.

In the fourth model which was the homogeneous reservoir with the permeability of 2000 mD, contained the oil with the viscosity of 90 cp and 150 ft oil thickness, after 25 years, both well completed with AICDs and ICDs reduced the WC by 0.3% when compared to the open hole.

5.2 RECOMMENDATIONS

The study of Autonomous inflow control devices was done successfully in this work, but for further study, the following recommendations were made:

Engineers on the field and researchers have to do further study on the AICVs performance, so as to establish the function (formula) which will be used to model AICVs and used in the simulators such as Eclipse and Computer Modelling Group (CMG).

The study of other inflow control devices, including Tube and hybrid channel ICDs, ER-AICDs, and fluidic diode AICDs and their economic analysis are recommended.

Optimization was done by considering the relationship between the results (trendline), for more detail another method of optimization should be used, such as by using optimization simulator such as Pipe-it software.

The installation of DFCs in the horizontal well perforating the oil reservoir has to consider the selection of proper packer which controls the annular flow.

The Fetkovich model was used on this Thesis, so the analysis on other aquifer model has to be done so as to see their effects.

6 REFERENCES

- Akbari, M., Gonzalez, . J. R. & Nadine , M., 2014. Considerations for Optimum Inflow Control Devices (ICDs) Selection and Placement in Horizontal Sections. *SPE*, p. 2.
- Al-Khelaiwi , F. T. M., 2013. *A Comprehensive Approach to the Design of Advanced Well Completions*, Edinburgh – Scotland, UK: Heriot-Watt University.
- Asheim, H., 2017. Flow towards horizontal wells ' Class notes'.
- Birchenko, V. M., 2010. Analytical Modelling of Wells with Inflow Control Devices. p. 78.
- Dake, L. P., 1998. *Fundamentals of Reservoir Engineering*. The Hague, The Netherlands: Elsevier Science B.V.
- Fernandes, P., Li, . Z. & Zhu, . D., 2009. Understanding the Roles of Inflow-Control Devices in Optimizing Horizontal-Well Performance.
- Guo, . B., 2016. *Petroleum Production System*. s.l.:University of Louisiana at Lafayette.
- Nnakaihe, S. E. et al., 2017. Enhancing the Effectiveness of Vertical Water Injection Wells With Inflow Control Devices (ICDs): Design, Simulation and Economics. *CScanada*.
- Nugraha, I. et al., 2016. Optimizing Reservoir Performance through Utilization of Autonomous Inflow Control Valve – Lessons Learnt from the World’s First Installation. Society of Petroleum Engineers..
- Shevchenko, E., 2013. *Experimental Study of Water Coning Phenomenon in Perforated Pipes Geometry*, Trondheim: NTNT.
- Whitson, C. H. & Brule, M. R., 2000. *PHASE BEHAVIOR, MONOGRAPH VOLUME 20*. Texas: s.n.
- Aadnoy, B. S., 2008. Autonomous Flow Control Valve or “intelligent” ICD.
- Ahmed, T., 2005. *Advanced Reservoir Engineering*. AMSTERDAM: Gulf Professional Publishing.
- Asheim, H., 1986 . MONA, An Accurate Two-Phase Well Flow Model Based on Phase Slippage. *SPE*, p. 221.
- Asheim, H., 2017. Production wells (Class notes).
- Berge, L. C., 2011. Troll Field - Completion Solutions Applied.

- Berge, . L. . C., 2011. Troll Field - Completion Solutions Applied.
- Birchenko, V. M., Muradov , K. M. & Davies., D. R., 2010. Reduction of the Horizontal Well's heel-toe Effect with Inflow Control Devices.
- Brill, . J. . P., 1987. *Multiphase Flow in Wells*, s.l.: Society of Petroleum Engineers.
- Daneshy, A. . A., Krasnov, . V. . A., Zimin, S. V. & Guo, B., 2010. ICD Design: Revisiting Objectives and Techniques. *SPE*, p. 2.
- Eltaher, E., Muradov, K. & Davies, D., 2014. Autonomous Inflow Control Control Valves- Their Modelling and Added Value. *SPE*.
- Elverhoy, A. B., Aakre, H. & Mathiesen, V., 2018. Autonomous Inflow Control for Maximizing Oil Recovery and Minimizing Water/Stream Production. *SPE*.
- Elverhoy, A. B., Aakre, H. & Mathiesen, V., 2018. Autonomous Inflow Control for Reducing the Water cut and /or Gas Oil Ratio.
- Fripp, M., Zhao, L., Least, B. & Halliburton, 2013. The Theory of a Fluidic Diode Autonomous Inflow Control Device.
- Håland, S., 2017. *Modelling and Analysis of Autonomous Inflow Control Devices*, Trondheim: NTNU.
- Halliburton, 2017. EquiFlow® Autonomous Inflow Control Devices.
- Halliburton, 2017. *Halliburton* page. [Internett]
Available at: www.halliburton.com
- Halvorsen, M. et al., 2012. Increased oil production at Troll by autonomous inflow control with RCP valves.
- Halvorsen, M. et al., 2016. Enhanced Oil Recovery On Troll Field By Implementing Autonomous. *SPE*.
- Halvorsen, M., Elseth, G. & Naevdal, O. M., 2012. Increased Oil Production at Troll by Autonomous Inflow control with RCP valves.
- Jadhav, N. & Zhambrovskii, D., 2017. Electrical Resistivity Autonomous Inflow Control Device ER-AICD.

James, E. J. & Hossain, M. M., 2017. Evaluation of Factors Influencing the Effectiveness of Passive and Autonomous Inflow Control Devices. *SPE*, p. 4.

Jovanov, I., 2016. *Performance of autonomous inflow control systems*, Stavanger: University of Stavanger.

Jubralla, A. F. & Cosgrove, P., 1996. Horizontal Wells Highlights. p. 14.

Kabir, C. S., Agamini, M. & Holguin, R. A., 2004. Production Strategy for Thin Oil columns in a Saturated Reservoirs.

Kabir, C. S., Agamini, M. & Holguin, R. A., 2004. Production Strategy for Thin Oil columns in a Saturated Reservoirs.

Lim, M., 2017. ICDs for Uncertainty and Heterogeneity Mitigation: Evaluation of Best Practice Design Strategies for Inflow Control Devices. *SPE*.

Marzooqi, A. A. et al., 2010. Wellbore Segmentation using Inflow Control Devices: Design and Optimisation Process.

Mathiesen, V., Aakre, H. & Werswick, B., 2013. A Flow Control Device and Method, Patent WO 2013/139601 A2..

Mathiesen, V., Werswick, B. & Aakre, H., 2016. *InflowControl*. [Online]. [Internet] Available at: <https://www.inflowcontrol.no/aicv-product-range/aicv-heavy-oil/> [Funnet 2018 02 10].

Ogunleye, A. O., 2012. Development of Vogel type Inflow Performance Relationship (IPR) for Horizontal wells. *SPE*.

Ohaegbulam, M. C., Izuwa, N. C. & Onwukwe, S. I., 2017. Analysis of Wellbore Pressure Drop on Horizontal Well Performance. *Volum Res 3*.

Oilprice.com, 2018. *Oil price.com*. [Internet] Available at: <https://oilprice.com/> [Funnet 15 06 2018].

page, H., 2017.. *Halliburton page*. [Internet] Available at: www.halliburton.com. [Funnet 13 09. 2017.].

Petrowiki, 2017. *Reserves estimation of thin oil columns*. [Internet] Available at: [http://petrowiki.org/index.php?title=Reserves estimation of thin oil columns&printable=yes](http://petrowiki.org/index.php?title=Reserves_estimation_of_thin_oil_columns&printable=yes)

Schlumberger, 2015. *Eclipse Reference Manual*. Version 2015.1 red. s.l.:s.n.

Schlumberger, 2018. [Internet] Available at: https://www.slb.com/resources/tech_reports/sand-control/resflow-icd-thailand-tr.aspx
[Funnet 17 05 2018].

Sharma, P., Gupta, D. K. & Kumar, M., 2015. *Application of Inflow Control Devices in Horizontal Well in Bottom water Drive Reservoir using Reservoir Simulation*, Dehradun: s.n.

Shi, H. et al., 2016. A New Method to Design and Optimize the ICD for Horizontal Wells.

Torbergsen, H. E. B., 2010. *Application and Design of Passive Inflow Control Devices on the Eni Goliat Oil Producer*, Stavanger,: University of Stavanger.

U.S. Department of Energy, 1998. Horizontal Wells : Subsurface Contaminants.

Zeng, Q., Wang, Z. & Yang, G., 2013. Comparative Study on Passive Inflow Control Devices by Numerical Simulation.

7 APPENDICES

Appendix 1: The oil properties used in the reservoir model

$$\mu_{od} = \left(0.32 + \frac{1.8 \cdot 10^7}{API^{4.53}}\right) * \left(\frac{360}{T+200}\right)^A \quad (66)$$

$$A = 10^{0.43 + \frac{8.33}{API}} \quad (67)$$

$$a = R_s(2.2 * 10^{-7} * R_s - 7.4 * 10^{-4}) \quad (68)$$

$$b = \frac{0.68}{10^c} + \frac{0.25}{10^d} + \frac{0.062}{10^c} \quad (69)$$

$$c = 8.62 * 10^{-5} * R_s \quad (70)$$

$$d = 1.10 * 10^{-3} * R_s \quad (71)$$

$$e = 3.74 * 10^{-3} * R_s \quad (72)$$

$$API = \frac{141.5}{\rho_o} - 131.5 \quad (73)$$

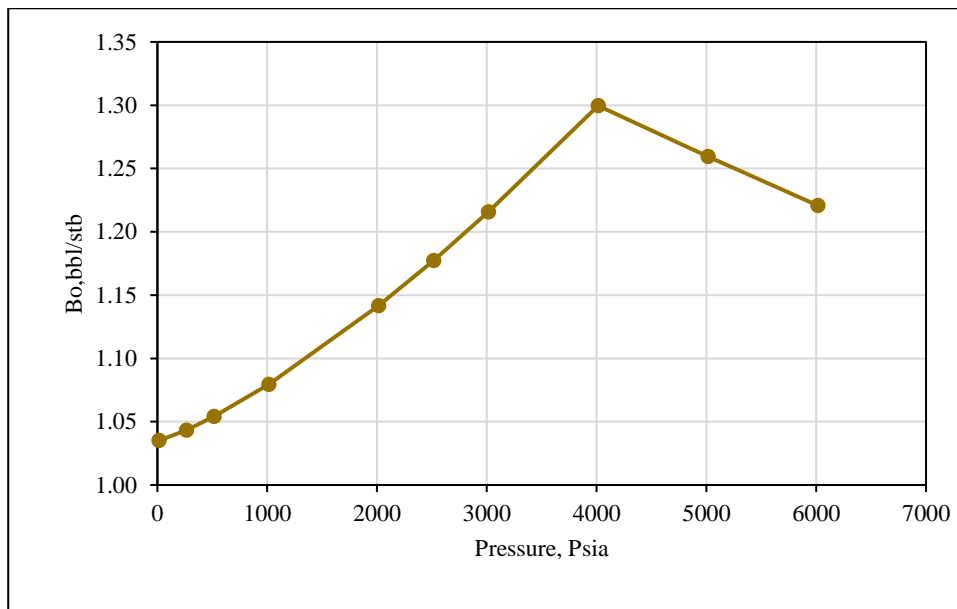


Figure 7-1: The variation of formation volume factor with the reservoir pressure for heavy oil

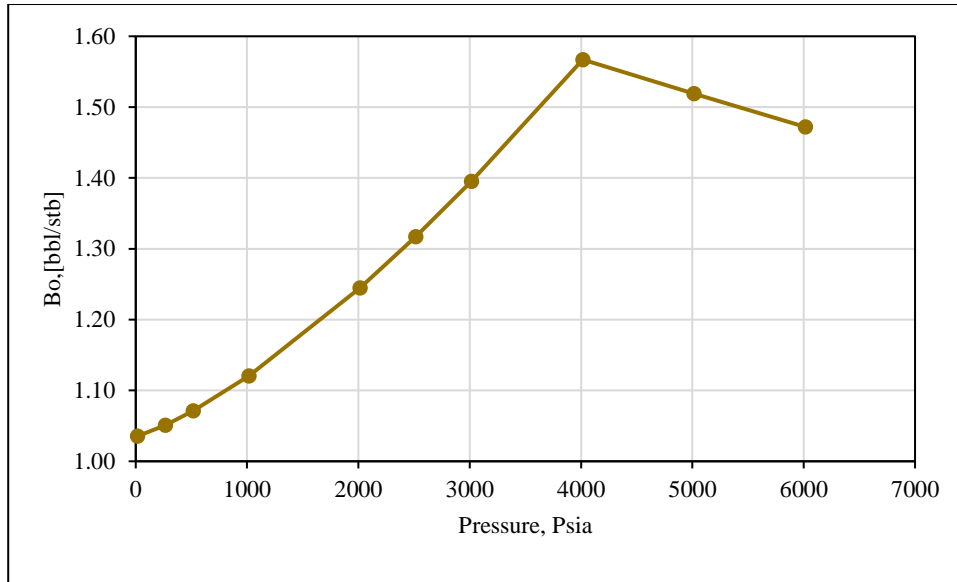


Figure 7-2: The variation of formation volume factor with the reservoir pressure for light oil

Appendix 2: The flowing rate through the DFCs

The flowing rate of the wellbore was 5000 stb/day

Flowing rate at local condition (Q)

$$Q = q_o * B_o$$

$$Q = 5000 * 1.27$$

$$Q = 6350 \text{ bbl./day}$$

Specific flowing rate (q_l)

$$q_l = \frac{q_o * B_o}{L_w}$$

$$q_l = \frac{6350}{7500}$$

Flowing rate per cell (q_{cell})

$$q_{cell} = q_l * l_{tubing}$$

$$q_{cell} = \frac{6350}{7500} * 500$$

The inflow through the DFCs (q_{DFC})

$$q_{DFC} = q_{cell} * \frac{L_{DFC}}{L_{tubing}}$$

$$q_{DFC} = \frac{6350}{7500} * 500 * \frac{40}{500}$$

$$q_{DFC} = 34 \text{ Bbl/day (225.08 l/hr)}$$

$$q_{DFC} = 190.8 \text{ ft}^3/\text{day}$$

Appendix 3: Procedure to design AICD function's parameters

Procedure to design AICD model

1. The AICD performance curve was digitized as shown in Figure 7-3

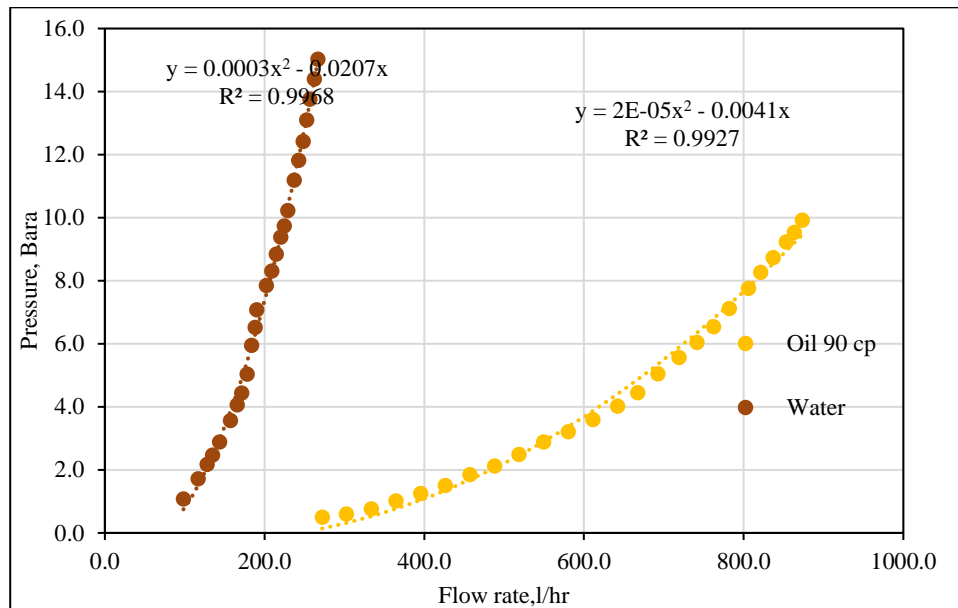


Figure 7-3: Performance curve of AICD in heavy oil

2. Unwanted fluid (water) of 225.08 l/hr l/hr was used to find the pressure drop.

$$\Delta P = 0.0003(225.08)^2 - 0.0207$$

$$\Delta P = 15.178 \text{ bara}$$

3. The value of K was found by using Equation (58), where the units of ΔP is Psia, ρ is lbm/ft³ and q is ft³/day.

$$K = \frac{\Delta P}{\rho * q^2}$$

$$K = \frac{15.178 * 14.5038}{64.79 * (190.8)^2}$$

$$K = 9.333 * 10^{-5}$$

Since the density calibration is water the value of K is equal to AICD strength (a_{AICD})

$$a_{AICD} = 9.333 * 10^{-5} \text{ psi}/((\text{lb}/\text{ft}^3)(\text{rft}^3/\text{day})^2)$$

4. The pressure drop in the oil was found by using Equation (58) by using a flow rate of 225.08 l/hr.

$$\Delta P = 2.5e - 5(225.08^2) - 0.0041(225.08)$$

$$\Delta P = 0.344 \text{ bara}$$

$$K = \frac{0.344 * 14.5038}{49.1 * 190.8^2}$$

$$K = 2.791 * 10^{-6}$$

5. The viscosity exponent (y) can be found by substituting a_{AICV} , densities, viscosities and K into Equation (59).

$$K = \left(\frac{\rho}{\rho_{cal}} \right) * \left(\frac{\mu_{cal}}{\mu} \right)^y * a_{AICV} \quad (24)$$

$$\left(\frac{1.45}{90} \right)^y = \frac{2.791 * 10^{-6} * 64.79}{9.333 * 10^{-5} * 49.1}$$

$$y = 0.79$$

Appendix 4: Procedure to design AICV model parameters

1. The AICV performance curve was digitized as shown in figure 7-4.

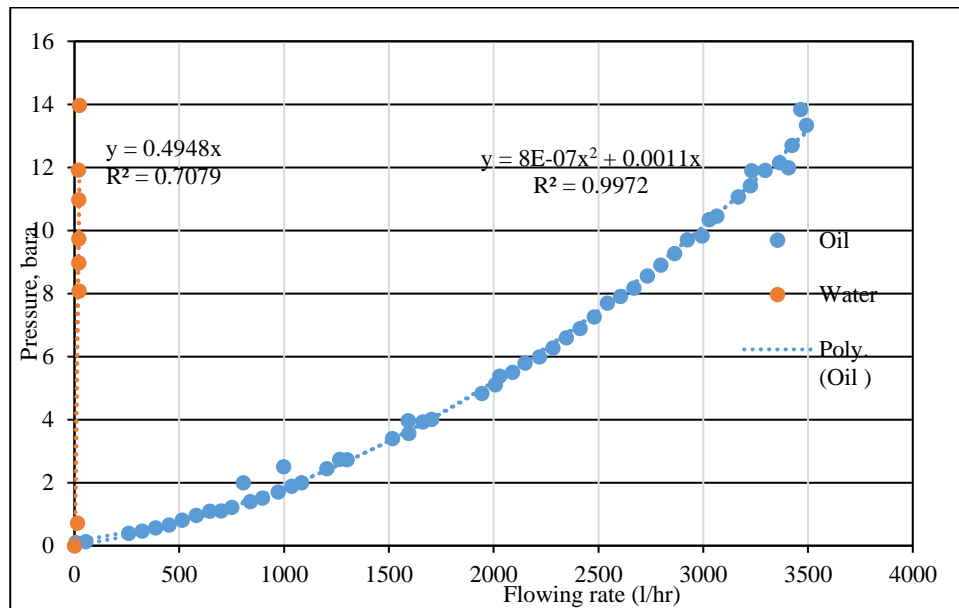


Figure 7-4: Digitized AICV fluid performance curve

2. Unwanted fluid (water) of 225.08 l/hr was used to find the pressure drop.

$$\Delta P = 0.4948(225.08)$$

$$\Delta P = 111.4 \text{ bara}$$

3. The value of K was found by using Equation (58).

$$K = \frac{\Delta P}{\rho * q^2}$$

$$K = \frac{111.4 * 14.5038}{64.79 * 190.8^2}$$

$$K = 6.8502 * 10^{-4}$$

Since the density calibration is water the value of K is equal to AICD strength (a_{AICD})

$$a_{AICV} = 6.8502 * 10^{-4} \text{ psi}/((\text{lb}/\text{ft}^3)(\text{rft}^3/\text{day})x)$$

4. The pressure drop of oil was found by using Equation (58) by using a flow rate of 225.08 l/hr.

$$\Delta P = 8e - 7(225.08^2) + 0.0011(225.08)$$

$$\Delta P = 0.288 \text{ bara}$$

$$K = \frac{0.288 * 14.5038}{49.1 * 190.8^2}$$

$$K = 2.337 * 10^{-6}$$

5. The viscosity exponent (y) can be found by substituting a_{AICV} , densities, viscosities and K into Equation (59).

$$\left(\frac{1.45}{90}\right)^y = \frac{2.337e - 6 * 64.39}{6.85e - 4 * 49.1}$$

$$y = 1.31$$

Appendix 5: Procedure to design AICD function's parameters for low viscous oil reservoir

Procedure to design AICD model

1. The AICD performance curve was digitized as shown in Figure 7-5

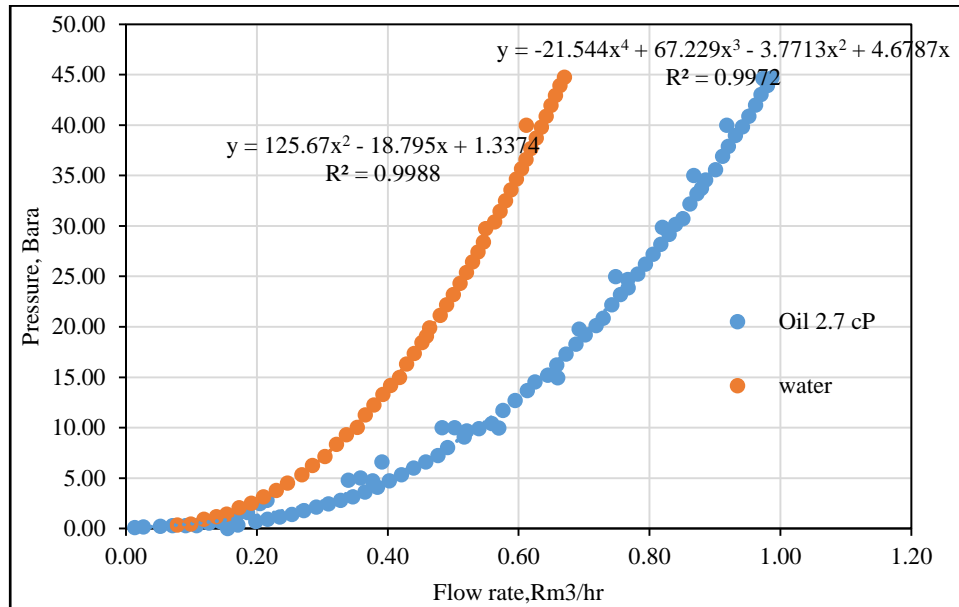


Figure 7-5: Performance curve of AICD in the low viscous oil reservoir

2. Unwanted fluid (water) of 225.08 l/hr l/hr was used to find the pressure drop.

$$\Delta P = 125.67(0.22508)^2 - 18.795(0.22508) + 1.3374$$

$$\Delta P = 3.474 \text{ bara}$$

3. The value of K was found by using Equation (58), where the units of ΔP is Psia, ρ is lbm/ft³ and q is ft³/day.

$$K = \frac{\Delta P}{\rho * q^2}$$

$$K = \frac{3.474 * 14.5038}{64.79 * (190.8)^2}$$

$$K = 2.136 * 10^{-5}$$

Since the density calibration is water the value of K is equal to AICD strength (a_{AICD})

$$a_{AICD} = 2.136 * 10^{-5} \text{ psi}/((\text{lb}/\text{ft}^3)(\text{rft}^3/\text{day})^2)$$

4. The pressure drop in the oil was found by using Equation (58) by using a flow rate of 225.08 l/hr.

$$\Delta P = (-21.544(0.22508^4) + 67.229(0.22508^3) - 3.7713(0.22508^2) + 4.6787(0.22508))$$

$$\Delta P = 1.573 \text{ bara}$$

$$K = \frac{1.573 * 14.5038}{49.1 * 190.8^2}$$

$$K = 1.276 * 10^{-5}$$

5. The viscosity exponent (y) can be found by substituting a_{AICV} , densities, viscosities and K into Equation (59).

$$K = \left(\frac{\rho}{\rho_{cal}} \right) * \left(\frac{\mu_{cal}}{\mu} \right)^y * a_{AICV} \quad (24)$$

$$\left(\frac{1.45}{2.7} \right)^y = \frac{1.27 * 10^{-5} * 64.79}{2.136 * 10^{-5} * 49.1}$$

$$y = 0.39$$

Appendix 6: Procedure to design AICV model parameters for low viscous oil reservoir model

1. The AICV performance curve was digitized as shown in Figure 7-6

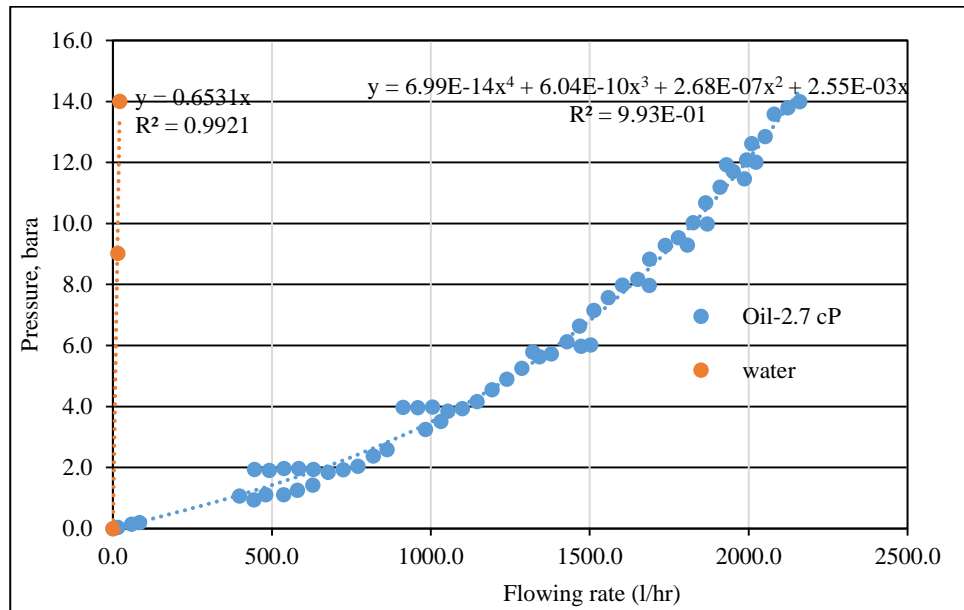


Figure 7-6: Digitized AICV fluid performance curve for low viscous oil reservoir

2. Unwanted fluid (water) of 225.08 l/hr was used to find the pressure drop.

$$\Delta P = 0.6531(225.08)$$

$$\Delta P = 147 \text{ bara}$$

3. The value of K was found by using Equation (58).

$$K = \frac{\Delta P}{\rho * q^2}$$

$$K = \frac{147 * 14.5038}{64.79 * 190.8^2}$$

$$K = 9.0393 * 10^{-4}$$

Since the density calibration is water the value of K is equal to AICD strength (a_{AICD})

$$a_{AICV} = 9.0393 * 10^{-4} \text{ psi}/((\text{lb}/\text{ft}^3)(\text{rft}^3/\text{day})x)$$

4. The pressure drop of oil was found by using Equation (58) by using a flow rate of 225.08 l/hr.

$$\Delta P = 6.99 * 10^{-14}(225.08^4) + 6.04 * 10^{-10}(225.08^3) + 2.68 * 10^{-7}(225.08^2) + 2.55 * 10^{-3}(225.08)$$

$$\Delta P = 0.594 \text{ bara}$$

$$K = \frac{0.594 * 14.5038}{49.1 * 190.8^2}$$

$$K = 4.8198 * 10^{-6}$$

5. The viscosity exponent (y) can be found by substituting a_{AICV} , densities, viscosities and K into Equation (59).

$$\left(\frac{1.45}{2.7}\right)^y = \frac{4.8198 * 10^{-6} * 64.39}{9.0393 * 10^{-4} * 49.1}$$

$$y = 3.97$$

Appendix 7: MATLAB code for optimization of the cross sectional area of ICDs by using the Golden ratio search method

```

Function[S] = golden1 (f)
%Input - f is the object function input as a string 'f'
% - a and b are the endpoints of the interval
% - delta is the tolerance for the abscissas
% - epsilon is the tolerance for the ordinates
%Output - S=(p,yp) contains the abscissa p and
% the ordinate yp of the maximum point
% - E=(dp,dy) contains the error bounds for p and yp
% - G is an n x 4 matrix: the kth row contains
% [ak ck dk bk]; the values of a, c, d, and b at the
% kth iteration
%%%%%%%%%%%%%%%%%%%%%%%%%%%%%%%%%%%%%%%%%%%%%%%%%%%%%%%%%%%%%%%%%%%%%%%%%%
% ICDs functions
f= @(x) -4e11*x.^2+8e8*x+2e6;
%Cross sectional Limits
a=6.9e-4;
b=1.2e-3;
%%%%%%%%%%%%%%%%%%%%%%%%%%%%%%%%%%%%%%%%%%%%%%%%%%%%%%%%%%%%%%%%%%%%%%%%%%
delta=1e-10;
epsilon=1e-2;
r1=(sqrt(5)-1)/2;
r2=1-r1;
h=b-a;
ya=feval(f,a);
yb=feval(f,b);
c=a+r2*h;
d=b-r2*h;
yc=feval(f,c);
yd=feval(f,d);
k=1;
A(k)=a;B(k)=b;
C(k)=c;D(k)=d;
while (abs(yb-ya)>epsilon) || (h>delta)
    k=k+1;
    if(yc>yd)
        b=d;
        yb=yd;
        d=c;
        yd=yc;
        h=b-a;
        c=a+r2*h;
        yc=feval(f,c);
    else
        a=c;
        ya=yc;
        c=d;
        yc=yd;
        h=b-a;
        d=b-r2*h;
        yd=feval(f,d);
    end
    A(k)=a;B(k)=b;C(k)=c;D(k)=d;
end
dp=abs(b-a);
dy=abs(yb-ya);
p=a;
yp=ya;
if(yb>ya)
    p=b;
    yp=yb;
end
G=[A' C' D' B']
S=[p yp]
E=[dp dy]

```

Appendix 8: MATLAB code for optimization of the strength of A ICDs (a) and Viscosity exponent (y) by using the Nelder - Mead method.

```

%% Preamble
clear; clc;
format long
f =@(x,y) (1e-4)*(5e14*x.^3-2e12*x.^2+2e9*x+3e7)+...
    0.9999*(3.14e4*y.^3-3.75e5*y.^2+1.22e6*y+3.1e7);
F =@(V) f(V(1),V(2));

V = [1.33e-5 ,0.09; 1.93e-4 ,0.14; 9.33e-5 ,0.59]; % Starting points
FV = [F(V(1,:)),F(V(2,:)),F(V(3,:))]; % Starting values
% Sort the starting points s.t. F(B) > F(G) <F(W)
[B,G,W,FB,FG,FW] = sortPoints(V,FV);

[X,Y] = meshgrid(linspace(-1,6),linspace(-2,5));
printDetails(B,G,W,FB,FG,FW,0);
plotFunc(X,Y,f,B,G,W);

i = 0; % Iterator
n = 4; % Maximum number of iterations
eps = 2e-4; % Error tolerance

%% Main loop
while (i < n) && (sqrt(sum((FB-FW).^2)) > eps)
    i = i + 1; % Manually increment i
    % Run Nelder-Mead algorithm
    [B,G,W,FB,FG,FW] = nelderMeadAlg(B,G,W,FB,FG,FW,F);
    % Sort vertices
    % The sorting can be done during Nelder-Mead to save computational
    % time, but for demonstrational purposes this is not done here.
    [B,G,W,FB,FG,FW] = sortPoints([B;G;W],[FB;FG;FW]);
    % Print details about our vertices
    printDetails(B,G,W,FB,FG,FW,i);
    if i == 10 % Zoom in on the plot
        [X,Y] = meshgrid(linspace(2.5,3.5),linspace(1.5,2.5));
    end
    if i == 20 % Zoom in even further on the plot
        [X,Y] = meshgrid(linspace(2.95,3.05),linspace(1.95,2.05));
    end
    plotFunc(X,Y,f,B,G,W);
end
fprintf('\n\nThe best point found was: (%10.10f, %10.10f) ',B(1),B(2));
fprintf(' with the function value: %10.10f\n',FB);

%% Help functions
% Functions defined inside scripts can only be seen by that script

%% Nelder-Mead Algorithm
function [B,G,W,FB,FG,FW] = nelderMeadAlg(B,G,W,FB,FG,FW,F)
    M = (B+G)/2;
    R = 2.*M - W;
    FR = F(R);
    if FR > FG
        % Reflect and possibly extend
        if FB > FR
            % Reflect
            W = R; FW = FR;
            fprintf('Reflection!\n');
        else
            % Try to expand since R is the best point
            E = 2.*R - M;
            FE = F(E);
            if FE > FB
                % Expansion is better, replace worst with expanded
                W = E; FW = FE;
                fprintf('Expansion!\n');
            else
                % Expansion is not better, replace worst with reflected
                W = R; FW = FR;
                fprintf('Reflection!\n');
            end
        end
    end
end

```

```

else
    % Contraction
    if FR > FW
        % Choose C2 if F(R) < F(W)
        W = R; FW = FR;
        fprintf('Reflection-');
    end
    C = (W+M)/2; FC = F(C);
    if FC > FW
        % Contract if F(C) < F(W)
        W = C; FW = FC;
        fprintf('Contraction!\n');
    else
        % Shrink towards B if F(C) < F(W)
        S = (B+W)/2; FS = F(S);
        W = S; FW = FS;
        G = M; FG = F(M);
        fprintf('Shrink!\n');
    end
end
end

%% Sorting algorithm
function [B,G,W,FB,FG,FW] = sortPoints(V,FV)
    %Sort the points according to function value
    V1 = V(1,:); F1 = FV(1);
    V2 = V(2,:); F2 = FV(2);
    V3 = V(3,:); F3 = FV(3);

    if (F3 >= F1) && (F3 >= F2)
        if (F2 >= F1)
            % F3 > F2 > F1
            [B,G,W] = deal(V3,V2,V1);
            [FB,FG,FW] = deal(F3,F2,F1);
        else
            % F3 > F1 > F2
            [B,G,W] = deal(V3, V1, V2);
            [FB,FG,FW] = deal(F3,F1,F2);
        end
    elseif (F1 >= F2) && (F1 >= F3)
        if (F2 >= F3)
            % F1 > F2 > F3
            [B,G,W] = deal(V1,V2,V3);
            [FB,FG,FW] = deal(F1,F2,F3);
        else
            % F1 > F3 > F2
            [B,G,W] = deal(V1,V3,V2);
            [FB,FG,FW] = deal(F1,F3,F2);
        end
    else % (F2 > F1) && (F2 > F3)
        if (F1 >= F3)
            % F2 > F1 > F3
            [B,G,W] = deal(V2,V1,V3);
            [FB,FG,FW] = deal(F2,F1,F3);
        else
            % F2 > F3 > F1
            [B,G,W] = deal(V2,V3,V1);
            [FB,FG,FW] = deal(F2,F3,F1);
        end
    end
end

%% Printing function
function printDetails(B,G,W,FB,FG,FW,i)
    fprintf('Iteration %3i:\t',i);
    fprintf('|B: %4.2f, %4.2f : %7.6f |\t',B(1),B(2),FB);
    fprintf('|G: %4.2f, %4.2f : %7.6f |\t',G(1),G(2),FG);
    fprintf('|W: %4.2f, %4.2f : %7.6f |\n',W(1),W(2),FW);
end

%% Plotting function
function plotFunc(X,Y,f,B,G,W)
    figure(1); clf;
    hold on
    contourf(X,Y,f(X,Y),30);
    title('Nelder-Mead Algorithm')
    xlabel('x-axis');

```

```
ylabel('y-axis');
axis image
colorbar();
plot([B(1), G(1), W(1), B(1)],...
      [B(2), G(2), W(2), B(2)],...
      '-','color',[0.8500 0.3250 0.0980],...
      'LineWidth', 2.5);
text(B(1),B(2),'B','color',[1 1 1]);
text(G(1),G(2),'G','color',[1 1 1]);
text(W(1),W(2),'W','color',[1 1 1]);
pause(1);
end
```

Appendix 9: Designed cross sectional areas of the ICDs

Table 7-1: The designed diameter and cross sectional area of the ICDs in the reservoir model

2

Sections	Units	I	II	III	IV
k	[mD]	5000	500	3000	1000
h	[ft]	100			
ρ_o	[lb/ft ³]	60.53			
q_o	[stb/day]	225			
B_o		1.08			
n		4			
μ_o	[cP]	90			
D	[ft]	1000			
L_w	[ft]	1000	2500	2500	1500
r_w	[ft]	0.5			
s		0			
A	[ft ²]	8.34E-05	0.00	7.91E-05	1.77E-04
d	[ft]	1.03E-02	0.00	1.00E-02	1.50E-02

Table 7-2: The designed diameter and cross sectional area of the ICDs in the reservoir model

3

Sections	Units	I	II	III	IV
k	[mD]	5000	500	3000	1000
h	[ft]	150			
ρ_o	[lb/ft ³]	54.6			
q_o	[stb/day]	225			
B_o		1.08			
n		4			
μ_o	[cP]	2.7			
D	[ft]	1000			
L_w	[ft]	1000	2500	2500	1500
r_w	[ft]	0.5			
s		0			
A	[ft ²]	7.04E-04	0.00	6.68E-04	1.49E-03
d	[ft]	3.00E-02	0.00	2.92E-02	4.36E-02

Appendix 10: Results for all four models

Table 7-3: The results for model 1

Model 1			
Completion type	open hole	ICDs	AICDs
Cumulative oil production[bbbl]	6.08E+07	6.12E+07	6.18E+07
RF	46.1%	46.4%	46.8%
WC	95.0%	95.00%	95.0%
Increase in cum. Oil production[bbbl]	0.00E+00	4.33E+05	9.63E+05
Revenue[Usd]	-	2.93E+07	6.53E+07
Net revenue [Usd]		2.09E+07	5.69E+07
Net revenue [price by -40%]		8.47E+06	2.92E+07
Net revenue [price +40%]		3.10E+07	7.92E+07

Table 7-4: The results for model 2

Model 2			
Completion type	open hole	ICDs	AICDs
Cumulative oil production [bbbl]	4.76E+07	4.78E+07	4.86E+07
RF	42.12%	42.26%	43.0%
WC	95.10%	95.33%	95.02%
Increase in cum. Oil production[bbbl]	0.00E+00	1.59E+05	1.01E+06
Revenue[Usd]	-	1.08E+07	6.86E+07
Net revenue [Usd]		2.41E+06	6.02E+07
Net revenue [price by -40%]		-2.18E+06	3.11E+07
Net revenue [price +40%]		6.10E+06	8.37E+07

Table 7-5: The results for model 3

Model 3			
Completion type	Open hole	ICDs	AICDs
Cumulative oil production[bbbl]	8.23E+07	8.25E+07	0.00E+00
RF	58.41%	58.615%	0.000%
WC	95.0%	95.0%	0.00%
Increase in cum. Oil production[bbbl]	0.00E+00	2.85E+05	-8.23E+07
Revenue[Usd]	-	1.93E+07	-5.58E+09
Net revenue [Usd]		1.09E+07	-5.59E+09
Net revenue [price by -40%]		2.73E+06	2.44E+06
Net revenue [price +40%]		1.76E+07	1.69E+07

Table 7-6: The results for model 4

Model 4			
Completion type	open hole	ICDs	AICDs
Cumulative oil production	6.62E+07	6.63E+07	6.63E+07
RF	50.23%	50.25%	50.26%
WC	95.0%	95.04%	95.0%
Increase in cum. Oil production[bbbl]	0.00E+00	2.74E+04	4.41E+04
Revenue[Usd]	-	1.86E+06	2.99E+06
Net revenue [Usd]		-6.54E+06	-5.41E+06
Net revenue [price by -40%]		-7.33E+06	-6.68E+06
Net revenue [price +40%]		-5.90E+06	-4.39E+06

Appendix 11: Other attachment of the results for all four models

These are the results attached in the Zip file.

- *Excel sheet “General results-optimal”*
This excel include the summary of all final results for all models.
- *Excel sheet “General results-unoptimal ”*
This excel include the results of unoptimized DFCs for all four models, the results were extracted from the Eclipse simulator.
- *Excel sheet “Area of ICDs-Heterogeneous ”*
This excel include the determination of cross sectional area in the heterogeneous reservoir.
- *Excel sheet “Area of ICDs-Homogeneous ”*
This excel include the determination of cross sectional area in the homogeneous reservoir.
- *Excel sheet “Digitized data ”*
This excel sheet include the which results from digitization
- *Excel sheet “fluid properties ”*
This excel sheet shows how PVT data were developed

Model 1

- *“Model 1 open”*
Eclipse code for open hole in reservoir model 1
- *“Model 1 ICD”*
Eclipse code for ICDs completion in reservoir model 1

- *“Model 1 AICV”*
Eclipse code for AICVs completion in reservoir model 1
- *“Model 1 AICD”*
Eclipse code for AICDs completion in reservoir model 1
- *“Model 1 ICD optimal”*
Eclipse code for ICDs completion (Optimized case) in reservoir model 1
- *“Model 1 AICD optimal”*
Eclipse code for AICDs completion (Optimized case) in reservoir model 1
- *Excel sheet “Model 1 ICD optimal ”*
It includes the results of the optimized ICDs in the model 1, the results were extracted from the Eclipse simulator.
- *Excel sheet “Model 1 AICD optimal”*
This excel includes the results of the optimized AICDs and AICVs in the model 1, the results were extracted from the Eclipse simulator.

Model 2

- *“Model 2 open”*
Eclipse code for open hole in reservoir model 2
- *“Model 2 ICD”*
Eclipse code for ICDs completion in reservoir model 2
- *“Model 2 AICV”*
Eclipse code for AICVs completion in reservoir model 2
- *“Model 2 AICD”*
Eclipse code for AICDs completion in reservoir model 2
- *“Model 2 ICD optimal”*
Eclipse code for ICDs completion (Optimized case) in reservoir model 2
- *“Model 2 AICD optimal”*
Eclipse code for AICDs completion (Optimized case) in reservoir model 2
- *Excel sheet “Model 2 ICD optimal ”*
It includes the results of the optimized ICDs in the model 2, the results were extracted from the Eclipse simulator.
- *Excel sheet “Model 2 AICD optimal ”*

This excel includes the results of the optimized AICDs and AICVs in the model 2, the results were extracted from the Eclipse simulator.

Model 3

- *“Model 3 open”*
Eclipse code for open hole in reservoir model 3
- *“Model 3 ICD”*
Eclipse code for ICDs completion in reservoir model 3
- *“Model 3 AICV”*
Eclipse code for AICVs completion in reservoir model 3
- *“Model 3 AICD”*
Eclipse code for AICDs completion in reservoir model 3
- *“Model 3 ICD optimal”*
Eclipse code for ICDs completion (Optimized case) in reservoir model 3
- *“Model 3 AICD optimal”*
Eclipse code for AICDs completion (Optimized case) in reservoir model 3
- *Excel sheet “Model 3 ICD optimal”*
It includes the results of the optimized ICDs in the model 3, the results were extracted from the Eclipse simulator.
- *Excel sheet “Model 3 AICD optimal”*
This excel includes the results of the optimized AICDs and AICVs in the model 3, the results were extracted from the Eclipse simulator.’

Model 4

- *“Model 4 open”*
Eclipse code for open hole in reservoir model 4
- *“Model 4 ICD”*
Eclipse code for ICDs completion in reservoir model 4
- *“Model 4 AICV”*
Eclipse code for AICVs completion in reservoir model 4
- *“Model 4 AICD”*
Eclipse code for AICDs completion in reservoir model 4
- *“Model 4 ICD optimal”*
Eclipse code for ICDs completion (Optimized case) in reservoir model 4

- *“Model 4 AICD optimal”*
Eclipse code for AICDs completion (Optimized case) in reservoir model 4
- *Excel sheet “Model 4 ICD optimal ”*
It includes the results of the optimized ICDs in the model 4, the results were extracted from the Eclipse simulator.
- *Excel sheet “Model 4 AICD optimal”*
This excel includes the results of the optimized AICDs and AICVs in the model 4, the results were extracted from the Eclipse simulator.

